

**GEOPHYSICAL EVALUATION OF SUBSURFACE LAYERS FOR
STRUCTURAL FOUNDATION USING ELECTRICAL
RESISTIVITY METHODS**

By:

**SURAJUDEEN HADI ADEMOLA
B.Sc Physics (U.I)
222814**

**A PROJECT SUBMITTED TO THE DEPARTMENT OF
PHYSICS, FACULTY OF SCIENCE, UNIVERSITY OF IBADAN,
IN PARTIAL FULFILMENT FOR THE AWARD OF BACHELOR
OF SCIENCE (B.Sc) DEGREE IN PHYSICS**

JANUARY, 2025

Certification

I certify that this project was carried out under my supervision by **Surajudeen Hadi Ademola**, with matriculation number **222814**, of the Department of Physics, Faculty of Science, University of Ibadan.

Dr. A. A. Adetoyinbo
B.Sc., M.Sc., Ph.D. (Ibadan)
Department of Physics, University of Ibadan
(Supervisor)

Date

Dedication

I dedicate this project to the Almighty God, whose wisdom, strength, and guidance have been my source of inspiration throughout this academic journey. To my beloved parents, whose unwavering love, sacrifices, and encouragement have shaped my path and fueled my ambition. Your prayers and support have been the foundation of my success.

Acknowledgements

First and foremost, I express my profound gratitude to Almighty God for granting me the strength, wisdom, and perseverance to complete this project successfully.

I would like to extend my sincere appreciation to my supervisor, **Dr. Adedeji Adegoke Adetoyinbo**, for his invaluable guidance, and unwavering support throughout this project. My sincere appreciation also to **Prof. Adekunle Kazeem Bello**, his expertise and mentorship have been instrumental in shaping this work.

A special appreciation goes to my family for their endless love, prayers, moral and financial support. Their unwavering belief in my abilities has been a constant source of motivation.

I am also thankful to my friends most especially **David Tolulope** and colleagues for their encouragement and assistance, as well as for creating an environment of collaboration and learning.

Finally, I acknowledge the contributions of everyone who, in one way or another, played a role in the successful completion of this project.

Abstract

The evaluation of subsurface conditions plays a pivotal role in understanding geological formations and assessing their suitability for various engineering and environmental applications. This project employed an integrated approach using geophysical methods to investigate subsurface properties at an open ground near the University of Ibadan Central Mosque (UI Mosque) and within Abubakar Abdulsalam Hall (AAH), University of Ibadan. A total of 20 Vertical Electrical Soundings (VES) were conducted using the Schlumberger array electrode configuration, with half-current electrode separation ($AB/2$) ranging from 1 to 55 m for each study area. Additionally, a total of five Profile Constant Separating Transverse (CST) measurements were obtained using the Wenner array electrode configuration, with electrode positions ranging from 0 to 150 m and 0 to 130 m, depending on the profile. These methods were employed to optimize depth-specific and lateral resistivity measurements, providing detailed insights into resistivity variations. The results enabled a comprehensive interpretation of subsurface features such as weak zones, potential failure planes, subsurface layers, soil types, fractures, anomalies, faults, and bedrock characteristics that could impact foundation stability.

The results obtained from the geoelectric sections revealed three primary subsurface geologic layers in both study areas: the topsoil, the weathered layer (comprising clay/sand and laterite), and the fractured basement/fresh bedrock. At the UI Mosque, the resistivity of the topsoil ranged from $220 \Omega\text{m}$ to $629.6 \Omega\text{m}$, with a mean value of $367.18 \Omega\text{m}$, and its thickness varied between 0.8 m and 1.1 m. The weathered layer exhibited a resistivity range of $60 \Omega\text{m}$ to $231 \Omega\text{m}$, with a mean value of $110.61 \Omega\text{m}$, and its thickness and depth ranged from 1.8 m to 3.0 m and 4.0 m to 22 m, respectively. The resistivity of the delineated fractured and fresh bedrock ranged from $27.7 \Omega\text{m}$ to $449.3 \Omega\text{m}$, although the depth of the fresh bedrock was undetermined. The resistivity and thickness of the subsurface layers indicate the suitability of the area for light to moderate civil engineering foundations. However, the presence of fractured zones may require further geotechnical evaluation for heavy structures.

Also, at the AAH site, the resistivity of the topsoil ranged from $186.9 \Omega\text{m}$ to $1222.0 \Omega\text{m}$, with a mean value of $422.5 \Omega\text{m}$, and its thickness varied between 0.5 m and 1.0 m. The weathered layer exhibited a resistivity range of $13.6 \Omega\text{m}$ to $70.0 \Omega\text{m}$, with a mean value of $29.6 \Omega\text{m}$, and its thickness and depth ranged from 1.4 m to 9.9 m and 1.9 m to 10.9 m, respectively. The resistivity of the delineated fractured and fresh bedrock ranged from $166.7 \Omega\text{m}$ to $834.5 \Omega\text{m}$. The resistivity and thickness of the subsurface layers indicate in this area showed that these fractured zones could indicate potential instability or the presence of water-bearing layers, which may

affect the load-bearing capacity of the subsurface materials. Therefore, a detailed geotechnical evaluation, including borehole drilling and core sampling, is recommended to assess the integrity of the bedrock and ensure the safety and stability of any heavy structures planned for the site.

Contents

Certification	i
Dedication	ii
Acknowledgements	iii
Abstract	iv
List of Figures	xii
List of Tables	xiii
Acronyms	xiii
1 CHAPTER 1: INTRODUCTION	1
1.1 Background to the Study	1
1.2 Research Problem	2
1.3 Aim and Objectives	3
1.3.1 Aim of the Study	3
1.3.2 Objectives of the Study	3
1.4 Justification of the Study	4
1.5 Geological Settings	4
1.5.1 The Study Location	4
1.5.2 The Study Area	5
1.6 Outline of the Thesis	9
2 CHAPTER 2: LITERATURE REVIEW	10
2.1 Introduction to Geophysical Methods in Civil Engineering	10
2.2 Overview of Geophysical Techniques	11

2.2.1	Ground Penetrating Radar (GPR)	11
2.2.2	Seismic Refraction Methods	12
2.2.3	Electrical Resistivity Methods	13
2.3	Theoretical Background of Electrical Resistivity Methods	14
2.3.1	General Principles of Electrical Resistivity Methods	14
2.3.2	Electric Current Flow in Subsurface Materials	15
2.3.3	Electrical Field and Potential	16
2.3.4	Apparent Resistivity	18
2.3.5	The General Four Electrode System	19
2.3.6	Electrode Configuration	19
2.4	Resistivity Surveying Techniques	22
2.4.1	Resistivity Surveying	22
2.4.2	Vertical Electrical Sounding	23
2.4.3	Constant Separation Traversing	24
2.4.4	Comparison of VES and CST	25
2.5	Previous Studies on Electrical Resistivity	26
2.5.1	Previous Studies in Nigeria	26
2.5.2	Comparison of Methods	26
2.6	Applications of Electrical Resistivity	27
2.6.1	Innovative Applications of Electrical Resistivity	27
2.6.2	Applications in Structural Health Monitoring	27
2.6.3	Applications in Building Foundation	27
2.7	Importance of Subsurface Evaluation for Foundation Design	28
2.7.1	Understanding Subsurface Conditions:	28
2.7.2	Benefits of Subsurface Evaluation:	28
2.7.3	Case Studies in Foundation Design:	28
2.7.4	Relevance to Sustainable Construction:	29
3	CHAPTER 3: MATERIALS AND METHODS	30
3.1	Introduction	30
3.2	Geophysical Investigation	30
3.3	Geophysical Survey Materials and Equipment	30

3.4	Methodology	32
3.4.1	Survey Design	32
3.4.2	Field Procedures	34
3.4.3	Data Acquisition	35
3.4.4	Data Processing	35
3.4.5	Interpretation Methods	35
3.5	Practical Curve Matching Techniques	36
3.5.1	Types of Possible Curves	36
3.5.2	Curve Matching Techniques Procedure Outlines	37
3.6	Limitations and Precautions	38
3.6.1	Limitations	38
3.6.2	Precautions	39
4	CHAPTER 4: RESULTS AND ANALYSIS	41
4.1	Introduction	41
4.2	Curve Match Techniques Results	41
4.3	Vertical Electrical Sounding Data Interpretation	43
4.3.1	VES 1 Station at UI Mosque	43
4.3.2	VES 2 Station at UI Mosque	44
4.3.3	VES 3 Station at UI Mosque	45
4.3.4	VES 4 Station at UI Mosque	46
4.3.5	VES 5 Station at UI Mosque	47
4.3.6	VES 6 Station at UI Mosque	48
4.3.7	VES 7 Station at UI Mosque	49
4.3.8	VES 8 Station at UI Mosque	50
4.3.9	VES 9 Station at UI Mosque	51
4.3.10	VES 10 Station at UI Mosque	52
4.3.11	VES 1 Station at AAH	53
4.3.12	VES 2 Station at AAH	54
4.3.13	VES 3 Station at AAH	55
4.3.14	VES 4 Station at AAH	56
4.3.15	VES 5 Station at AAH	57

4.3.16	VES 6 Station at AAH	58
4.3.17	VES 7 Station at AAH	59
4.3.18	VES 8 Station at AAH	60
4.3.19	VES 9 Station at AAH	61
4.3.20	VES 10 Station at AAH	62
4.4	Constant Separation Traversing Data Interpretation	63
4.5	Interpretation of the Profiles	67
4.5.1	Resisitivty Variations	67
4.5.2	Profile 1 at UI Mosque	68
4.5.3	Profile 2 at UI Mosque	68
4.5.4	Profile 3 at UI Mosque	68
4.5.5	Profile 1 at AAH	69
4.5.6	Profile 2 at AAH	69
4.6	Geoelectric Section along the Profiles using Surfer	70
4.6.1	UI Mosque Profile 1 Geoelectric Section	70
4.6.2	UI Mosque Profile 2 Geoelectric Section	71
4.6.3	UI Mosque Profile 3 Geoelectric Section	72
4.6.4	Abubakar Abdulsalam Hall Profile 1 Geoelectric Section	73
4.6.5	Abubakar Abdulsalam Hall Profile 2 Geoelectric Section	74
4.7	Geoelectric Parameters and the Inferred Lithology of the Study Area	74
4.7.1	Model Interpretation of Layers for UI Mosque Study Area	75
4.7.2	Model Interpretation of Layers for AAH Study Area	76
5	CHAPTER 5: SUMMARY, CONCLUSION, AND RECOMMENDATIONS	79
5.1	SUMMARY	79
5.2	RECOMMENDATIONS	79
5.3	CONCLUSION	80
REFERENCES		81
APPENDIX		85

List of Figures

1.1	Map showing Nigeria from the World Map generated using QGIS.	5
1.2	Combined maps for the study location and study area generated by QGIS.	7
1.3	Combined maps for the study areas generated by QGIS.	8
2.1	Diagram illustrating electrical current flow through subsurface [Pearson <i>et al.</i> , 2023]	15
2.2	Diagram illustrating electrical field with equipotential and current flow lines [Jamaluddin <i>et al.</i> , 2019]	17
2.3	Graph showing an apparent resistivity curve for a typical VES survey [Sanuade <i>et al.</i> , 2019]	18
2.4	Comparison of the Schlumberger and Wenner array electrode configurations	21
3.1	The Resistivity Meter used for the Survey.	31
3.2	Electrode Arrangement of Wenner and Schlumberger Configuration [James <i>et al.</i> , 2011]	32
3.3	Survey Layout for UI Mosque Study Area	33
3.4	Survey Layout for AAH Study Area	34
3.5	An Electrode Injected to the Ground	34
3.6	The four Curves Types for typical Three Layered Model [Amit <i>et al.</i> , 2018]	37
4.1	Two Curve Matching Result gotten from the plot on log-log graph	42
4.2	Graphical Representation of VES 1	43
4.3	Graphical Representation of VES 2	44
4.4	Graphical Representation of VES 3	45
4.5	Graphical Representation of VES 4	46
4.6	Graphical Representation of VES 5	47
4.7	Graphical Representation of VES 6	48
4.8	Graphical Representation of VES 7	49

4.9	Graphical Representation of VES 8	50
4.10	Graphical Representation of VES 9	51
4.11	Graphical Representation of VES 10	52
4.12	Graphical Representation of VES 1	53
4.13	Graphical Representation of VES 2	54
4.14	Graphical Representation of VES 3	55
4.15	Graphical Representation of VES 4	56
4.16	Graphical Representation of VES 5	57
4.17	Graphical Representation of VES 6	58
4.18	Graphical Representation of VES 7	59
4.19	Graphical Representation of VES 8	60
4.20	Graphical Representation of VES 9	61
4.21	Graphical Representation of VES 10	62
4.22	2D View of CST Profile 1	63
4.23	2D View of CST Profile 2	64
4.24	2D View of CST Profile 3	65
4.25	2D View of CST Profile 1 at AAH	66
4.26	2D View of CST Profile 2 at AAH	67
4.27	Geoelectric Section along Profile 1 at UI Mosque using Surfer	70
4.28	Geoelectric Section along Profile 2 at UI Mosque using Surfer	71
4.29	Geoelectric Section along Profile 3 at UI Mosque using Surfer	72
4.30	Geoelectric Section along Profile 1 at AAH using Surfer	73
4.31	Geoelectric Section along Profile 2 at AAH using Surfer	74

List of Tables

4.1	Interpretation of Layers at UI Mosque Study Area	76
4.2	Interpretation of Layers at AAH Study Area	78
5.1	VES 1-5 Data obtained from Filed Work at UI Mosque	85
5.2	VES 6-10 Data obtained from Filed Work at UI Mosque	86
5.3	VES 1-5 Data obtained from Filed Work at AAH	87
5.4	VES 6 - 10 Data obtained from Field Work at AAH	87

Acronyms

AAH – Abubakar Abdulsalam Hall

UI – University of Ibadan

QGIS – Quantum Geographic Information System

VES – Vertical Electrical Sounding

CST – Constant Separation Traversing

ERT – Electrical Resistivity Tomography

Surfer – A software program that helps to create 2D and 3D models of from geospatial data

WINRESIST – A software program that creates one-dimensional 1D electrical resistivity models

DIPROWIN – A software program that creates two-dimensional 2D electrical resistivity models

CHAPTER 1: INTRODUCTION

1.1 Background to the Study

Building failures, a prevalent issue in various regions, often result from poor soil conditions, inadequate site investigations, and a lack of understanding of the underlying subsurface structure. (**Amadi, et al., 2012**) highlight that improper foundation designs and insufficient knowledge of the structural distribution of subsurface layers are leading contributors to such failures. Also, (**Kværna and Øygarden 2006**) emphasized that soil instability often caused by moisture fluctuations, plays a significant role in compromising the structural integrity of buildings. To mitigate these risks, comprehensive geophysical surveys are vital for analyzing the properties of the ground before construction.

Recent studies have expanded the scope of geophysical methods like Vertical Electrical Sounding (VES) and Constant Separation Traversing (CST) to include subsurface mapping, groundwater exploration, and geotechnical evaluations. (**Adetoyinbo, et al., 2023**), in their work published in the *International Journal of Scientific and Applied Research*, used VES to assess groundwater potential and subsurface characteristics in Idi-Ayunre, Ibadan. Their study identified significant geological features, such as fracture zones and aquifer units, revealing areas with low groundwater prospects. Similarly, (**Ogunseye, et al., 2022**), in their work published in the *Journal of Environmental Studies*, analyzed the geochemical properties of soils in Mokola, Ibadan, using soil samples and laboratory tests. Their findings highlighted the presence of heavy metal contamination, emphasizing its potential impact on groundwater quality and the importance of including geochemical assessments in subsurface investigations. The application of Constant Separation Traversing (CST) has also gained significant attention for its role in evaluating lateral resistivity variations and detecting geological discontinuities. (**Anomohanran 2013**) applied CST to investigate lateral subsurface variations in the Niger Delta region, highlighting its effectiveness in detecting faults, fractures, and lithological boundaries that may compromise the stability of engineering foundations. Their findings demonstrated how CST complements VES by providing lateral profiling of resistivity, offering a more comprehensive understanding of subsurface conditions. Furthermore, (**Ismaila, et al., 2019**) used CST in combination with VES to assess subsurface layers for road construction projects in Ilorin, Nigeria. Their work revealed significant variations

in soil composition and resistivity, emphasizing the need for lateral resistivity profiling in regions with heterogeneous geological settings.

Geophysical surveys, including VES and CST, are particularly significant in regions where soil heterogeneity poses risks to construction activities. For example, (**Agada, et al., 2013**) investigated subsurface characteristics in an area prone to structural failures. Their findings revealed that geological discontinuities, such as fractures and dislocations, were primary contributors to differential settlements and structural disintegration. This underscores the importance of employing methods like VES and CST, which can delineate subsurface features with precision. Electrical resistivity surveys have emerged as a popular method in geotechnical investigations due to their high spatial resolution, cost-effectiveness, and non-destructive nature. This method measures the ability of subsurface materials to conduct electrical currents, enabling the identification of various layers, voids, fractures, and lithological features. As noted by (**Griffiths and Barker 1993**), and corroborated by (**Soupios, et al., 2006**), these surveys provide critical data that can prevent construction failures by ensuring that foundation designs align with the physical and structural characteristics of the site.

Furthermore, (**Warner 2004**) and (**Ozevin, et al., 2017**) emphasized that geophysical techniques are indispensable tools for assessing the bearing capacity of soils. These methods enable civil engineers to identify areas of concern, such as seepage zones and clayey substrata, which can cause excessive settlement and cracking in buildings. By incorporating such techniques into site investigations, construction projects can significantly reduce the risks associated with geotechnical failures. In practical terms, electrical resistivity methods, including VES and CST, have been successfully applied in various engineering projects to identify and map subsurface structures. According to (**Lapenna, et al., 2005**), these methods are invaluable for delineating depth variations, subsurface discontinuities, and lithological interfaces that may affect foundation stability. In addition to their technical benefits, they offer a cost-effective solution compared to traditional drilling methods, making them accessible for large-scale geotechnical investigations.

In summary, the integration of Vertical Electrical Sounding (VES) and Constant Separation Traversing (CST) represents an innovative approach to geotechnical site investigation by addressing challenges related to subsurface heterogeneity and providing insights into lateral and vertical variations, these methods mitigate risks of construction failure. This study employs these techniques to evaluate the geotechnical characteristics of the subsurface within the study area, contributing to safer and more sustainable civil engineering practices.

1.2 Research Problem

Inadequate knowledge of subsurface conditions remains a critical factor contributing to building failures, particularly in regions with complex and heterogeneous geological settings. Engineers often face challenges in accurately assessing subsurface characteristics, which leads to poorly designed foundations that are unable to prevent excessive settling, structural cracking, or outright

collapse. Despite advancements in construction technology, many civil engineering projects still suffer from cost overruns and safety concerns stemming from improper site investigations. While geophysical methods like Vertical Electrical Sounding (VES) and Constant Separation Traversing (CST) have demonstrated significant potential in subsurface characterization, their application in civil engineering foundation designs remains underexplored. This gap in the integration of effective site investigation techniques results in a lack of precise and actionable data, which not only compromises structural stability but also incurs substantial economic and safety risks.

1.3 Aim and Objectives

1.3.1 Aim of the Study

The aim of this project is to evaluate the subsurface layers for structural foundation design by employing electrical resistivity methods, specifically Vertical Electrical Sounding (VES) with Schlumberger configuration and Constant Separation Traversing (CST) with Wenner configuration, aiming to provide actionable insights for foundation stability.

1.3.2 Objectives of the Study

The specific objectives of this study are to:

- Map the subsurface layers and determine their resistivity values using VES and CST methods.
- Identify weak zones, fractures, and groundwater presence that may affect the stability of civil engineering foundations.
- Analyze the depth, thickness, and resistivity of subsurface layers to assess their suitability for various foundation types.
- Detect lateral variations such as faults, fractures, or discontinuities using CST to complement the vertical subsurface evaluation.
- Correlate resistivity values with lithological and geotechnical properties, such as soil type, compaction, and strength.
- Combine VES and CST data to generate 3D visualization of the subsurface using specialized geophysical software, enhancing the interpretation and understanding of subsurface features.
- Provide engineering recommendations for foundation design based on geophysical findings, ensuring safety, cost-efficiency, and structural stability in the study area.

1.4 Justification of the Study

Understanding subsurface layers is essential for civil engineering foundation design, as inadequate knowledge can lead to structural failures, safety risks, and financial losses. The use of Vertical Electrical Sounding (VES) and Constant Separation Traversing (CST) offers a powerful, cost-effective, and non-invasive approach to addressing these challenges.

Previous studies, such as (**Coker 2012**) in Akobo area of Ibadan and (**Adagunodo, et al., 2013**) in Oniye, Southwestern Nigeria, demonstrated the utility of VES for groundwater exploration and fracture detection. Similarly, research by (**Farinde 2015**) focused on integrating geophysical and geotechnical methods for road construction at the University of Ibadan. However, these studies often emphasized resource exploration or general geotechnical characterizations rather than specifically addressing civil engineering foundation requirements.

Regions with heterogeneous soil conditions, such as Ibadan, require tailored and localized geophysical evaluations to mitigate risks like differential settlement and soil instability. While earlier works have provided valuable geological insights, a significant gap remains in leveraging these findings for actionable recommendations in foundation design.

This study aims to fill this gap by explicitly integrating VES and CST methods to evaluate the lithological and structural characteristics of subsurface layers. VES will focus on vertical resistivity profiling, while CST will provide complementary lateral resistivity variations, making it possible to detect faults or fractures that could compromise foundation stability. By correlating resistivity data with geotechnical properties, this research delivers practical insights into soil properties, lithological variations, and structural integrity, enhancing the safety and cost-efficiency of construction practices.

Unlike previous studies, this project emphasizes civil engineering applications, offering a novel approach to geophysical evaluations tailored for foundation design. The findings will contribute to safe and sustainable construction practices, bridging the gap between geophysical insights and practical engineering solutions in complex geological settings.

1.5 Geological Settings

1.5.1 The Study Location

Nigeria, located in West Africa, offers a rich and varied geological tapestry for geophysical research on subsurface layers, particularly for civil engineering foundations. The country's geology ranges from the ancient crystalline basement complex in the southwest, composed of migmatites, gneisses, and granites, to several significant sedimentary basins like the Niger Delta, the Benue Trough, and the Chad Basin. The basement complex's extensive weathering creates a regolith that significantly impacts foundation stability, necessitating thorough geophysical investigation to understand its depth and characteristics. The sedimentary basins, especially the Niger Delta, present complex

stratigraphy with layers of sand, silt, and clay, which have substantial implications for foundation design due to their variable thickness and composition. Hydrogeologically, Nigeria shows diversity with groundwater confined to fractured and weathered zones in the basement areas, contrasting with the broader aquifers in sedimentary regions, affecting soil moisture and stability. Structurally, the presence of faults, folds, and fractures across the nation dictates the subsurface's response to structural loads, crucial for avoiding issues like differential settlement. Even within these broad geological zones, local variability due to tectonic activity, erosion, and sediment deposition makes each site unique, particularly in areas like Ibadan where soil conditions can be highly heterogeneous.

Previous geophysical studies in Nigeria have laid a foundation for understanding how techniques like VES and CST can be applied to map and interpret these geological features for civil engineering purposes on how to ensure the safety and sustainability of civil engineering projects through geophysical evaluation of subsurface conditions.

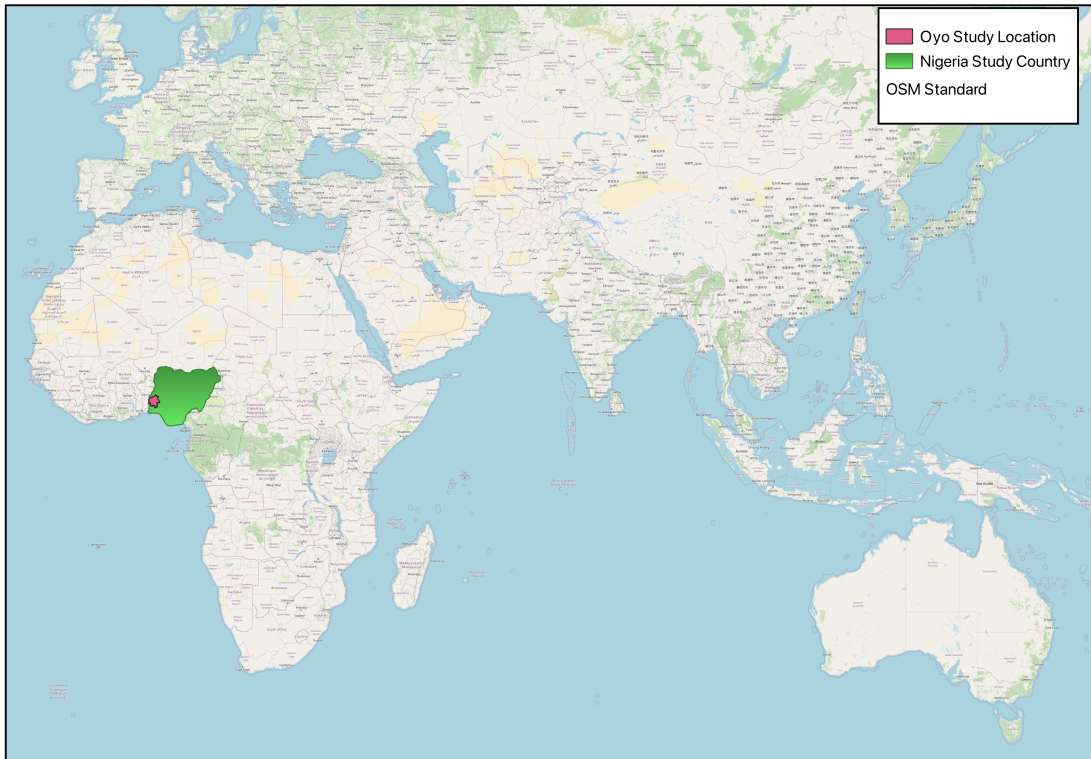


Figure 1.1: Map showing Nigeria from the World Map generated using QGIS.

1.5.2 The Study Area

The geophysical investigation for this study was conducted across two distinct locations within Ibadan North Local Government at the University of Ibadan, Oyo State, Nigeria. This study area lies within the southwestern part of Nigeria, each chosen to represent different geological and soil conditions pertinent to civil engineering foundation design.

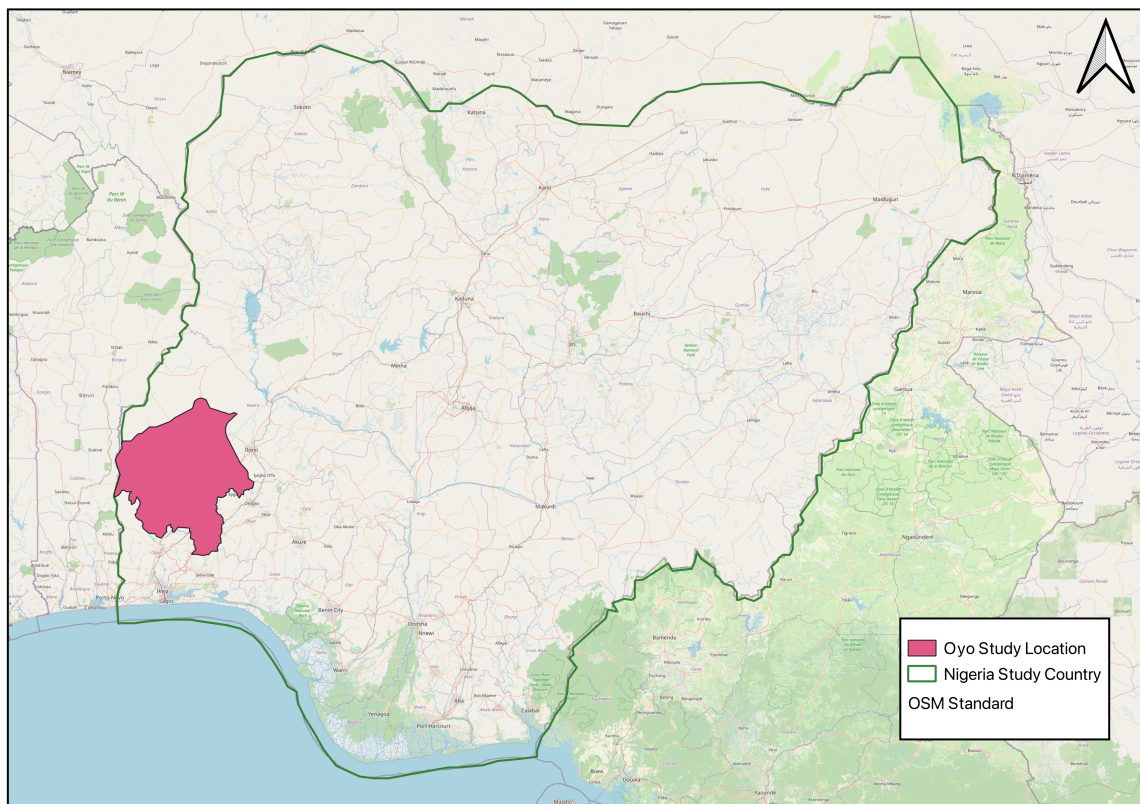
First Location:

Located at Emotan Lane in an open site at the University of Ibadan Central Mosque (UI Mosque), Ibadan, the survey covered an area centered around coordinates 7.44662° N, 3.89960° E, extending across multiple points within the site. This site lies within the southwestern part of Nigeria. This area is characterized by the crystalline basement complex, typical of the region, with significant weathering that could impact foundation stability. Here, 10 Vertical Electrical Soundings (VES) were executed using the Schlumberger electrode configuration, and 3 Constant Separation Traversing (CST) profiles were conducted with the Wenner electrode configuration.

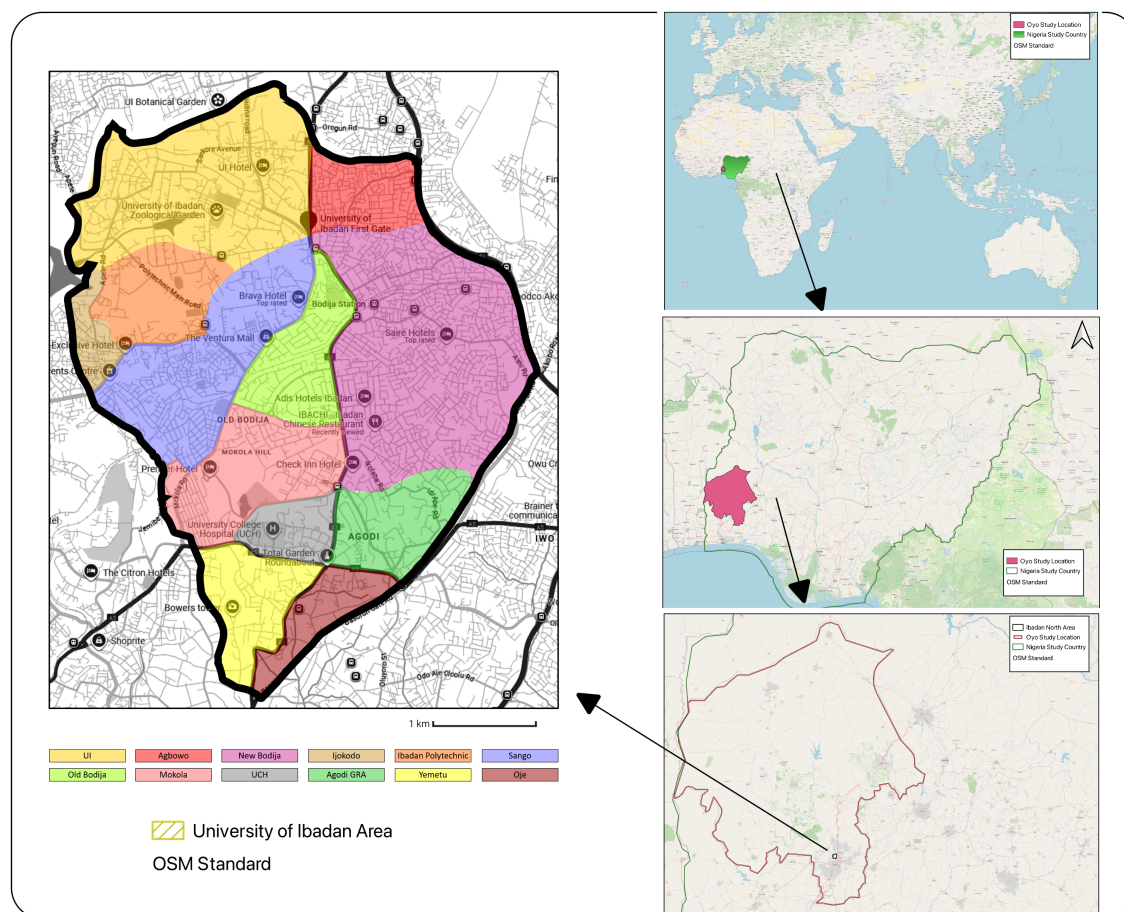
Second Location:

The second investigation site is at Appleton Road in Abubakar Abdulsalam Hall (AAH), University of Ibadan, the survey covered an area centered around coordinates 7.43933° N, 3.89449° E. This location also represents the geological complexity of the area, featuring a mix of basement rocks with potential for varying soil compositions due to its proximity to different geological features. This site was chosen to assess how these conditions affect foundation stability and to understand the variability in soil composition. Here, 10 VES were similarly carried out, and 2 CST profiles were established.

Both areas were selected to provide a comprehensive understanding of the subsurface conditions within the University of Ibadan campus, ensuring the findings can be directly applicable to civil engineering practices in similar geological settings. The precise coordinates of these sites were meticulously recorded to enable accurate geophysical surveying and to facilitate future reference or validation of the study results.



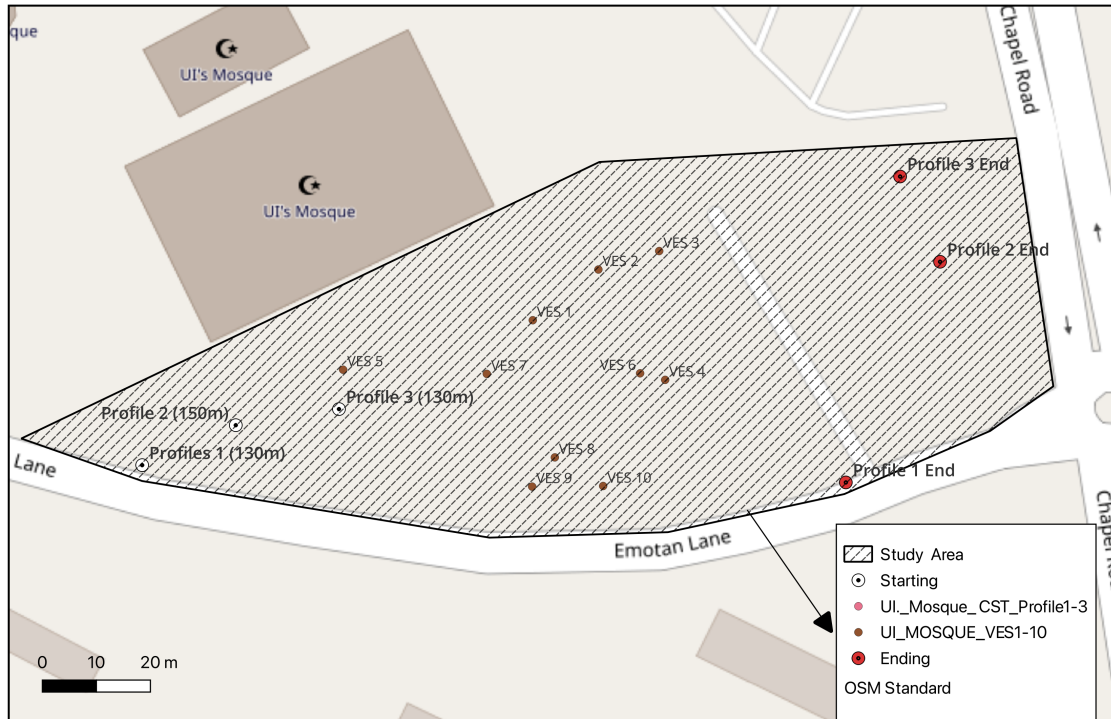
(a) Map showing Oyo State Region from Nigeria Map.



(b) Map of Ibadan North highlighting the University of Ibadan Study Area.

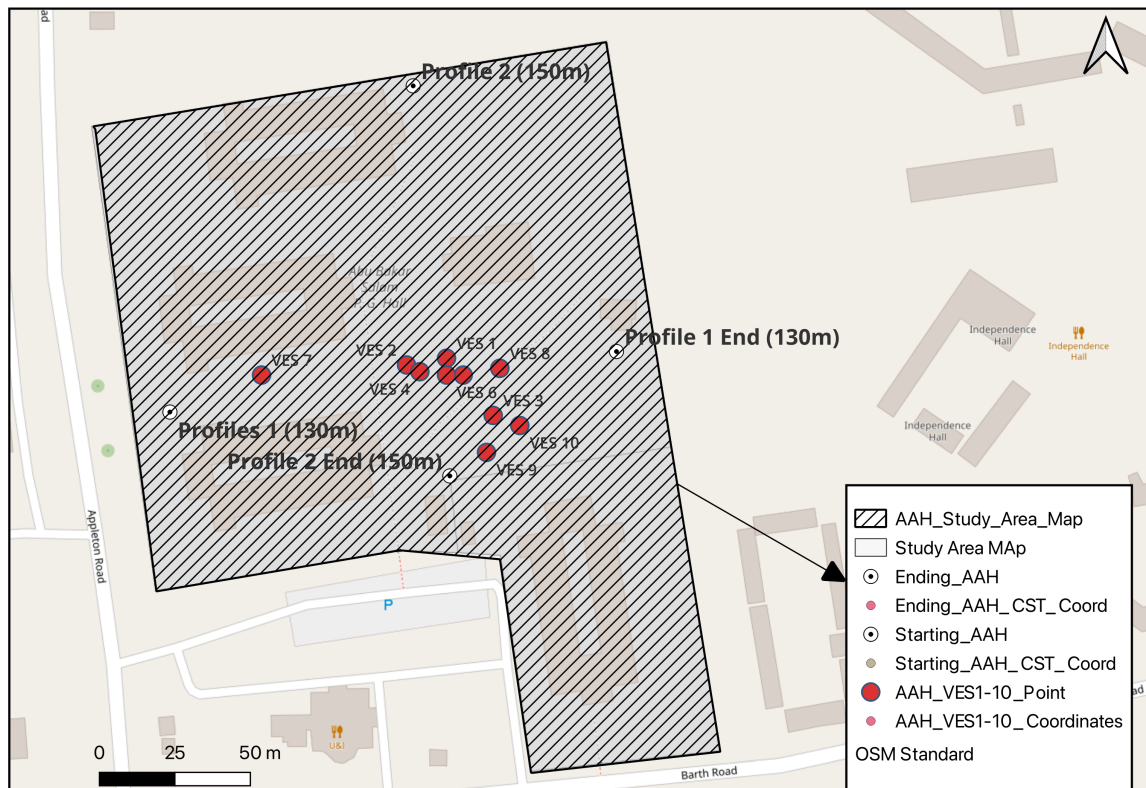
Figure 1.2: Combined maps for the study location and study area generated by QGIS.

UI MOSQUE STUDY AREA



(a) Coordinates: 7.44662° N, 3.89960° E.

ABUBAKAR ABDULSALAM HALL STUDY AREA MAP



(b) Coordinates: 7.43933° N, 3.89449° E.

Figure 1.3: Combined maps for the study areas generated by QGIS.

1.6 Outline of the Thesis

This thesis is organized into five chapters:

- Chapter 1: Introduction, including the aims, objectives, the study location and area including the significance of the study.
- Chapter 2: Literature Review, providing a detailed discussion of previous research, theoretical principles, applications, challenges and the limitations of the study.
- Chapter 3: Materials and Methods of the research and analysis.
- Chapter 4: The results, analysis, combination of VES and CST and further discussion.
- Chapter 5: Summary, Conclusion and Recommendations

References and appendix were also included at the end of the project

CHAPTER 2: LITERATURE REVIEW

2.1 Introduction to Geophysical Methods in Civil Engineering

Geophysical methods are generally non-invasive or non destructive methods long used in the construction industry for investigation of the subsurface. Principally, these are used for the detection of geologic anomalies such as cavities and voids, detection of buried pipes and other utilities, detection of water bearing aquifers for well development, exploitation of quarries and in determining soil stratification or layering. In addition, the methods provide a means for verifying as constructed pavement thicknesses in a continuous unbroken image of the pavement structural configuration or determining rebar embedment and layout non destructively.

The use of Geophysical methods confers advantages as they generally speed up the process of investigation, provide continuous streams of information not otherwise available in discrete sampling or invasive procedures and give advance information on what to expect for a given locality before a more detailed and costly soil exploration is even planned. Thus Geophysical methods are a force multiplier for the engineer and allow the user to identify potential problem areas or target areas even before the start of a detailed Soil Exploration program.

Geophysical methods are not a replacement to a detailed soil exploration program; rather they augment these programs to yield more meaningful and area extensive but more intensive information at the fraction of the time and cost. Geophysical Methods have been around for quite some time. These are non invasive procedures employed in order to determine subsurface soil conditions and geologic anomalies such as cavities and voids or buried objects such as pipelines. Geophysical methods are used for various purposes in Civil Engineering Investigation of the subsurface. The advent of high speed computers and fast signal processors have vastly improved the technology and resulted in increased reliability and signal clarity in the use of these methods.

(Emilio M. et al., 2010) in their Paper titled *Geophysical Methods in Civil Engineering - Practical Applications* presented their local practical experience in the deployment of Geophysical methods and equipment to address and provide solutions to various practical problems where conventional approaches may not give adequate information or may not provide it in a faster or more accurate way. Geophysical methods address the need for more information compared

to conventional borings, these are not substitute to actual soil borings particularly when soil design parameters (strength and compressibility) are needed. However, borings may provide only limited discrete information points or are limited because of budgetary restrictions while Geophysical methods may provide a continuous data stream or even three dimensional images of the desired target of interest. Thus these two methods are complementary and would provide a more meaningful information record when done together or when augmented by each other. These methods are not a substitute for detailed borings except for specific objectives which do not require strength characterization or design strength or compressibility parameters, they can sometimes yield more meaningful results and thus corroborate results of other methods.

2.2 Overview of Geophysical Techniques

Geophysical techniques offer innovative, non-invasive solutions for subsurface investigations, which are crucial in civil engineering projects. These methods provide reliable data on subsurface conditions, enabling engineers to make informed decisions regarding foundation designs, groundwater exploration, and the detection of subsurface anomalies. Among the most prominent techniques are **Ground Penetrating Radar (GPR)**, **Seismic Refraction**, and **Electrical Resistivity Methods**, each with unique principles, applications, and limitations.

2.2.1 Ground Penetrating Radar (GPR)

Ground Penetrating Radar (GPR) is a geophysical method that uses electromagnetic radar pulses to investigate the subsurface. Initially developed for military applications, such as detecting mines and buried weapons, GPR has become an essential tool in civil engineering due to its ability to provide high-resolution, real-time subsurface imaging (**Annan, 2005**).

Principle of Ground Penetrating Radar

GPR operates by transmitting electromagnetic radar impulses into the ground. The radar waves are reflected or absorbed based on the material's stiffness, moisture content, and composition. Reflected signals are captured by a receiving antenna and processed in real time to produce a subsurface image. The depth of investigation is inversely proportional to the radar frequency: higher frequencies provide better resolution at shallow depths, while lower frequencies are used for deeper penetration (**Reynolds, 2011**).

Applications of Ground Penetrating Radar

In a highway construction project, GPR is used to measure pavement thickness to millimeter precision, enabling dispute resolution and ensuring compliance with quality standards. GPR is versatile, with applications including:

- Detection of cavities, voids, and geologic anomalies.
- Locating buried objects, such as pipelines, rebar, and archaeological artifacts.
- Environmental scanning for waste landfill detection.
- Measuring roadway and pavement thickness for quality assurance.
- Structural assessment of concrete to detect embedded objects (**Annan, 2005**).

Inherent Limitations of Ground Penetrating Radar

- Signal attenuation in conductive soils, such as clay, reduces penetration depth.
- The method's resolution decreases with increasing depth.
- Interpretation requires expertise and can be affected by noise and interference (**Reynolds, 2011**).

2.2.2 Seismic Refraction Methods

In a slope stabilization project, seismic refraction identified fault zones and sloping bedrock, enabling engineers to optimize foundation placement and reduce risks of structural failure. Seismic refraction is a method that utilizes shock waves to analyze subsurface structures and material properties. It is particularly effective for investigating stratigraphy and mechanical properties of soils and rocks (**Telford et al., 1990**).

Principle of Seismic Refraction Methods

Shock waves are generated by striking a steel plate with a hammer or using explosives. These waves travel through the ground, refracting and reflecting at material boundaries. Geophones positioned along a linear spread detect these waves, and their arrival times are recorded by a seismograph. The velocity of wave propagation provides insights into the stiffness and composition of subsurface layers (**Reynolds, 2011**).

Applications of Seismic Refraction Methods

- Determining subsurface stratification and soil stiffness.
- Identifying faults, fractures, and cavities.
- Assessing sloping bedrock and geologic anomalies.
- Ensuring foundation stability in construction projects (**Telford et al., 1990**).

Field Procedure of Seismic Refraction Methods

A typical seismic refraction layout, known as a “spread,” involves 12 to 24 geophones. Multiple “shots” are conducted to ensure thorough coverage and accurate detection of subsurface anomalies. Each shot provides detailed data on layer characteristics and velocities (**Reynolds, 2011**).

2.2.3 Electrical Resistivity Methods

Surface electrical resistivity surveying is based on the principle that the distribution of electrical potential in the ground around a current-carrying electrode depends on the electrical resistivities and distribution of the surrounding soils and rocks. The usual practice in the field is to apply an electrical direct current (DC) between two electrodes implanted in the ground and to measure the difference of potential between two additional electrodes that do not carry current. Usually, the potential electrodes are in line between the current electrodes, but in principle, they can be located anywhere. The current used is either direct current, commutated direct current (i.e., a square-wave alternating current), or AC of low frequency (typically about 20 Hz). All analysis and interpretation are done on the basis of direct currents. The distribution of potential can be related theoretically to ground resistivities and their distribution for some simple cases, notably, the case of a horizontally stratified ground and the case of homogeneous masses separated by vertical planes (e.g., a vertical fault with a large throw or a vertical dike). For other kinds of resistivity distributions, interpretation is usually done by qualitative comparison of observed response with that of idealized hypothetical models or on the basis of empirical methods (**Telford et al., 1990**).

Mineral grains comprised of soils and rocks are essentially nonconductive, except in some exotic materials such as metallic ores, so the resistivity of soils and rocks is governed primarily by the amount of pore water, its resistivity, and the arrangement of the pores. To the extent that differences of lithology are accompanied by differences of resistivity, resistivity surveys can be useful in detecting bodies of anomalous materials or in estimating the depths of bedrock surfaces. In coarse, granular soils, the groundwater surface is generally marked by an abrupt change in water saturation and thus by a change of resistivity. In fine-grained soils, however, there may be no such resistivity change coinciding with a piezometric surface. Generally, since the resistivity of a soil or rock is controlled primarily by the pore water conditions, there are wide ranges in resistivity for any particular soil or rock type, and resistivity values cannot be directly interpreted in terms of soil type or lithology. Commonly, however, zones of distinctive resistivity can be associated with specific soil or rock units on the basis of local field or drill hole information, and resistivity surveys can be used profitably to extend field investigations into areas with very limited or nonexistent data. Also, resistivity surveys may be used as a reconnaissance method, to detect anomalies that can be further investigated by complementary geophysical methods and/or drill holes (**Binley, 2015**).

The electrical resistivity method has some inherent limitations that affect the resolution and accuracy that may be expected from it. Like all methods using measurements of a potential

field, the value of a measurement obtained at any location represents a weighted average of the effects produced over a large volume of material, with the nearby portions contributing most heavily. This tends to produce smooth curves, which do not lend themselves to high resolution for interpretations. Another feature common to all potential field geophysical methods is that a particular distribution of potential at the ground surface does not generally have a unique interpretation. Although these limitations should be recognized, the non-uniqueness or ambiguity of the resistivity method is scarcely less than with the other geophysical methods. For these reasons, it is always advisable to use several complementary geophysical methods in an integrated exploration program rather than relying on a single exploration method. A single resistivity measurement requires four electrodes coupled to the ground and provides the apparent resistivity of the materials located between the potential electrodes. These surveys typically utilize multiple electrode pairs arranged in various configurations (i.e., spatial geometries), chosen based on site parameters and survey objectives (**Binley, 2015**).

2.3 Theoretical Background of Electrical Resistivity Methods

2.3.1 General Principles of Electrical Resistivity Methods

The principle of electrical resistivity is based on Ohm's Law, which relates the flow of electric current through a material to its resistivity. Subsurface materials exhibit varying resistivity based on their composition, moisture content, and porosity. Conductive materials such as clays and water-saturated zones show low resistivity, while compact, dry rocks display high resistivity values. This variation allows for the characterization of subsurface layers.

Principle of Resistivity

Ohm's Law relates voltage (V), current (I), and resistance (R) through the equation:

$$R = \frac{V}{I} \quad (2.1)$$

In the context of subsurface investigations, resistivity (ρ) is calculated by considering the geometric dimensions of the material:

$$\rho = R \frac{A}{L} \quad (2.2)$$

where:

- ρ = Resistivity of the material ($\Omega \cdot m$),
- R = Measured resistance (Ω),
- A = Cross-sectional area of the material (m^2),
- L = Length of the material (m).

Key Concept:

Conductive materials like clays and water-saturated zones have low resistivity, while dry, compact rocks and non-porous materials exhibit high resistivity. This contrast enables the detection of geological features such as aquifers, fractures, and stratigraphic boundaries.

2.3.2 Electric Current Flow in Subsurface Materials

When an electric current is introduced into the subsurface, it spreads radially through the soil or rock. The current's behavior depends on the material's resistivity, with high-resistivity materials offering greater resistance to current flow and low-resistivity materials allowing easier passage. The electric field generated by the current is measured using potential electrodes.

Equation for Current Density:

$$J = \sigma E \quad (2.3)$$

where:

- J = Current density (A/m^2),
- σ = Electrical conductivity ($1/\rho, S/m$),
- E = Electric field intensity (V/m).

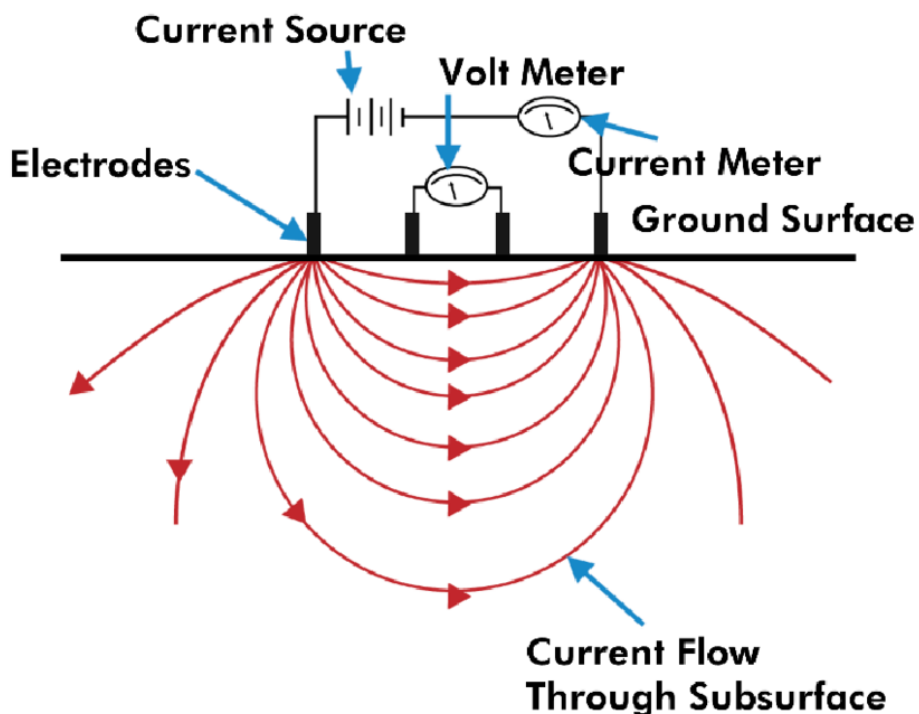


Figure 2.1: Diagram illustrating electrical current flow through subsurface [Pearson *et al.*, 2023]

2.3.3 Electrical Field and Potential

When current is injected into the subsurface, it creates an electrical field. The potential difference (ΔV) measured across two points is influenced by the resistivity of the intervening materials. Equipotential lines and current flow lines provide a visual representation of how the electrical field is distributed within the subsurface, aiding in the interpretation of resistivity data (**Telford et al., 1990**). Coulomb established that the force of attraction or repulsion between two charged spheres is proportional to the product of the individual electric fields and inversely proportional to the square of the distance between the centers of the spheres. The electric field of a charge is a force \mathbf{F} exerted on another unit charge using Coulomb's law (**Reynolds, 2011**).

The force \mathbf{F} is given by:

$$\mathbf{F} \propto \frac{q_1 q_2}{r^2} \quad (2.4)$$

Introducing the constant of proportionality k_e , the equation becomes:

$$\mathbf{F} = k_e \frac{q_1 q_2}{r^2} \quad (2.5)$$

where:

- \mathbf{F} is the force between the charges (in newtons, N),
- k_e is Coulomb's constant, approximately $8.987 \times 10^9 \text{ N} \cdot \text{m}^2 \cdot \text{C}^{-2}$,
- q_1 and q_2 are the magnitudes of the charges (in coulombs, C),
- r is the distance between the charges (in meters, m).

The electric field (\mathbf{E}) at a point in space is defined as the force (\mathbf{F}) per unit charge (q):

$$\mathbf{E} = \frac{\mathbf{F}}{q} = k_e \frac{q}{r^2} \quad (2.6)$$

This equation indicates that the electric field is radially outward for a positive charge and radially inward for a negative charge (**Reynolds, 2011**).

Derivation of Electric Potential Formula

Electric potential (V) at a point is defined as the work done in bringing a unit positive charge from infinity to that point in an electric field. The relationship between electric potential and the electric field is given by:

$$V = - \int \mathbf{E} \cdot d\mathbf{r} \quad (2.7)$$

Substituting $\mathbf{E} = k_e \frac{q}{r^2}$ into the equation:

$$V = - \int_{r_0}^r \left(k_e \frac{q}{r^2} \right) dr \quad (2.8)$$

Evaluating the integral:

$$V = -k_e q \int_{r_0}^r \frac{1}{r^2} dr \quad (2.9)$$

$$V = -k_e q \left[-\frac{1}{r} \right]_{r_0}^r \quad (2.10)$$

$$V = k_e q \left(\frac{1}{r_0} - \frac{1}{r} \right) \quad (2.11)$$

For simplicity, when $r_0 = \infty$, the potential at infinity is considered zero, and the equation becomes:

$$V = k_e \frac{q}{r} \quad (2.12)$$

This equation shows that the electric potential at a distance r from a charge q is directly proportional to the charge and inversely proportional to the distance (Reynolds, 2011).

Application to Resistivity Surveys

In resistivity surveys, the potential difference (ΔV) between two points on the subsurface is measured, and the apparent resistivity (ρ_a) is calculated. This potential difference is influenced by the distribution of current flow lines and equipotential surfaces, which vary based on subsurface resistivity (Telford *et al.*, 1990).

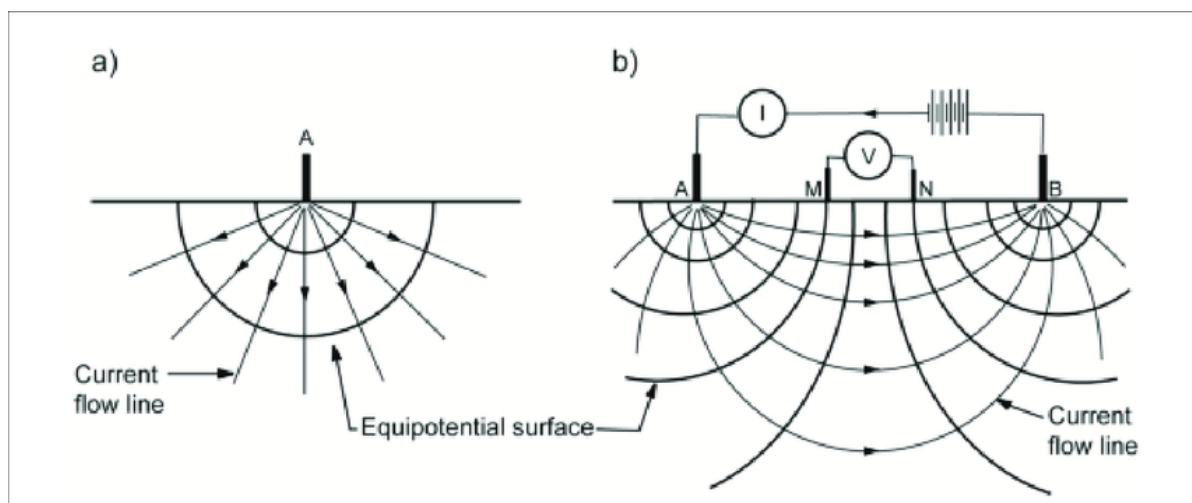


Figure 2.2: Diagram illustrating electrical field with equipotential and current flow lines [Jamaluddin *et al.*, 2019]

2.3.4 Apparent Resistivity

Data from resistivity surveys are customarily presented and interpreted in the form of values of apparent resistivity ρ_a . Apparent resistivity is defined as the resistivity of an electrically homogeneous and isotropic half-space that would yield the measured relationship between the applied current and the potential difference for a particular arrangement and spacing of electrodes. Wherever these measurements are made over a real heterogeneous earth, as distinguished from the fictitious homogeneous half-space, the symbol ρ is replaced by ρ_a for apparent resistivity.

Apparent resistivity is the bulk resistivity value obtained from field measurements. It is calculated using:

$$\rho_a = K \frac{\Delta V}{I} \quad (2.13)$$

where:

- ρ_a = Apparent Resistivity (Ωm),
- ΔV = Measured Potential Difference (V),
- I = The Injected current (A).

Apparent resistivity is interpreted to estimate true resistivity, accounting for geological and geometric influences. Understanding apparent resistivity is crucial for interpreting field data and creating subsurface models.

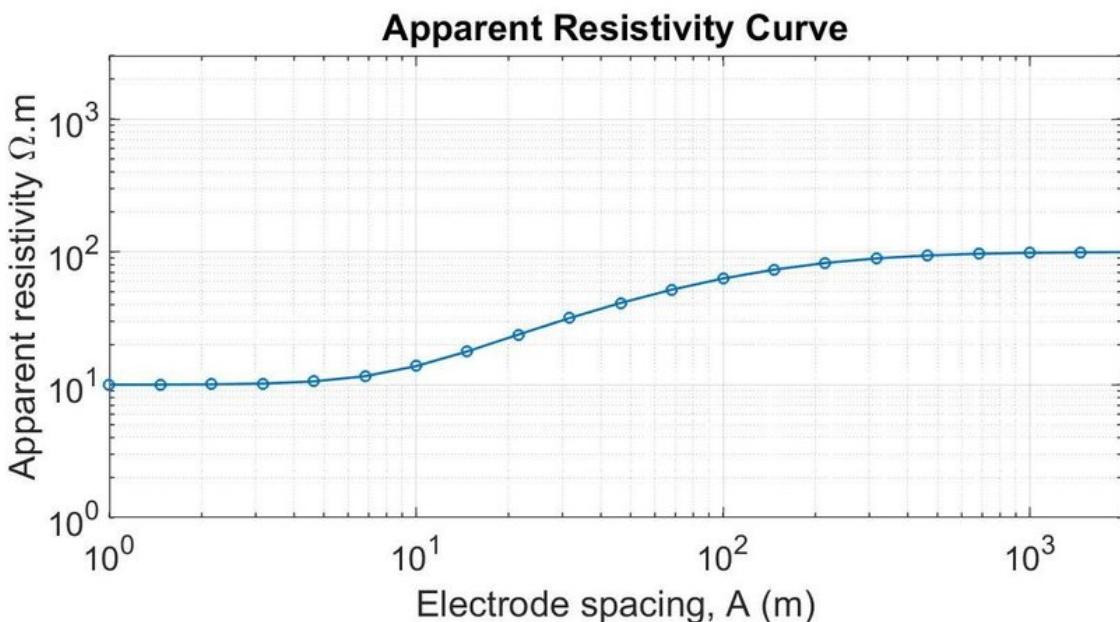


Figure 2.3: Graph showing an apparent resistivity curve for a typical VES survey [Sanuade *et al.*, 2019]

2.3.5 The General Four Electrode System

The four-electrode system is a standard configuration for resistivity surveys, comprising two current electrodes (A and B) and two potential electrodes (M and N). This setup minimizes contact resistance effects and ensures accurate measurements. The purpose is to measure the electrical resistivity of materials or earth layers by eliminating contact resistance between the electrodes and the material (**Binley, 2015**).

Consider an arrangement consisting of a pair of current electrodes and a pair of potential electrodes. The current electrodes A and B act as source and sink, respectively. At the detection electrode C, the potential due to the source A is:

$$\phi_C = \frac{\rho I}{2\pi} \left(\frac{1}{r_{AC}} - \frac{1}{r_{CB}} \right) \quad (2.14)$$

Similarly, the resultant potential at D is:

$$\phi_D = \frac{\rho I}{2\pi} \left(\frac{1}{r_{AD}} - \frac{1}{r_{DB}} \right) \quad (2.15)$$

The potential difference measured by a voltmeter connected between C and D is:

$$\phi = \frac{\rho I}{2\pi} \left\{ \left(\frac{1}{r_{AC}} - \frac{1}{r_{CB}} \right) - \left(\frac{1}{r_{AD}} - \frac{1}{r_{DB}} \right) \right\} \quad (2.16)$$

All quantities in this equation can be measured at the ground surface except the resistivity, which is given by:

$$\rho_a = 2\pi \frac{\phi}{I} \left\{ \frac{1}{\left(\frac{1}{r_{AC}} - \frac{1}{r_{CB}} \right) - \left(\frac{1}{r_{AD}} - \frac{1}{r_{DB}} \right)} \right\} \quad (2.17)$$

This resistivity is known as apparent resistivity, which is equivalent to the true resistivity only when the latter is uniform throughout the subsurface. Otherwise, it must be looked upon as the most convenient way to represent the resistivity in the subsurface based on surface measurements. If the electrodes are laid out along a line and their separations are increased systematically, the change in apparent resistivity (as defined in Equation (6)) with electrode spacing makes it possible to determine the variation of resistivity with depth, within limits of precision that depend on the subsurface layering configuration (**Telford *et al.*, 1990**).

2.3.6 Electrode Configuration

Electrode configuration (electrode array) A geometrical pattern of electrodes used in electrical sounding, constant-separation traversing, and induced polarization surveys. Usual configurations comprise two current electrodes and two potential electrodes whose separations are known and

defined by a geometric factor. Common configurations include the Schlumberger arrays, Wenner arrays and dipole-dipole (**Loke, 2004**).

Schlumberger Array:

Ideal for vertical profiling and depth estimation and commonly used in **Vertical Electrical Sounding (VES)** Surveying. For this array, in the limit as a approaches zero, the quantity V/a approaches the value of the potential gradient at the midpoint of the array. In practice, the sensitivity of the instruments limits the ratio of s to a and usually keeps it within the limits of about 3 to 30. Therefore, it is typical practice to use a finite electrode spacing. The apparent resistivity (ρ_a) is:

$$\rho_a = \pi a \left[\frac{s^2}{a} - \frac{a}{4} \right] \frac{V}{I} = \pi a \left[\left(\frac{s}{a} \right)^2 - \frac{1}{4} \right] \frac{V}{I}, \quad (2.18)$$

Wenner Array:

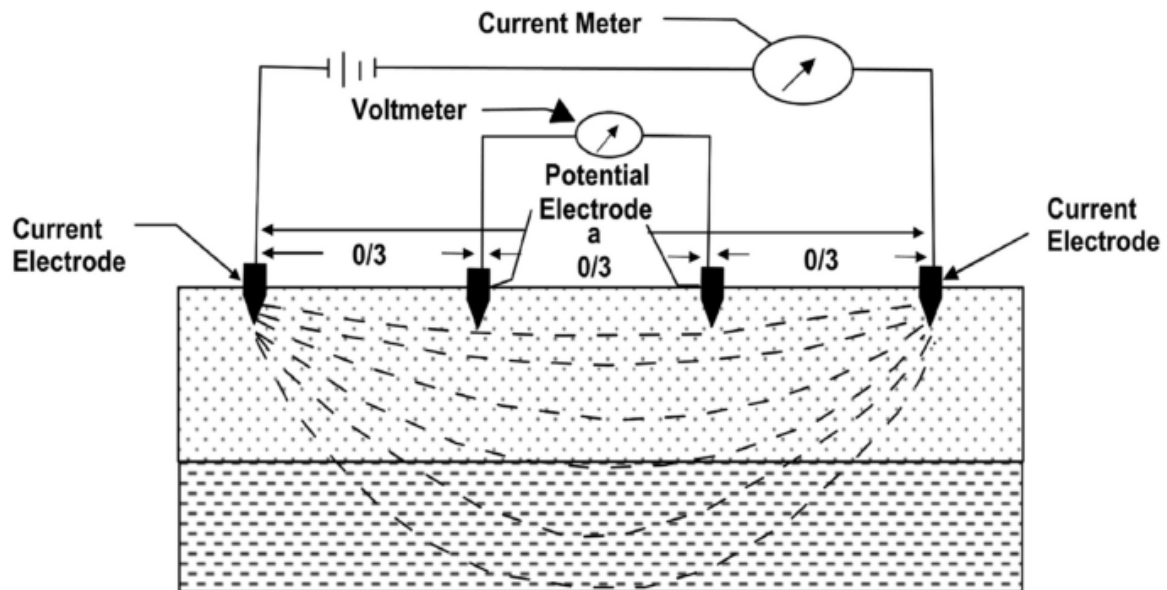
This is suitable for horizontal profiling with uniform sensitivity and commonly used in **Constant Separation Traversing (CST)** Surveying. This array consists of four electrodes in line, separated by equal intervals, denoted a . After derivation, the user will find that the geometric factor K is equal to a , so the apparent resistivity is given by:

$$\rho_a = \pi a \left[\frac{s^2}{a} - \frac{a}{4} \right] \frac{V}{I} = \pi a \left[\left(\frac{s}{a} \right)^2 - \frac{1}{4} \right] \frac{V}{I}, \quad (2.19)$$

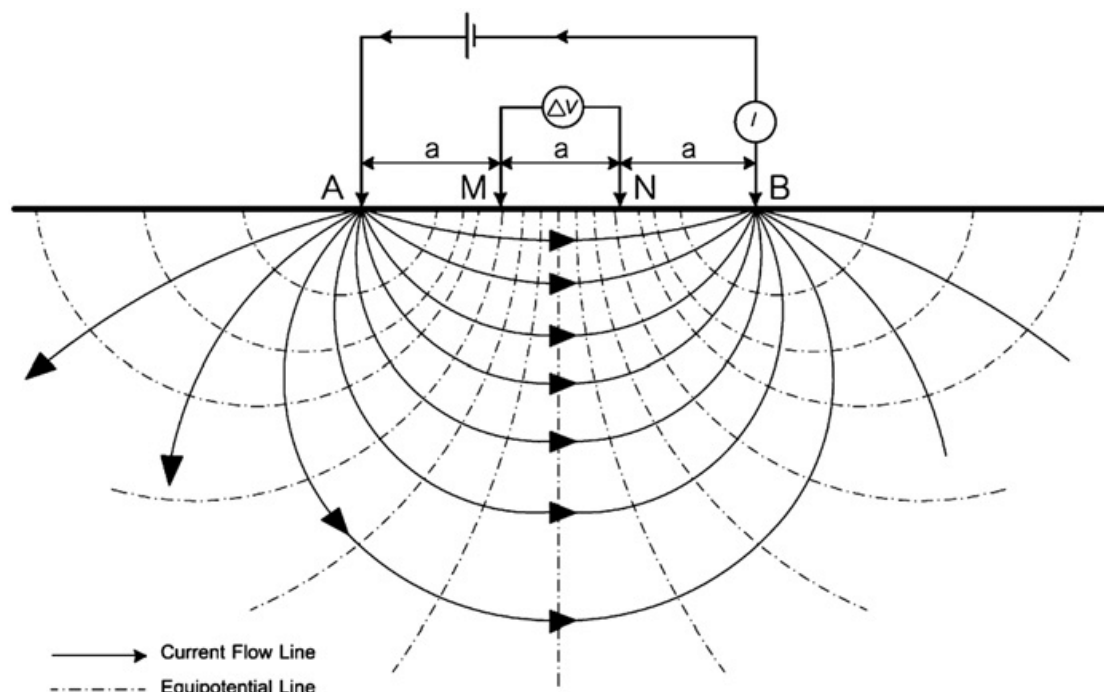
Dipole-Dipole Array:

It provides high-resolution imaging for lateral changes. The dipole-dipole array is one member of a family of arrays using dipoles (closely spaced electrode pairs) to measure the curvature of the potential field. If the separation between both pairs of electrodes is the same a , and the separation between the centers of the dipoles is restricted to $a(n+1)$, the apparent resistivity is given by:

$$\rho_a = \pi a n(n+1)(n+2) \frac{V}{I}, \quad (2.20)$$



(a) Schematic diagram of the Schlumberger array electrode configuration [Afuwai *et al.*, 2019]



(b) Schematic diagram of the Wenner array electrode configuration [Wiwattanachang *et al.*, 2011]

Figure 2.4: Comparison of the Schlumberger and Wenner array electrode configurations

2.4 Resistivity Surveying Techniques

2.4.1 Resistivity Surveying

Resistivity surveying is a geophysical method used to explore and characterize the subsurface by measuring the electrical properties of the ground. This technique is particularly valuable for mapping various geological features such as stratigraphy, fractures, faults, and groundwater zones. By injecting electrical current into the ground and measuring the resulting potential differences, resistivity surveying provides insights into the distribution of materials with different electrical resistivities beneath the Earth's surface. These measurements are crucial for a variety of applications including environmental studies, engineering projects, archaeological investigations, and hydrogeological assessments.

The principle behind resistivity surveying is based on the fact that different materials, like clay, sand, rock, or water, have distinct electrical resistivities. For instance, water-saturated zones typically have lower resistivity due to the conductive nature of dissolved salts, whereas dry, compact rocks might show higher resistivity. By interpreting these resistivity variations, geophysicists can infer the presence of different subsurface layers or structures.

(GEOLOGYSCIENCE)

Steps for carrying out Resistivity Surveying:

1. **Planning the Survey:** Before setting up, a detailed plan is created considering the survey objectives, the area's geology, and any known subsurface features. This includes choosing the appropriate electrode configuration (like Wenner, Schlumberger, or Dipole-Dipole arrays) based on the depth and resolution required. (**Loke, M.H. 2011**)
2. **Set Up Electrodes Along the Survey Line:** Electrodes are strategically placed along a predetermined line or grid pattern. The spacing between electrodes can vary depending on the desired resolution and depth of investigation. For deep surveys, wider spacing might be used, while for shallow investigations, closer spacing is preferred. (**archive.epa.gov**)
3. **Inject Current Using an External Source:** An external power source, typically a battery or generator, is used to inject a known current into the ground through two current electrodes. The choice of current magnitude is important as it should be sufficient to produce measurable potential differences without causing electrode polarization or overheating. (**epa.gov**)
4. **Measure Potential Differences at Specific Electrode Configurations:** Using two potential electrodes, the voltage difference resulting from the current flow is measured. This step is repeated at various configurations or along the survey line to gather comprehensive data. Modern resistivity meters automate this process, ensuring precision in measurements. (**archive.epa.gov**)

5. Calculate Apparent Resistivity and Analyze Results: The apparent resistivity is calculated using formulas that incorporate the measured potential difference, the injected current, and the geometric factor of the electrode array. This apparent resistivity might not directly represent the true resistivity due to the complex nature of subsurface materials but provides a basis for interpretation. (**Loke, M.H. 2011**)

- *Data Processing:* Collected data is processed to remove noise, correct for any systematic errors, and sometimes to transform the data into a more interpretable form like 2D or 3D resistivity models.
- *Interpretation:* Geophysical software or manual interpretation methods are used to analyze the resistivity data. This step involves correlating resistivity values with known geological properties, which might require integration with other geophysical or geological data.
- *Validation:* Often, the results are validated through drilling or other direct methods to confirm the presence of predicted features like aquifers or fault lines.

2.4.2 Vertical Electrical Sounding

The vertical electrical sounding or geoelectric method is one of the most used electrical geophysical techniques thanks to its simplicity and relative low cost. These are especially useful in hydrogeological studies where it is necessary to define and characterize deep phreatic levels. Vertical electrical sounding or SEV are a geophysical technique that, by means of electricity, allows recognizing or distinguishing the different geological formations that are found in depth and delimiting them. Electrical or electromagnetic geophysical techniques are based on measuring the resistivity of materials or conductivity. (**EGSCIENCES**)

Vertical Electrical Sounding (VES) is one-dimensional direct current electrical resistivity method, which consists of introducing a continuous electrical current of known intensity into the ground through two or more emitting electrodes, commonly called A and B, and measuring the electric potential difference using another pair of receiving electrodes, M and N, in this way it is possible to obtain the induced potential and the vertical distribution of the resistivities of the traversed formations. Using this method, the depth of study is directly proportional to the distance between the current electrodes and/or the potential electrodes used, so that the greater the separation distance between the electrodes, the greater the depth of the soil to be studied, while a spacing between the electrodes will measure the resistivity distribution in the subsurface at shallower depths. In this method, the results are compared with the common resistivities of the different materials, which allows them to be differentiated from each other. (**EGSCIENCES**)

The current injection electrodes A and B, and the potential measurement electrodes M and N, are arranged aligned in a certain structure, for this different configurations called “electrode device” are used, some of the most used are the Schlumberger configuration , Wenner and Dipole-Dipole. (**EGSCIENCES**)

2.4.3 Constant Separation Traversing

The object of electric horizontal profiling or combined Traversing approach is to detect the lateral variations in the resistivity of the ground. In Schlumberger method of electrical profiling, the current electrodes (AB) remains fixed at a relatively large distance, for instance, a few hundred meters, and the potential electrodes (MN) with a small constant separation (**Sharma 1986**).

The appearance of the resistivity profile obtained by horizontal profiling will depend not only on the positions of the potential electrodes M and N, but also on the positions of the current electrodes A and B with respect to the inhomogeneities in the earth and the reason behind that is that all electrodes are moved after each measurement (**Kunetz, 1966**).

The effect of vertical structures e.g. (faults, fissures, dikes, veins, and shear zones) is lateral. If these features crop out, abrupt discontinuities in the slope of (ρ_a) curves are obtained as the mobile electrode configuration crosses the vertical resistivity boundary. Many of key features found in the resistivity anomalies over a vertical fault are found also in anomalies over near vertical structures. The fault represents a vertical contact problem between two media of differing resistivity. Therefore, the calculated curves for (ρ_a) are discontinuous at the vertical boundary. The discontinuity will be evident in practice as a steep gradient in the resistivity curve (**Sharma, 1986**).

The traversing obtained by moving an electrode spread with fixed electrode separation along a traverse line, the array of electrodes being aligned either in the direction of the traverse (longitudinal traverse) or at right angles to it (transverse traverse). The former technique is more efficient as only a single electrode has to be moved from one end of the spread to the other, and the electrodes reconnected, between adjacent readings. The Vertical discontinuity distorts the direction of current flow and thus the overall distribution of potential in its vicinity.

2.4.4 Comparison of VES and CST

Aspect	VES (Vertical Electrical Sounding)	CST (Constant Separation Traversing)
Application	Used for determining vertical variations in subsurface resistivity, often for geological or hydrological studies.	Used for mapping horizontal variations in subsurface resistivity over a specific area.
Field Survey	Involves inserting electrodes into the ground at different depths along a vertical profile to measure resistivity changes with depth.	Electrodes are placed at a constant separation, and measurements are taken as the array is moved horizontally across the survey area.
Cost	Costs include equipment, labor for setting up electrodes at various depths, and data analysis.	Similar costs but potentially less labor-intensive as electrode setup is simpler with fixed separation.
Formula	Resistivity is calculated using formulas like $\rho_a = \pi a \left[\frac{s^2}{a} - \frac{a}{4} \right] \frac{V}{I}$.	Similar resistivity formulas but applied in a horizontal context, often using a Wenner or Schlumberger array configuration.
Purpose	To provide a vertical profile of resistivity, useful for identifying depth to bedrock, water table, or different soil layers.	To provide a horizontal map of resistivity, useful for detecting lateral changes like faults, buried structures, or contaminant plumes.
Advantages	Offers detailed information on vertical resistivity changes, which can be critical for depth-specific investigations.	Efficient for covering large areas to identify lateral resistivity variations, providing a broader spatial understanding.
Challenges	Requires precise depth control and can be influenced by surface conditions; time-consuming for deep profiling.	Less detailed in vertical resolution, and lateral resolution depends on electrode spacing; can be affected by surface irregularities.

2.5 Previous Studies on Electrical Resistivity

2.5.1 Previous Studies in Nigeria

Several authors have contributed to the application of electrical resistivity methods in civil engineering investigations. **Akintoye *et al.*, (2018)** investigated the subsurface conditions of an unstable slope in southwestern Nigeria using the electrical resistivity method. The study employed the Schlumberger configuration to delineate weak zones and fractures, revealing that high resistivity anomalies correspond to compact lithological units, while low resistivity zones indicate water-saturated regions. The results were used to recommend appropriate foundation designs for slope stabilization. **Adeyemi and Bello (2020)** conducted a geophysical evaluation of construction sites in Lagos, Nigeria, to identify potential risks associated with heterogeneous subsurface layers. Using Vertical Electrical Sounding (VES), the authors mapped lithological variations and identified zones of high porosity and low bearing capacity. The findings highlighted the importance of resistivity surveys in mitigating structural failures. **Olayemi *et al.*, (2021)** applied electrical resistivity tomography (ERT) to assess subsurface integrity for a proposed bridge site. The study identified a highly fractured zone beneath the surface, which could pose a risk to structural stability. The authors recommended relocating the foundation to a more stable area, emphasizing the reliability of ERT in civil engineering applications. **James and Olatunji (2019)** focused on the use of geophysics for groundwater exploration in arid regions. Though primarily aimed at water resource management, their work demonstrated the potential of resistivity methods in identifying zones with sufficient bearing capacity for construction purposes.

2.5.2 Comparison of Methods

Various configurations have been used in resistivity surveys, including Schlumberger, Wenner, and Dipole-Dipole arrays. **(Eze *et al.*, 2017)** compared these methods for subsurface investigations and found that the Schlumberger array is more effective for deep-layer detection, while the Wenner array provides better horizontal resolution. Their research underscores the need to select an appropriate configuration based on site-specific requirements. **(Telford *et al.*, 1990)** further elaborated on the principles of resistivity methods, offering insights into how the Wenner array can be adapted for high-resolution near-surface investigations. This is a seminal text that discusses various resistivity techniques and provides a detailed analysis of their applications in subsurface investigations. The authors emphasized that while the Schlumberger configuration excels in depth penetration, the Wenner method remains superior for detailed mapping of near-surface anomalies.

(Reynolds 2011) provides a comprehensive guide on geophysical methods used in engineering, including electrical resistivity. He discusses how resistivity surveys are instrumental in civil engineering projects, especially in urban areas where the variability of subsurface properties poses significant challenges.

2.6 Applications of Electrical Resistivity

2.6.1 Innovative Applications of Electrical Resistivity

In recent years, there has been an increasing application of electrical resistivity methods in more complex subsurface investigations. **Steeple and Chilton (2001)** focused on the use of resistivity in mapping groundwater contamination in urban areas. They highlighted how advanced electrical resistivity tomography (ERT) can help locate pollution plumes in aquifers, enabling more efficient management of groundwater resources, this underscores the growing versatility of resistivity methods in addressing both environmental and engineering concerns.

Loke (2016) provides a detailed exploration of the technological advancements in resistivity methods. He describes new developments in data acquisition systems, such as multi-electrode arrays, that have made resistivity surveys faster and more accurate. This book serves as a crucial resource for understanding the technical evolution of electrical resistivity methods and their broader application in modern engineering and environmental investigations.

2.6.2 Applications in Structural Health Monitoring

Electrical resistivity methods have also been explored for monitoring the health of structures over time. **Bermúdez *et al.*, (2020)** demonstrated how electrical resistivity tomography can be employed to monitor the condition of reinforced concrete structures, detecting early signs of deterioration such as corrosion. Their study showed how resistivity surveys could be used for the non-destructive testing of infrastructure, offering a sustainable and cost-effective alternative to traditional inspection methods. **Caldwell and Brown (2004)** conducted a study on the application of resistivity imaging for the monitoring of railway tracks. Their work showed that electrical resistivity could be used to detect subtle shifts in the ground around the tracks, which could indicate potential risks like landslides or subsidence. Their findings suggest that resistivity surveys can play a critical role in maintaining the integrity of transport infrastructure, especially in areas prone to natural disasters.

2.6.3 Applications in Building Foundation

Falae (2014) carried out a geophysical survey using Vertical Electrical Sounding (VES) at Ibese Southwestern Nigeria to determine the geophysical parameters that can be used to evaluate the structural competence of the subsurface geological characteristics of the site for construction purposes and building development. The Schlumberger configuration was used for the data acquisition. One-dimensional numerical inversion of individual DC resistivity was used to enhance the processing of the results for better achievement of the aim of the study. Models obtained from the 2D inversion of each VES were used for construction of geo-electric sections which exhibit the main geo-electric characteristics of the geological units present in the area.

2.7 Importance of Subsurface Evaluation for Foundation Design

Subsurface evaluation is a critical aspect of civil engineering, particularly in foundation design, as the stability, safety, and longevity of structures heavily depend on the underlying ground conditions. Inadequate knowledge of subsurface characteristics often leads to construction challenges, foundation failures, and increased project costs.

2.7.1 Understanding Subsurface Conditions:

The subsurface environment is inherently heterogeneous, comprising varying soil types, rock layers, and groundwater conditions. Evaluating these factors provides insights into:

- **Soil Properties:** Characteristics such as density, cohesion, and angle of internal friction influence a soil's load-bearing capacity and compressibility.
- **Rock Layers:** The depth and quality of bedrock can affect the choice of foundation type and its depth.
- **Groundwater Table:** The presence of groundwater impacts soil strength and stability, making its identification crucial for waterproofing and structural integrity.

2.7.2 Benefits of Subsurface Evaluation:

- **Foundation Stability:** Subsurface evaluation ensures that the chosen foundation type is compatible with site-specific conditions, reducing the risk of settlement or failure.
- **Cost Efficiency:** Early identification of subsurface issues prevents unforeseen complications during construction, minimizing delays and cost overruns.
- **Environmental Safety:** Identifying geological hazards such as faults or contaminated soils mitigates risks to the structure and surrounding environment.
- **Design Optimization:** Provides engineers with critical data for designing efficient and durable foundations tailored to site-specific conditions.

2.7.3 Case Studies in Foundation Design:

Several studies have demonstrated the importance of subsurface evaluation including **Akintoye et al., (2018)** used seismic refraction to detect weak zones in an unstable slope, enabling optimized foundation design for slope stabilization. **Adeyemi and Bello (2020)** applied Vertical Electrical Sounding (VES) to map lithological variations in Lagos, Nigeria, identifying zones of low bearing

capacity and mitigating risks of structural failure. **Olayemi *et al.*, (2021)** employed electrical resistivity tomography (ERT) to identify a fractured zone beneath a proposed bridge site, leading to the relocation of the foundation for safety.

2.7.4 Relevance to Sustainable Construction:

Subsurface evaluation aligns with sustainable construction practices by:

- Minimizing material wastage through accurate design.
- Reducing the environmental impact of construction failures.
- Enhancing the resilience of structures against natural hazards.

CHAPTER 3: MATERIALS AND METHODS

3.1 Introduction

This chapter outlines the geophysical investigation, materials, equipment, and methodologies employed in the geophysical evaluation of subsurface layers for civil engineering foundation design using electrical resistivity methods. The methods described here focus on Vertical Electrical Sounding (VES) and Constant Separation Traversing (CST), which were selected for their effectiveness in capturing vertical and lateral variations in subsurface resistivity. This chapter also discusses survey design, data acquisition, processing, interpretation, precautions, and limitations encountered during the study.

3.2 Geophysical Investigation

In this project work, the geophysical survey was carried out using Vertical Electrical Sounding (VES) with the Schlumberger array electrode configuration and Constant Separation Traversing (CST) with the Wenner array electrode configuration. A total of **20 VES** profiles and **5 CST** profiles were conducted. The coordinates of the points in the selected area were taken, and the results were collated. The electrical resistivity method involves injecting current into the ground and measuring the resulting potential difference to determine subsurface resistivity variations. These variations help delineate different geological layers, assess lithological properties, and detect fractures or faults.

3.3 Geophysical Survey Materials and Equipment

The success of a geophysical survey depends on the appropriate selection and utilization of specialized materials and equipment. The following tools were employed:

- **Resistivity Meter:** The core device used to inject current into the ground and measure the resulting potential difference. A digital resistivity meter (e.g., ABEM Terrameter) shown in

fig 3.1 was utilized for precise and reliable measurements.

- **Steel Metal Electrodes:** Used as current and potential electrodes for injecting current into the ground and measuring potential differences. Electrodes were securely inserted into the soil to ensure good contact.
- **Connecting Wire Cables:** Insulated cables connected the resistivity meter to the electrodes, ensuring stable current flow and accurate measurements.
- **Measuring Tape:** Used to measure and maintain accurate spacing between electrodes according to the selected configuration.
- **Hammer:** Assisted in driving electrodes into hard or compact ground surfaces.
- **Clips:** Metal clips were used to secure the cables to the electrodes and maintain strong connections.
- **Compass:** Used to align survey lines and ensure consistent electrode orientation relative to the site layout.
- **Global Positioning System (GPS):** Employed to accurately record the geographical coordinates of each survey station.
- **Data Recording Materials:** Included field notebooks, data sheets, and digital storage devices for logging measurements and observations.



Figure 3.1: The Resistivity Meter used for the Survey.

3.4 Methodology

3.4.1 Survey Design

- **Selection of Electrode Configurations:** Two configurations were selected to address different investigation goals:

- **Schlumberger Configuration:**

This configuration was chosen for VES due to its ability to penetrate deeper into the subsurface by gradually increasing the current electrode spacing. It provides detailed depth-specific resistivity data and is cost-effective for deep investigations.

- **Wenner Configuration:**

This configuration was employed for CST as it is sensitive to lateral variations in resistivity, making it ideal for detecting horizontal changes in subsurface layers. Its simplicity in setup allows for rapid data acquisition over large areas.

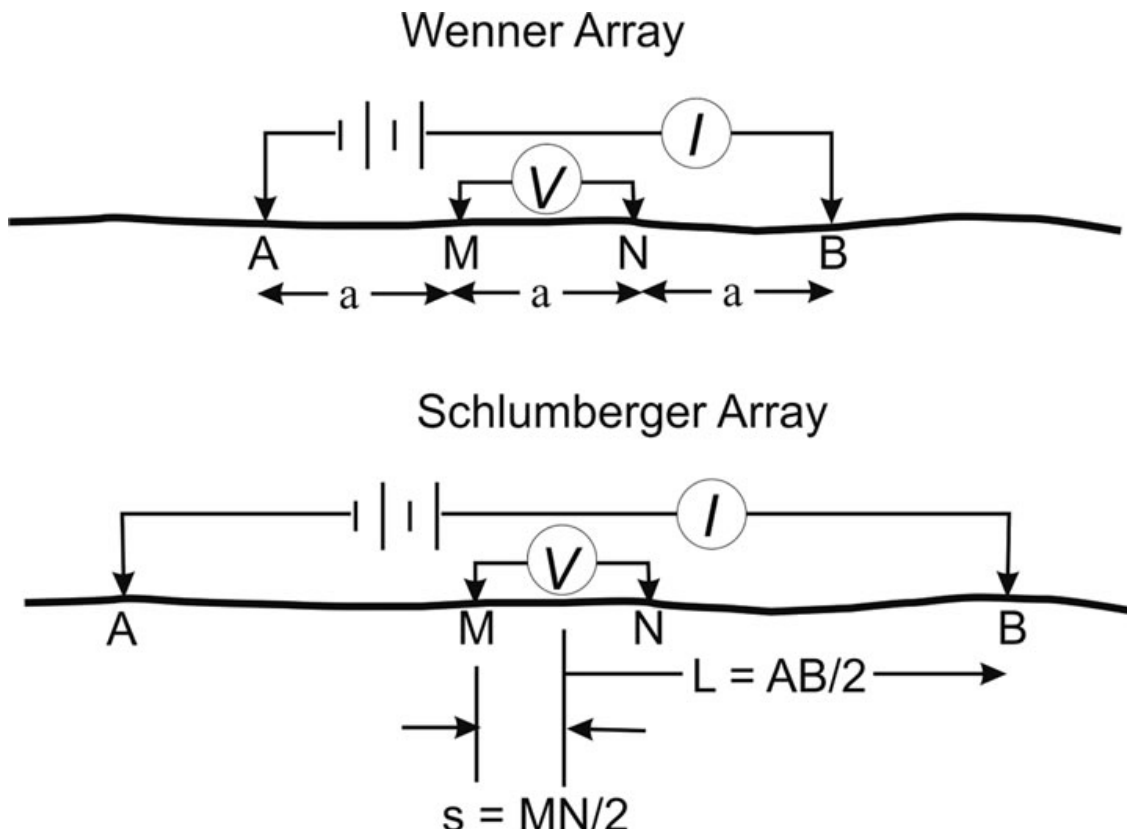


Figure 3.2: Electrode Arrangement of Wenner and Schlumberger Configuration [James *et al.*, 2011]

- Survey Layout:** The study area was systematically covered with 3 parallel profiles at first study area and 2 parallel profiles at second study area, denoted as Profile 1 (130m), Profile 2 (150m) and Profile 3 (130m) at first study area, and Profile 1 (130 m) and Profile 2 (150 m) at second study area, spaced apart to ensure adequate coverage. Profile endpoints and starting points are clearly marked, ensuring proper alignment during the survey. The profiles were oriented to maximize data collection over the expected subsurface structures, as informed by the geological context of the area. The survey also incorporated Vertical Electrical Sounding (VES) points, numbered VES1 to VES10 for each study area, which are distributed across the area for localized subsurface investigations. GPS was used to precisely locate the electrode positions, ensuring consistency and repeatability of the survey. Additionally, a grid-like "Box Layer" is superimposed over the study area for spatial referencing and visualization of the coverage.

Here is the attached figure showing the survey layout for both study areas:

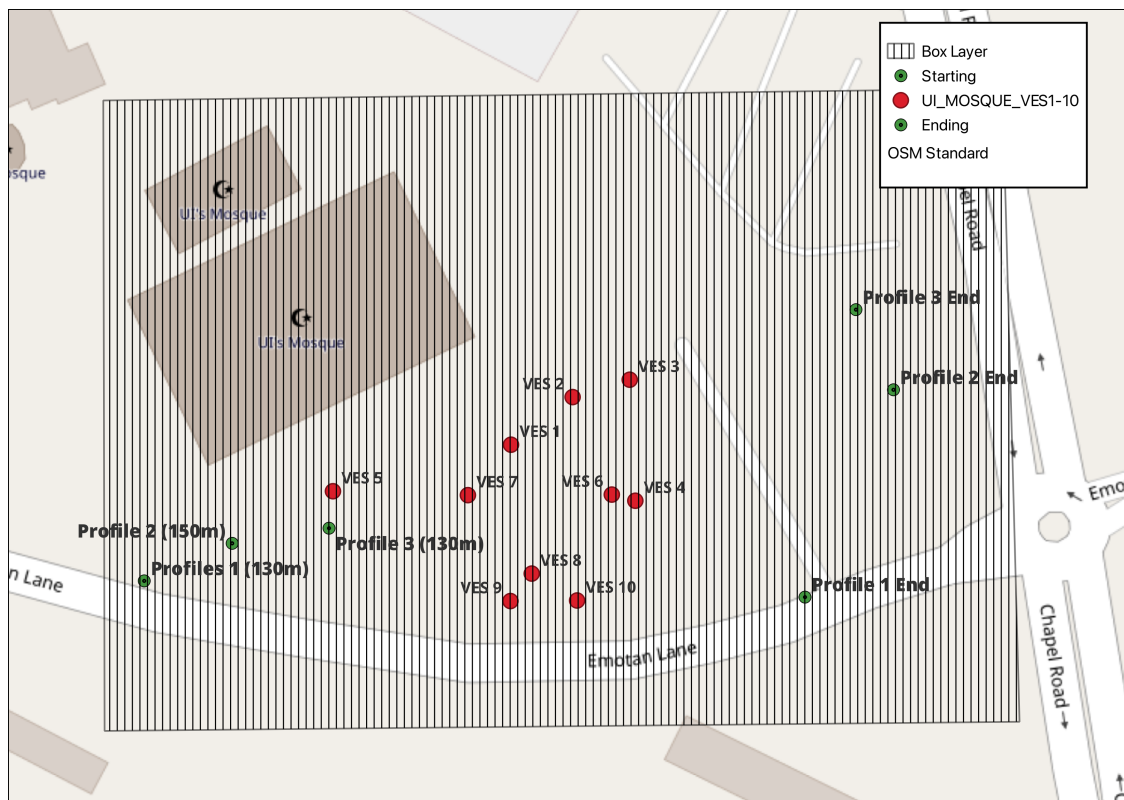


Figure 3.3: Survey Layout for UI Mosque Study Area

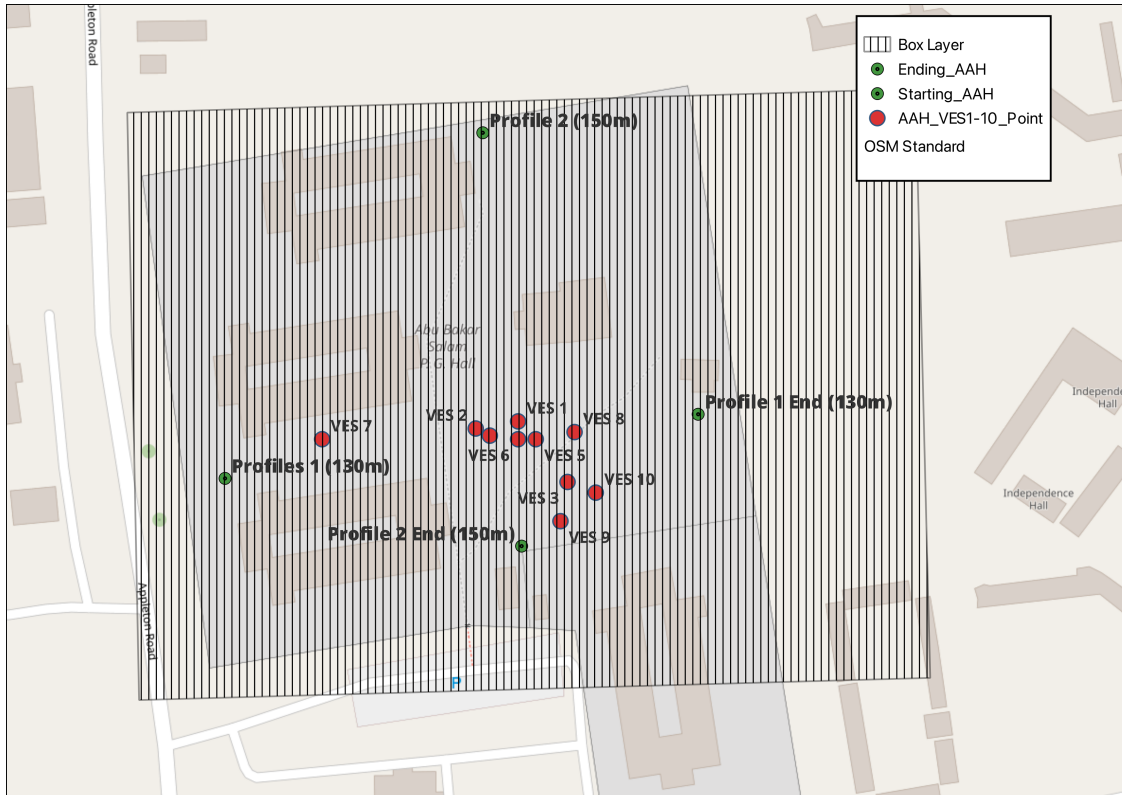


Figure 3.4: Survey Layout for AAH Study Area

3.4.2 Field Procedures

- Electrode Placement:** Electrodes were inserted into the ground at specified intervals based on the chosen configuration. Care was taken to ensure firm contact with the soil, especially in dry or compacted areas.



Figure 3.5: An Electrode Injected to the Ground

- **Current Injection and Measurement:** A steady electrical current was injected into the ground through the outer electrodes. The potential difference was measured across the inner electrodes using the resistivity meter. Environmental factors such as moisture levels and soil conductivity were monitored to optimize measurements.

3.4.3 Data Acquisition

1. Vertical Electrical Sounding Data Acquisition

Data was collected at fixed points and the coordinates were recorded along the survey line by gradually increasing the spacing between current electrodes. The resulting apparent resistivity values were plotted against electrode spacing to generate depth profiles.

2. Constant Separation Traversing Data Acquisition

The electrode array was moved laterally along the survey lines with a fixed electrode spacing. Here the starting coordinates and the ending coordinates were recorded and apparent resistivity values were recorded at regular intervals to map horizontal variations in subsurface resistivity.

3.4.4 Data Processing

- **Software Used:** The data was processed using software such as WINRESIST to get 1D with VES data for 2D and 3D resistivity modeling. DIPROWIN software was employed for contour plotting and visualization with CST data. Surfer software was used to get the geoelectric section along the profiles.
- **Data Correction:** Corrections were applied to remove noise caused by electrode polarization, environmental factors, or measurement errors. Calibration checks were performed to ensure the reliability of the resistivity meter.
- **Inversion Techniques:** The apparent resistivity values were inverted to obtain true resistivity, using iterative algorithms to refine the models. The final output included detailed resistivity profiles and maps.

3.4.5 Interpretation Methods

- **Resistivity Models:** The processed data was used to construct 2D and 3D models of subsurface resistivity. These models highlighted lithological layers, groundwater zones, and potential weak zones.
- **Correlation with Geological Data:** Resistivity results were correlated with known geological features in the study area, including borehole logs and previous studies.

- **Validation:** Validation of the results was achieved by comparing the interpreted data with existing geological maps and, where available, borehole data.

3.5 Practical Curve Matching Techniques

Curve matching is a critical component of interpreting geophysical resistivity data. It involves comparing the field-derived apparent resistivity curves with theoretical or standard curves to deduce subsurface characteristics. This process allows for the estimation of layer resistivities, thicknesses, and depths, which are vital for understanding subsurface structures and anomalies.

In using the curve matching method, the field data are plotted on a log-log graph on a transparent overlay, called the tracing paper. The tracing paper is then placed on the master curve in such a way that their vertical and horizontal axes are always parallel. Vertical electrical sounding field curves can be interpreted qualitatively using simple curve shapes, semi-quantitatively using graphical model curves, or quantitatively with computer models.

3.5.1 Types of Possible Curves

The resistivity curves observed during Vertical Electrical Sounding (VES) are influenced by the number and arrangement of subsurface layers, as well as their resistivity contrasts. The apparent resistivity curve for a three-layer structure generally has one of four typical shapes, determined by the vertical sequence of resistivity in the layers. These include:

- **H-Type Curve:** Characterized by a low-resistivity layer sandwiched between two high-resistivity layers. This is typical for weathered basement or clay layers underlain by fresh bedrock.
- **A-Type Curve:** Exhibits a progressive increase in resistivity with depth, often indicative of compact and drier subsurface materials.
- **K-Type Curve:** Shows a high-resistivity layer between two low-resistivity layers. This configuration can suggest sandy or gravelly layers between moist soil or clay.
- **Q-Type Curve:** Characterized by a gradual decrease in resistivity with depth, often indicative of a conductive basement or saturated zones.

These curves provide initial insights into subsurface conditions and guide subsequent data processing and interpretation.

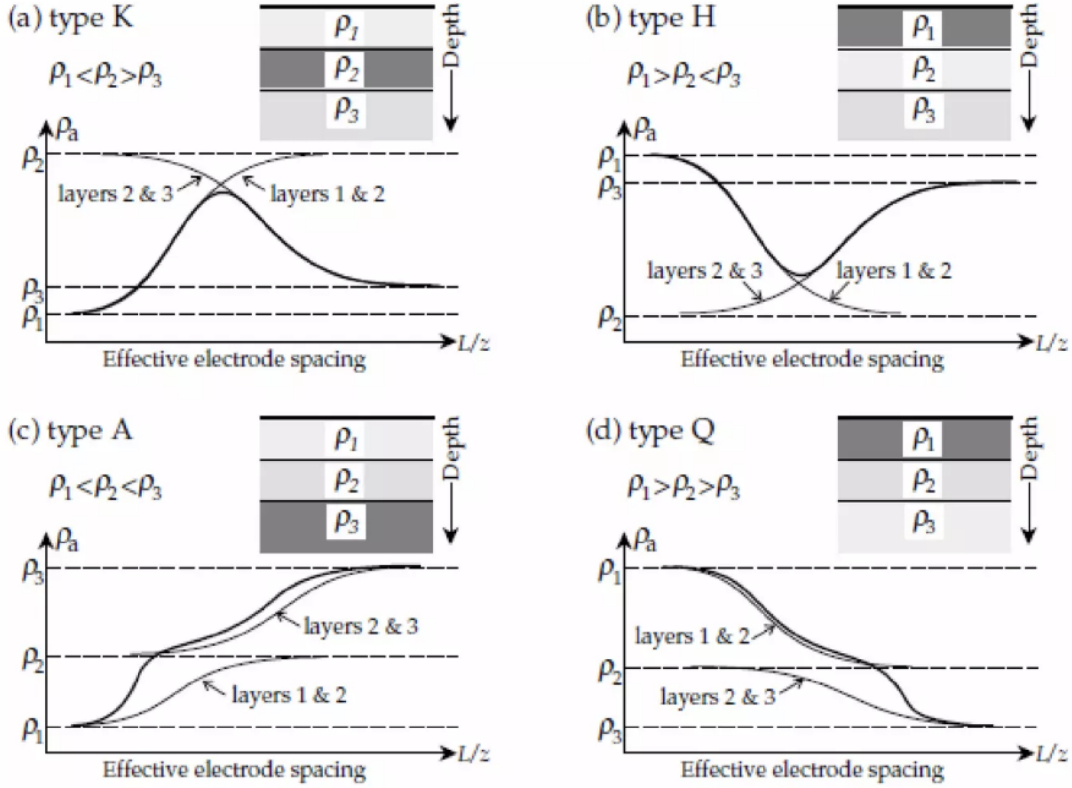


Figure 3.6: The four Curves Types for typical Three Layered Model [Amit *et al.*, 2018]

When there are more than three layers with different resistivity on a field curves, several letters combination are used to classify the curves type. For example, In Four-Layer Geoelectric sections, there are 8 possible relations:

- $\rho_1 > \rho_2 < \rho_3 < \rho_4$ **HA Type**
- $\rho_1 > \rho_2 < \rho_3 > \rho_4$ **HK Type**
- $\rho_1 < \rho_2 < \rho_3 < \rho_4$ **AA Type**
- $\rho_1 < \rho_2 < \rho_3 > \rho_4$ **AK Type**
- $\rho_1 < \rho_2 > \rho_3 < \rho_4$ **KH Type**
- $\rho_1 < \rho_2 > \rho_3 > \rho_4$ **KQ Type**
- $\rho_1 > \rho_2 > \rho_3 < \rho_4$ **QH Type**
- $\rho_1 > \rho_2 > \rho_3 > \rho_4$ **QQ Type**

3.5.2 Curve Matching Techniques Procedure Outlines

The curve matching process involves systematic steps to ensure accurate interpretation of field data. The following outlines the procedure:

1. **Plot Field Data:** The apparent resistivity values from field measurements are plotted on a log-log graph against electrode spacing ($AB/2$).
2. **Initial Visual Comparison:** The plotted curve is visually compared with standard theoretical master curves to identify a similar pattern.
3. **Scaling Master Curves:** The master curves are scaled to match the field data. This involves adjusting the scale factor for resistivity and electrode spacing.
4. **Layer Parameter Estimation:** From the matched curve, the layer resistivities, thicknesses, and depths are estimated for initial interpretation.
5. **Iterative Refinement:** Advanced software tools like WINRESIST are used to refine the initial estimates, reducing interpretation errors and improving accuracy.

This structured approach ensures that the derived subsurface models are reliable and consistent with field observations.

3.6 Limitations and Precautions

3.6.1 Limitations

Electrical resistivity methods (ERM) are widely used for subsurface investigations, but they are not without limitations. These limitations can arise from environmental factors, methodological constraints, and inherent characteristics of the subsurface. Some of the key limitations include:

- **Sensitivity to Noise:** ERM is highly sensitive to noise from external sources such as power lines, stray currents, and metallic objects in the survey area. These factors can distort measurements and affect data quality.
- **Limited Depth Penetration:** The depth of investigation is constrained by the maximum spacing of current electrodes. For deeper investigations, larger electrode spacing is required, which may not be feasible in restricted spaces or urban environments (**Binley, 2015**).
- **Ambiguity in Interpretation:** Resistivity results are inherently non-unique, meaning that different subsurface conditions can produce similar resistivity patterns. This can lead to misinterpretation if additional validation methods, such as borehole logs, are not used (**Reynolds, 2011**).
- **Effect of Geological Complexity:** In areas with highly heterogeneous geology, such as fractured zones or mixed lithologies, interpreting resistivity data can be challenging due to overlapping resistivity values (**Olayemi et al., 2021**).

- **Dependence on Soil Moisture:** The resistivity of subsurface materials is strongly influenced by moisture content. Seasonal variations in soil moisture can lead to inconsistent results if surveys are conducted at different times of the year (**Farinde *et al.*, 2015**).
- **Environmental Impact:** In some cases, the insertion of electrodes can disturb the soil or vegetation. This is particularly a concern in sensitive ecological areas or agricultural lands.
- **Equipment Limitations:** The accuracy of resistivity measurements is dependent on the quality and calibration of the equipment used. Older or poorly maintained instruments can produce unreliable results.
- **Time and Labor Intensive:** Setting up electrodes and conducting surveys over large areas can be time-consuming, especially in rough terrains or areas with accessibility issues.

3.6.2 Precautions

To minimize the limitations of electrical resistivity methods and ensure reliable results, the following precautions should be taken:

1. **Ensure Proper Electrode Contact:** Electrodes should be securely inserted into the ground to achieve good electrical contact. In dry or rocky areas, water or conductive gel can be used to improve contact.
2. **Avoid Areas with High Noise Levels:** Surveys should be conducted away from power lines, pipelines, and other sources of electrical interference. If unavoidable, filters should be used to remove noise from the data.
3. **Conduct Surveys During Stable Weather Conditions:** Avoid conducting surveys during extreme weather conditions, such as heavy rains or droughts, as these can affect soil resistivity and distort results.
4. **Perform Regular Equipment Calibration:** The resistivity meter and other instruments should be calibrated before use to ensure accurate measurements. Regular maintenance is essential to avoid equipment malfunction.
5. **Validate Results with Additional Methods:** To reduce ambiguity, resistivity results should be validated using borehole data, geological maps, or other geophysical methods like seismic or ground-penetrating radar (**Reynolds, 2011**).
6. **Use Appropriate Electrode Configurations:** Select the electrode configuration (e.g., Schlumberger or Wenner) that best suits the survey objectives and site conditions. This ensures optimal resolution and depth coverage.
7. **Minimize Environmental Impact:** Take measures to reduce soil and vegetation disturbance when placing electrodes, especially in environmentally sensitive areas.

8. **Plan for Accessibility:** In areas with difficult terrain or limited access, plan the survey layout in advance to ensure all necessary locations can be reached without compromising data quality.
9. **Conduct Pre-Survey Reconnaissance:** Assess the site for potential obstacles, such as rocks, buried utilities, or water bodies, that may interfere with the survey.
10. **Record Detailed Field Notes:** Document all field conditions, instrument settings, and environmental factors during the survey. This information is crucial for data interpretation and troubleshooting.

CHAPTER 4: RESULTS AND ANALYSIS

4.1 Introduction

This chapter presents a comprehensive overview of the results obtained from the geophysical surveys conducted at two distinct study areas: Emotan Lane near the University of Ibadan Central Mosque, and Appleton Road in Abubakar Abdulsalam Hall within the University of Ibadan campus. These results are analyzed and interpreted to understand the subsurface resistivity variations, geological features, and structural anomalies, including subsurface layers, faults, and other resistivity contrasts. The data acquisition processes utilized both Vertical Electrical Sounding (VES) and Constant Separation Traversing (CST) techniques, employing the Schlumberger and Wenner array configurations, respectively. These methods were chosen for their reliability and effectiveness in delineating subsurface structures and identifying resistivity anomalies.

This chapter also provides insights into the resistivity characteristics of the basement complex and their implications for understanding the structural integrity, fault systems, and other geophysical anomalies in the study areas. The findings are presented in the form of tables, graphs, and contour maps to enhance clarity and support the discussions.

4.2 Curve Match Techniques Results

The results of the curve matching process provide a detailed understanding of the subsurface properties at each VES station. The following were observed in this study:

- The dominant curve types identified in the study areas were **H-Type**, indicating a combination of weathered and Fresh bedrock layers.
- Resistivity values for the topsoil ranged between 100 and 500 Ωm in first study area and ranged between 150 and 450 Ωm , reflecting variations in soil composition and moisture content.
- Weathered basement layers exhibited resistivity values ranging from 50 to 150 Ωm , consistent

with clayey or saturated zones.

- Fresh bedrock layers showed resistivity values exceeding 1,000 Ωm , indicative of hard, compact bedrock.
- Layer thicknesses varied between 1 m and 30 m, with deeper layers observed at VES stations closer to fault zones.

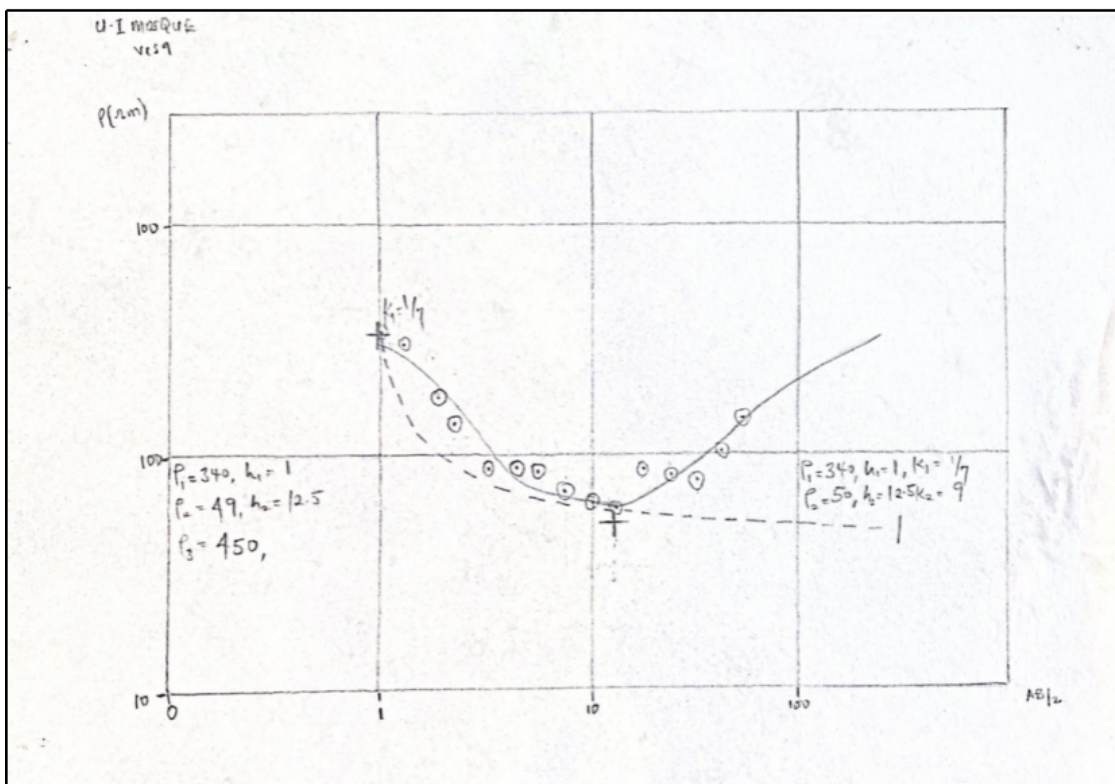
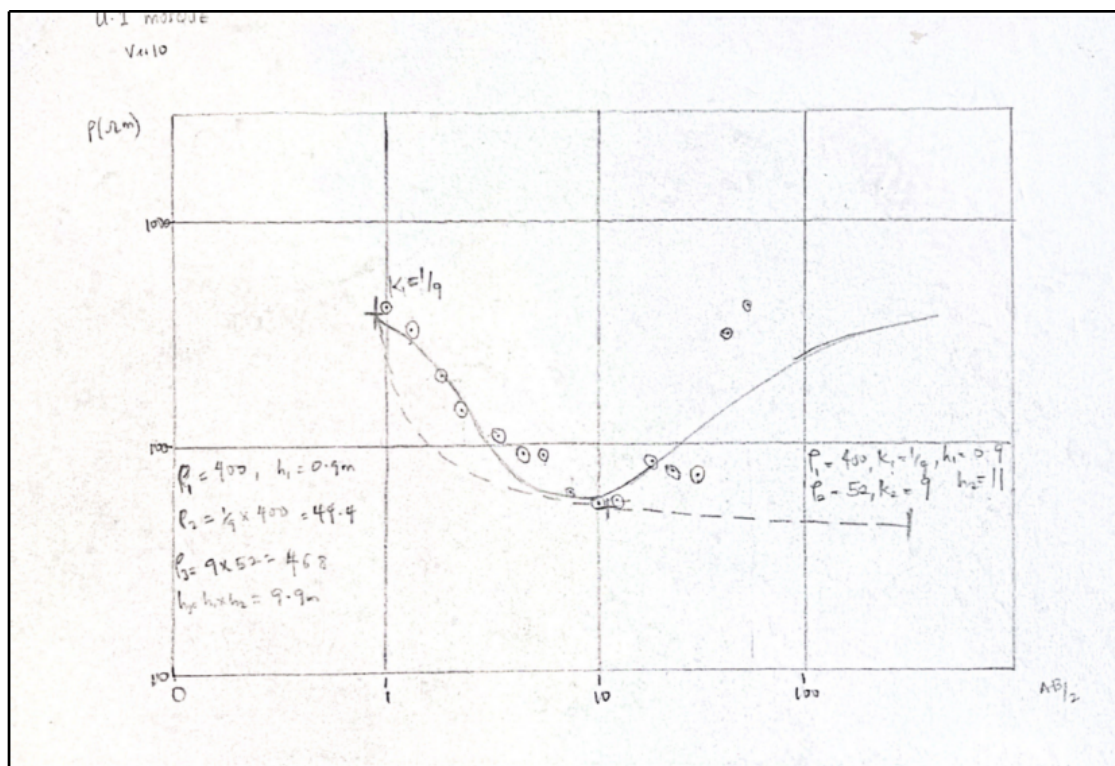


Figure 4.1: Two Curve Matching Result gotten from the plot on log-log graph

4.3 Vertical Electrical Sounding Data Interpretation

4.3.1 VES 1 Station at UI Mosque

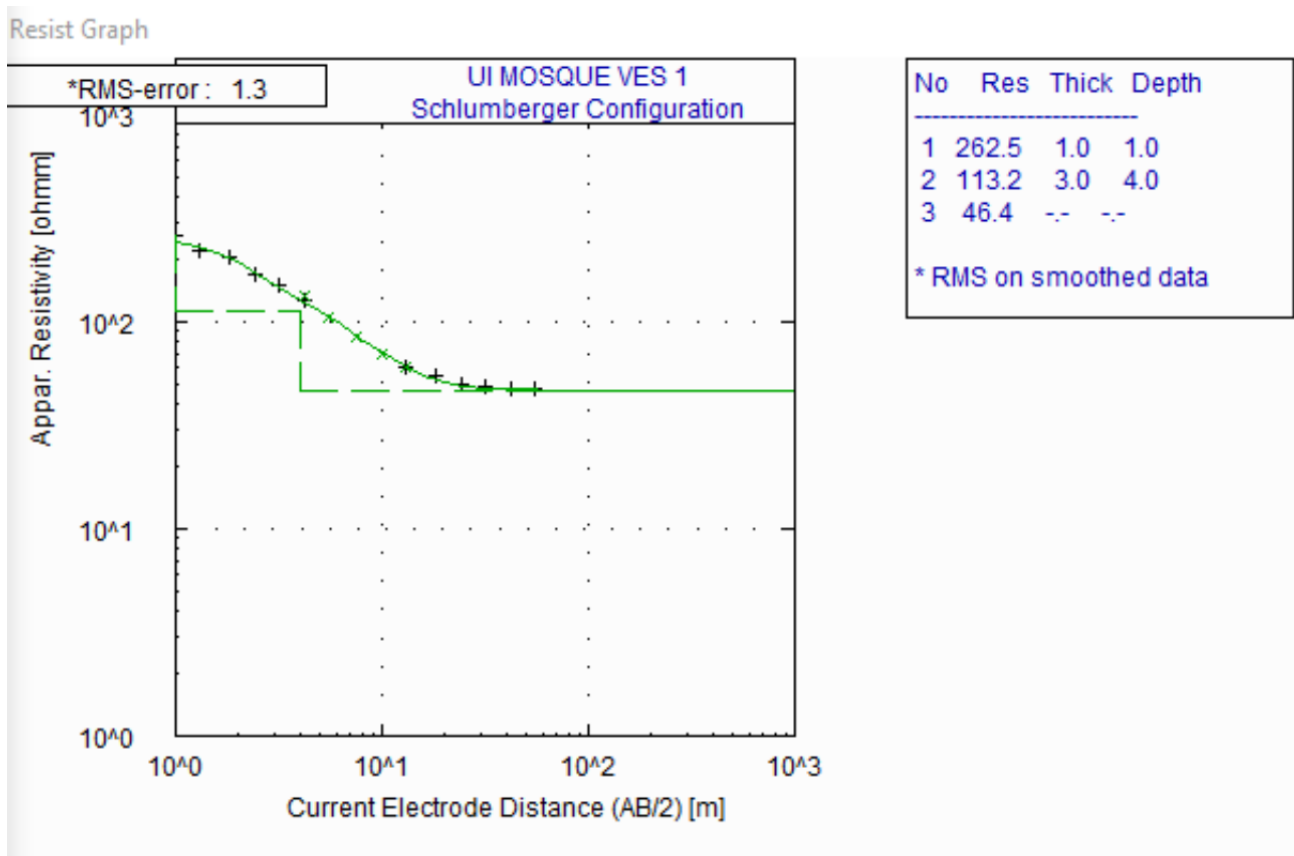


Figure 4.2: Graphical Representation of VES 1

The VES curve for UI Mosque VES 1 in fig. 4.2 suggests an **Q-type pattern**, characterized by a descending resistivity trend, indicating a three-layer subsurface model. The first layer, with a resistivity of $262.5 \Omega\text{m}$ and a thickness of 1.0 m , represents the topsoil, likely composed of dry sandy soil or lateritic materials. Below this is the intermediate layer, which has a resistivity of $113.2 \Omega\text{m}$ and a thickness of 3.0 m , likely indicating clayey soil or moist sandy material due to its more conductive nature. The third layer, with a resistivity of $46.4 \Omega\text{m}$ and undefined thickness, is interpreted as a basement layer consisting of fractured or weathered rock, potentially saturated with water.

The subsurface lithology suggests a dry and resistive topsoil, a more conductive clay-rich intermediate layer, and a water-saturated or fractured basement rock. No significant faulting is apparent in the data, but the low resistivity of the third layer indicates high moisture content or fractures, which could affect foundation stability. While the top layer is stable, its thinness limits its load-bearing capacity. The intermediate layer's compressible clay content may not support heavy foundations without proper treatment. The bottom layer's water saturation or fractured condition warrants further geotechnical investigation to ensure suitability for construction.

4.3.2 VES 2 Station at UI Mosque

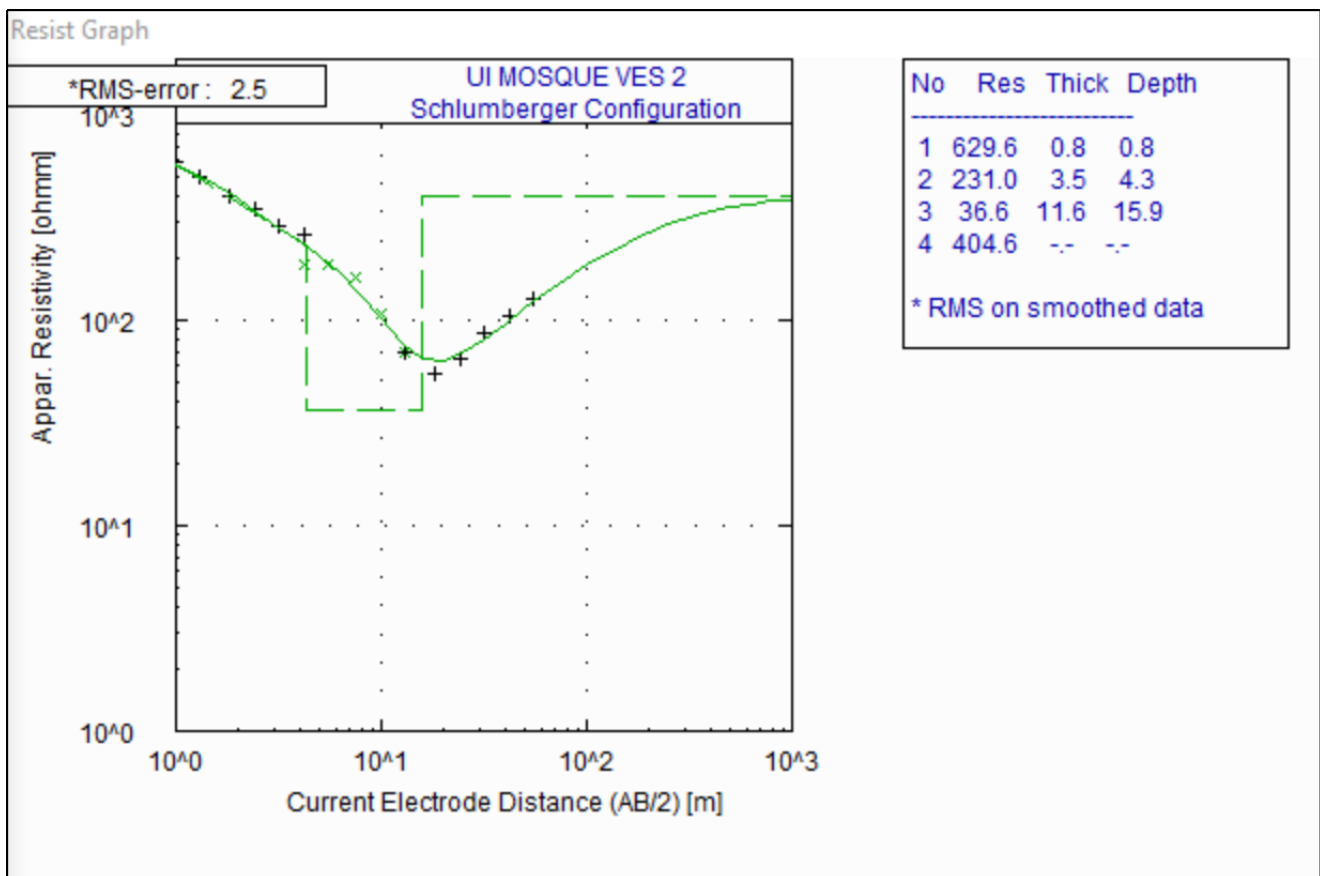


Figure 4.3: Graphical Representation of VES 2

The curve exhibits a **QH-type trend** in fig. 4.3, characterized by an initial descent in resistivity, followed by an ascent, and then another descent. This indicates a four-layer subsurface model with alternating resistive and conductive layers. The resistivity and thickness data for each layer are as follows: Layer 1 (Topsoil) has a resistivity of $629.6 \Omega \text{ m}$ and a thickness of 0.8 m , corresponding to a depth of 0.8 m . Layer 2 (Intermediate) has a resistivity of $231.0 \Omega \text{ m}$ and a thickness of 3.5 m , reaching a depth of 4.3 m . Layer 3 (Basement Transition) exhibits a resistivity of $36.6 \Omega \text{ m}$ and a thickness of 11.6 m , extending to a depth of 15.9 m . Finally, Layer 4 (Basement Rock) has a resistivity of $404.6 \Omega \text{ m}$, but its thickness and depth are not specified. The subsurface lithology can be described as follows: Layer 1 (Topsoil) is dry and resistive, likely composed of sand or laterite; Layer 2 (Intermediate) is moderately resistive, suggesting weathered rock or moist sandy material; Layer 3 (Transition Zone) is highly conductive, likely consisting of clay-rich or water-saturated soil; and Layer 4 (Basement) is resistive, representing fractured or fresh bedrock rock.

For foundation suitability, Layer 1 ($0\text{--}0.8 \text{ m}$) is suitable for shallow foundations if compacted. Layer 2 ($0.8\text{--}4.3 \text{ m}$) may require evaluation for stability. Layer 3 ($4.3\text{--}15.9 \text{ m}$) presents poor foundation conditions due to low resistivity, indicating potential compressibility or water saturation, necessitating deep foundations (e.g., piles). Layer 4 (below 15.9 m) is ideal for foundation support if bedrock is confirmed.

4.3.3 VES 3 Station at UI Mosque

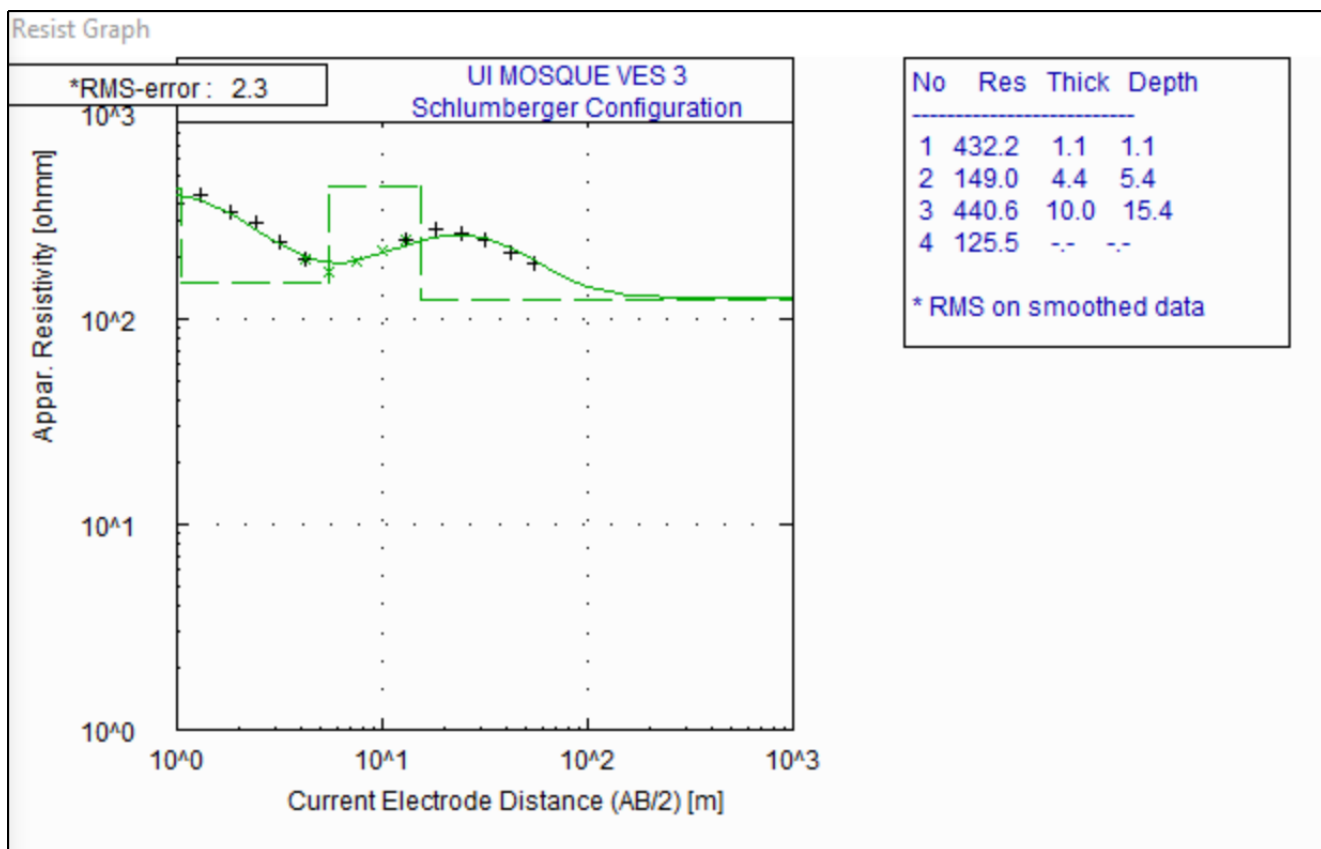


Figure 4.4: Graphical Representation of VES 3

The resistivity pattern shown in fig. 4.4 indicates a **H-Type Curve**. The resistivity and thickness data for the layers are as follows: Layer 1 has a resistivity of 432.2 $\Omega\cdot m$ and a thickness of 1.1 m, corresponding to a depth of 1.1 m. Layer 2 has a resistivity of 149.0 $\Omega\cdot m$ and a thickness of 4.4 m, extending to a depth of 5.4 m. Layer 3 has a resistivity of 440.6 $\Omega\cdot m$ and a thickness of 10.0 m, reaching a depth of 15.4 m. Layer 4 has a resistivity of 125.5 $\Omega\cdot m$ and extends beyond the measured depth. The lithology interpretation suggests that Layer 1, with high resistivity, represents dry or compacted material, such as laterite or dry sand. Layer 2, with lower resistivity, could indicate clay or water-saturated soil. Layer 3, with increased resistivity, suggests compacted rock or unsaturated sandstone. Layer 4, with lower resistivity, points to a water-bearing formation or weathered rock.

For foundation suitability, Layer 1 (0-1.1 m) is suitable for shallow foundations if compact. Layer 2 (1.1-5.4 m) requires evaluation due to possible instability. Layer 3 (5.4-15.4 m) is more stable for deep foundations. Layer 4 below 15.4m should be assessed for load-bearing capacity before construction.

4.3.4 VES 4 Station at UI Mosque

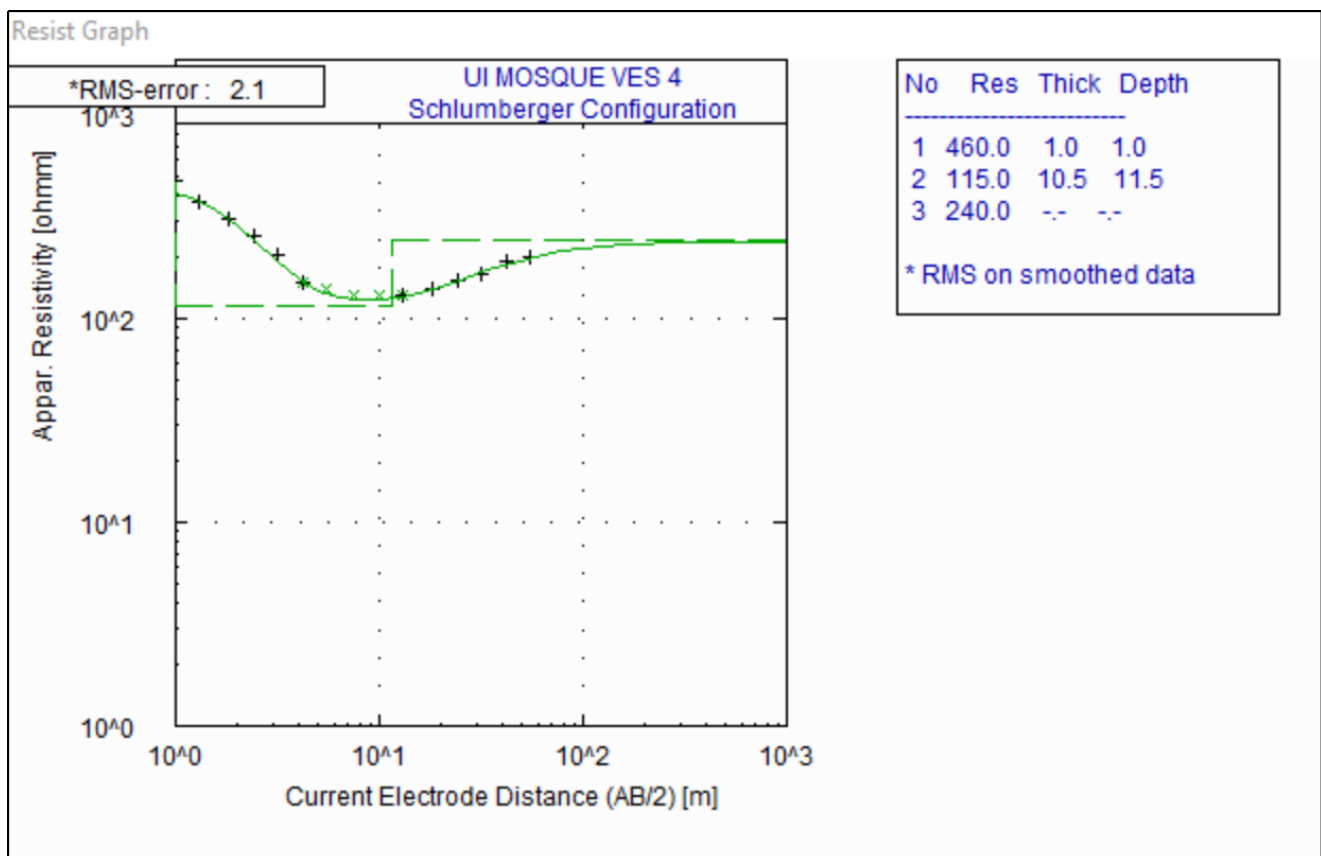


Figure 4.5: Graphical Representation of VES 4

The resistivity data shown in fig. 4.5 indicates that the resistivity drops significantly from Layer 1 to Layer 2, and then partially increases in Layer 3. This suggests a **H-Type** curve with a transition zone between more resistive material and a moderately resistive layer. The resistivity and thickness data for the layers are as follows: Layer 1 has a resistivity of $460 \Omega \text{ m}$ and a thickness of 1.0 m , corresponding to a depth of 1.0 m . Layer 2 has a resistivity of $115.0 \Omega \text{ m}$ and a thickness of 10.5 m , extending to a depth of 11.5 m . Layer 3 has a resistivity of $240 \Omega \text{ m}$, but its thickness and depth are not determined.

The lithology interpretation for the layers is as follows: Layer 1, with a high resistivity, could indicate dry, resistive material such as sand or laterite. Layer 2, with moderate resistivity, may suggest weathered rock or moist sandy material. Layer 3, with a higher resistivity than Layer 2 but lower than Layer 1, could represent fractured rock or a transition zone between weathered material and solid basement rock.

4.3.5 VES 5 Station at UI Mosque

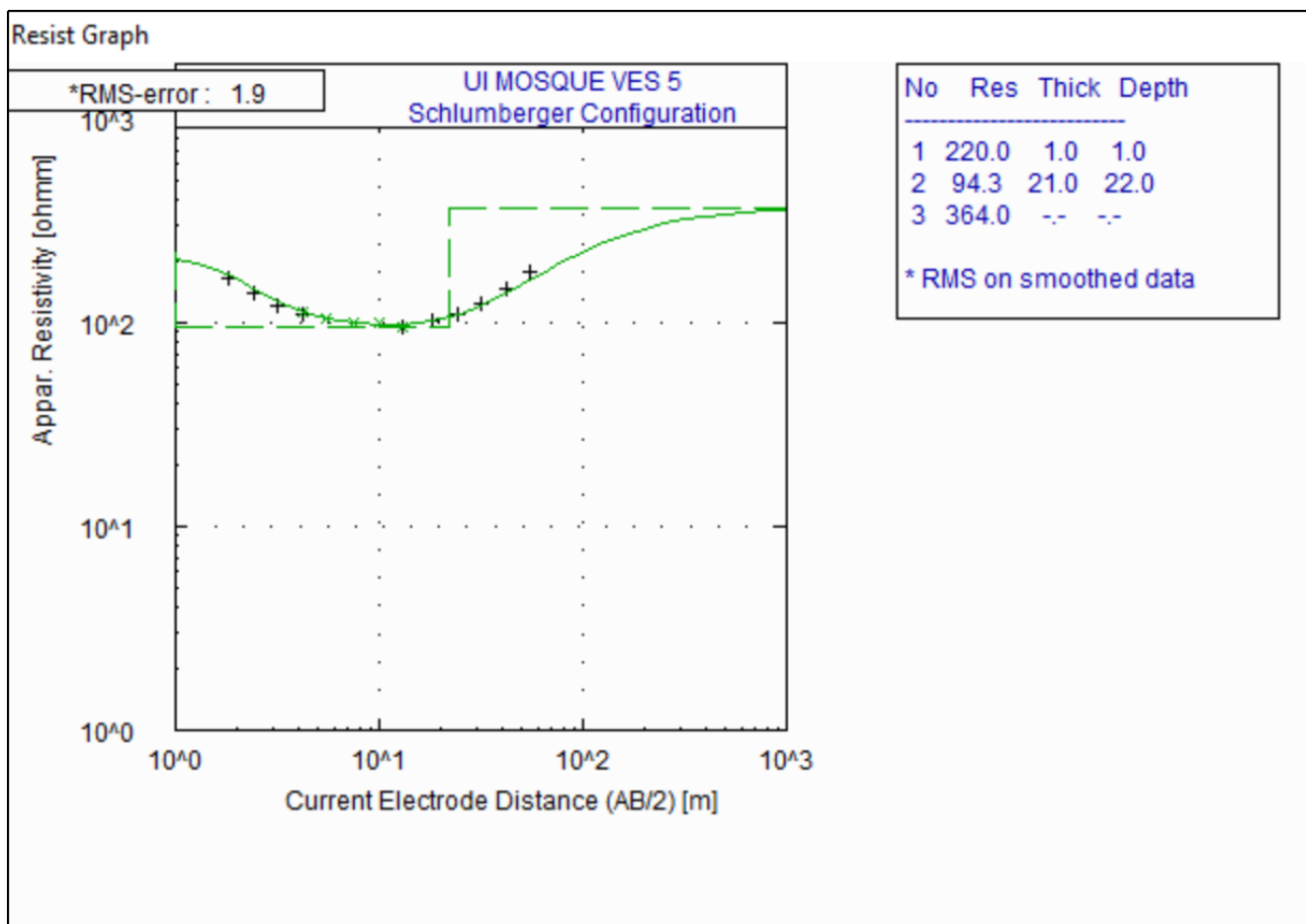


Figure 4.6: Graphical Representation of VES 5

Fig. 4.6 above curve is typical **H-Type** curve, the resistivity and thickness data for the layers are as follows: Layer 1 has a resistivity of $220 \Omega \text{ m}$ and a thickness of 1.0 m , corresponding to a depth of 1.0 m . Layer 2 has a resistivity of $94.3 \Omega \text{ m}$ and a thickness of 21.0 m , extending to a depth of 22.0 m . Layer 3 has a resistivity of $364 \Omega \text{ m}$, but its thickness and depth not determined

The lithology interpretation for the layers is as follows: Layer 1, with a relatively moderate resistivity, may represent a type of soil or weathered material such as sand or laterite. Layer 2, with a significantly lower resistivity, likely indicates a conductive layer such as clay, water-saturated soil, or a more saturated transition zone. Layer 3, with a higher resistivity, may correspond to solid rock, possibly fractured basement rock or dry, resistive material beneath the conductive zone.

4.3.6 VES 6 Station at UI Mosque

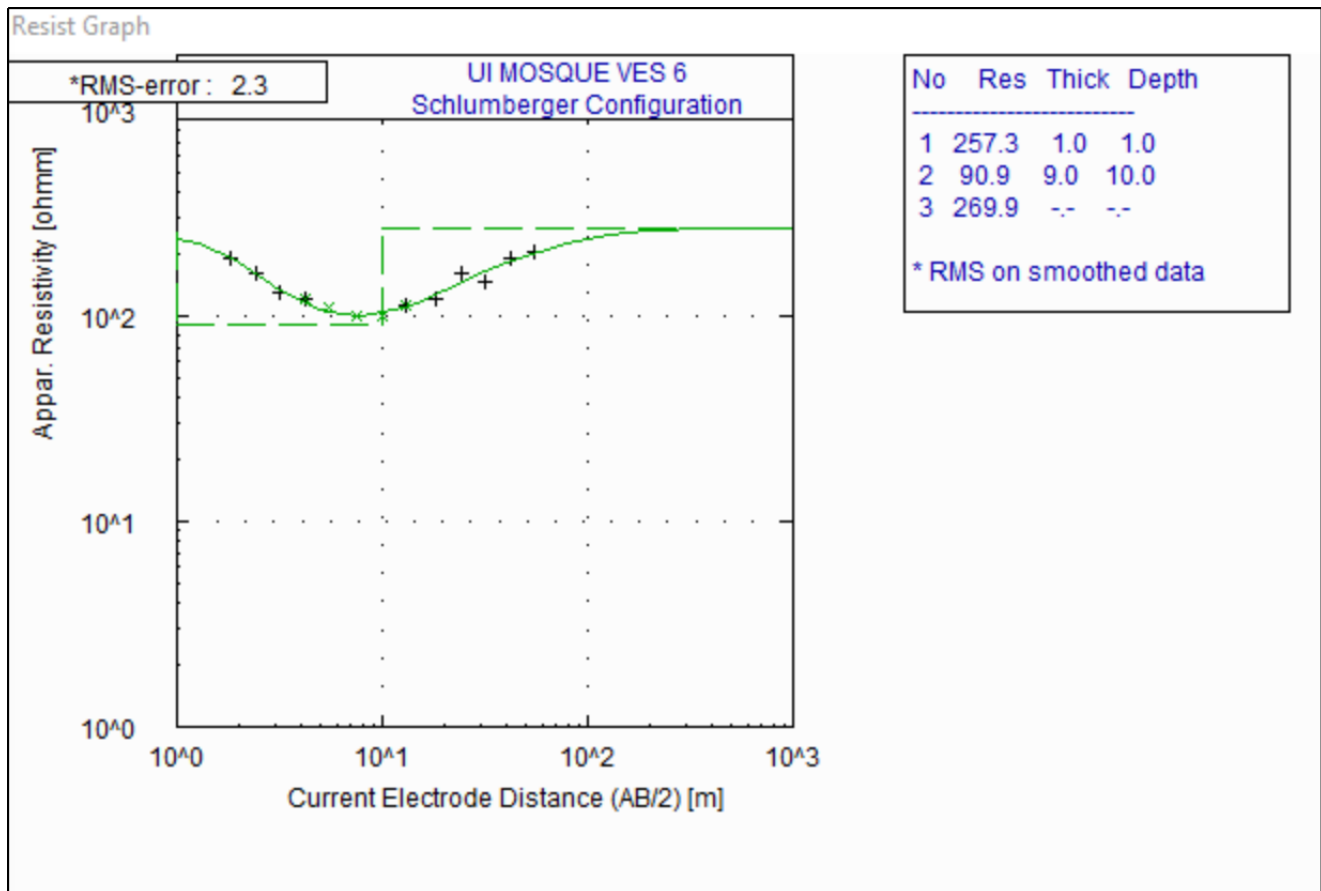


Figure 4.7: Graphical Representation of VES 6

In fig. 4.7, the resistivity and thickness data for the layers are as follows: Layer 1 has a resistivity of $257.3 \Omega \text{ m}$ and a thickness of 1.0 m , corresponding to a depth of 1.0 m . Layer 2 has a resistivity of $90.9 \Omega \text{ m}$ and a thickness of 9.0 m , extending to a depth of 10.0 m . Layer 3 has a resistivity of $269.9 \Omega \text{ m}$, but its thickness and depth are not determined.

The lithology interpretation for the layers is as follows: Layer 1, with a relatively high resistivity, could represent dry, resistive material such as sand or laterite. Layer 2, with a lower resistivity, likely represents a conductive layer, such as clay, moist sandy material, or water-saturated soil. Layer 3, with a resistivity similar to Layer 1, suggests a return to resistive conditions, possibly indicating a transition to a solid or fractured basement rock. This is typical **H-Type** curves.

4.3.7 VES 7 Station at UI Mosque

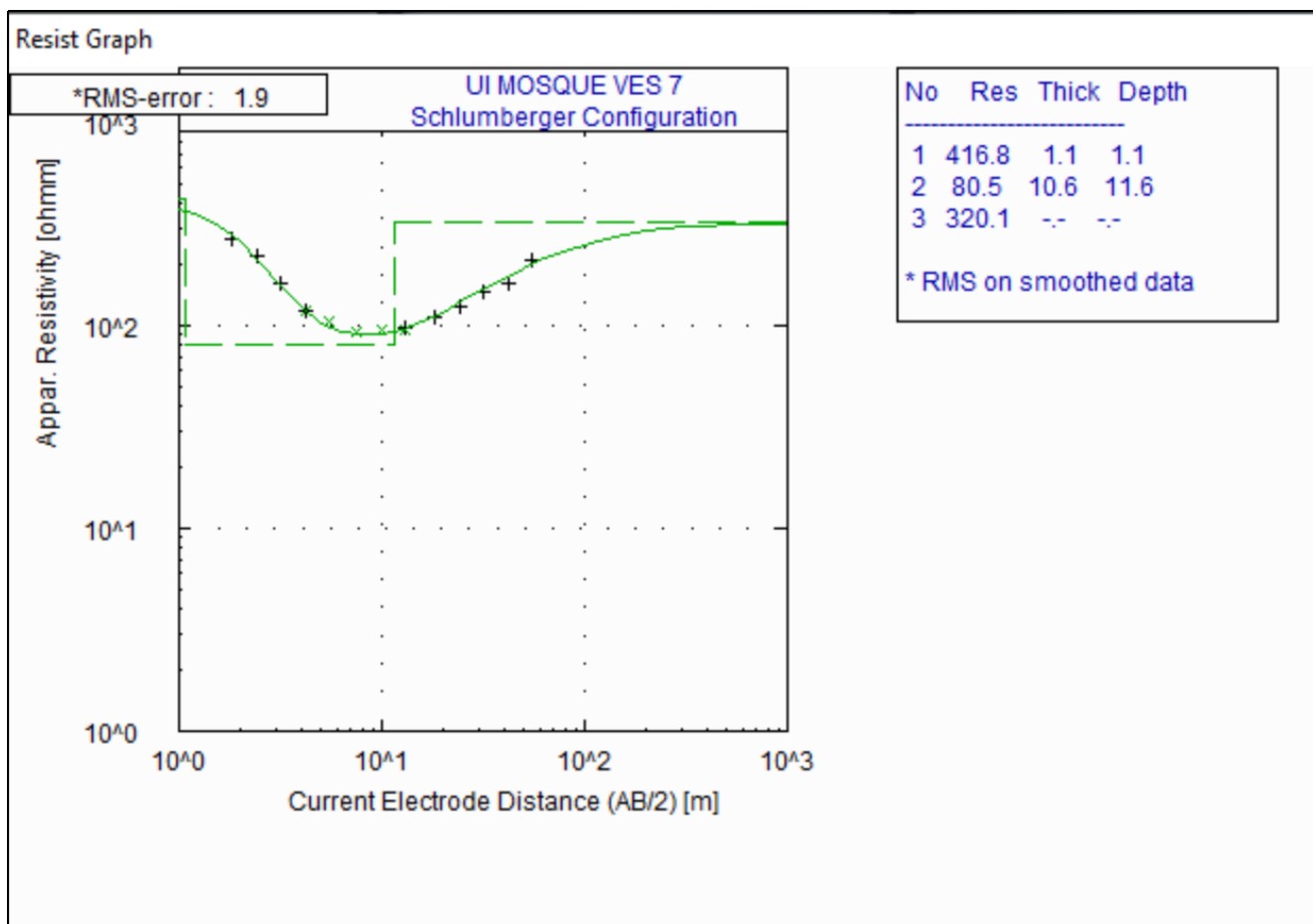


Figure 4.8: Graphical Representation of VES 7

In fig. 4.8 The resistivity decreases in Layer 2 and then increases again in Layer 3, suggesting a **H-Type** curve with a conductive layer (Layer 2) beneath a resistive top layer (Layer 1) and a return to resistivity at greater depth (Layer 3). The resistivity and thickness data for the layers are as follows: Layer 1 has a resistivity of $416.8 \Omega \text{ m}$ and a thickness of 1.1 m , corresponding to a depth of 1.1 m . Layer 2 has a resistivity of $80.5 \Omega \text{ m}$ and a thickness of 10.6 m , extending to a depth of 11.6 m . Layer 3 has a resistivity of $320.1 \Omega \text{ m}$.

The lithology interpretation for the layers is as follows: Layer 1, with a high resistivity, likely represents dry, resistive material such as sand or laterite. Layer 2, with a significantly lower resistivity, is likely to be a conductive zone, such as clay, water-saturated soil, or a weathered material. Layer 3, with a higher resistivity than Layer 2, could represent fractured rock or solid basement rock, which is more resistive than the overlying conductive material.

4.3.8 VES 8 Station at UI Mosque

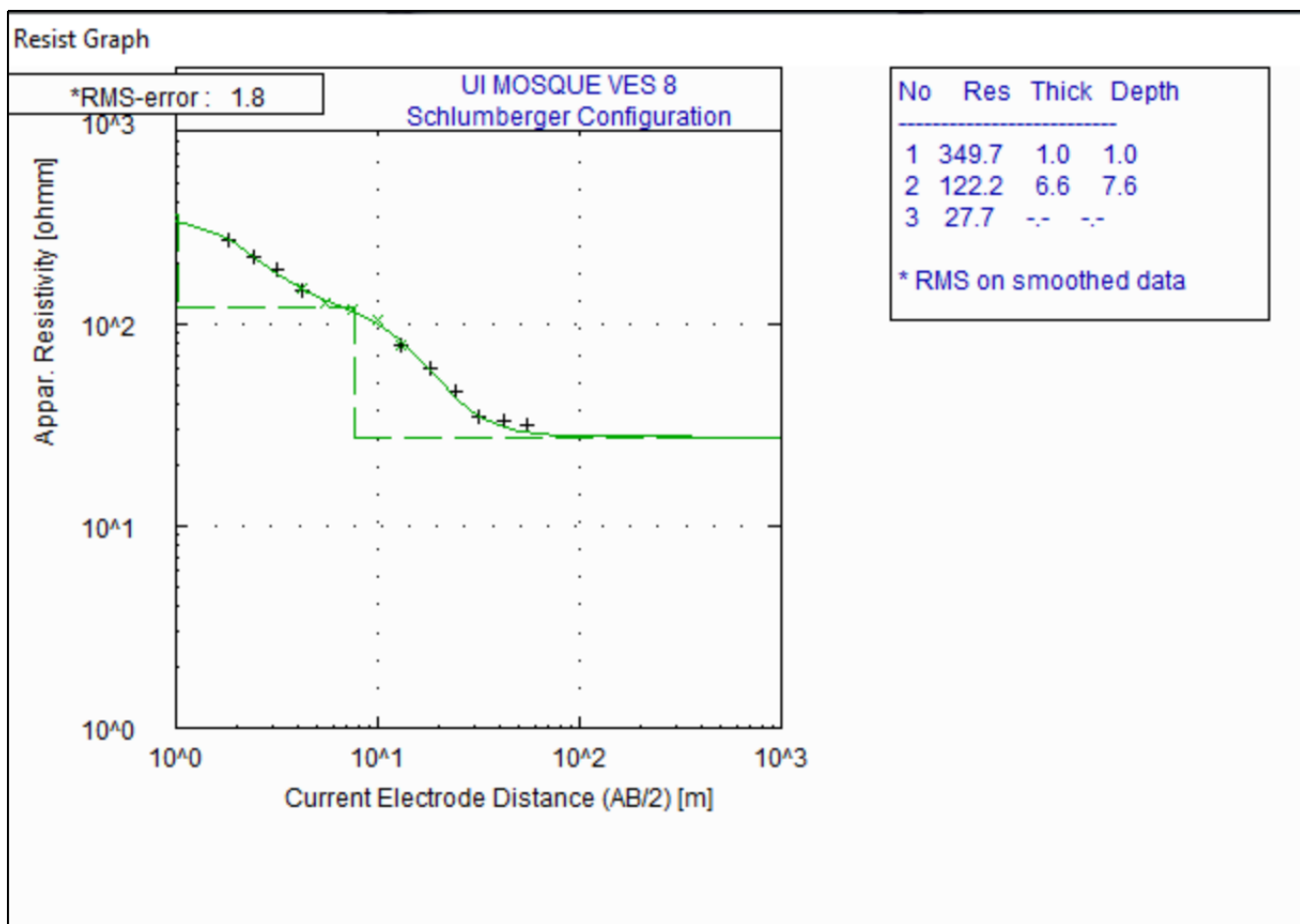


Figure 4.9: Graphical Representation of VES 8

In fig. 4.9, the resistivity decreases significantly from Layer 1 to Layer 2 and further decreases in Layer 3, which suggests a three-layer curve with a progressively more conductive layer at greater depths. This pattern is indicative of a **Q-Type** curve. The resistivity and thickness data for the layers are as follows: Layer 1 has a resistivity of $349.7 \Omega m$ and a thickness of $1.0 m$, corresponding to a depth of $1.0 m$. Layer 2 has a resistivity of $122.2 \Omega m$ and a thickness of $6.6 m$, extending to a depth of $7.6 m$. Layer 3 has a resistivity of $27.7 \Omega m$.

The lithology interpretation for the layers is as follows: Layer 1, with a relatively high resistivity, likely represents dry, resistive material such as sand or laterite. Layer 2, with moderate resistivity, could represent weathered rock, moist sandy material, or a transition zone. Layer 3, with a very low resistivity, suggests a conductive layer, possibly clay-rich, water-saturated soil, or a highly conductive transition zone.

4.3.9 VES 9 Station at UI Mosque

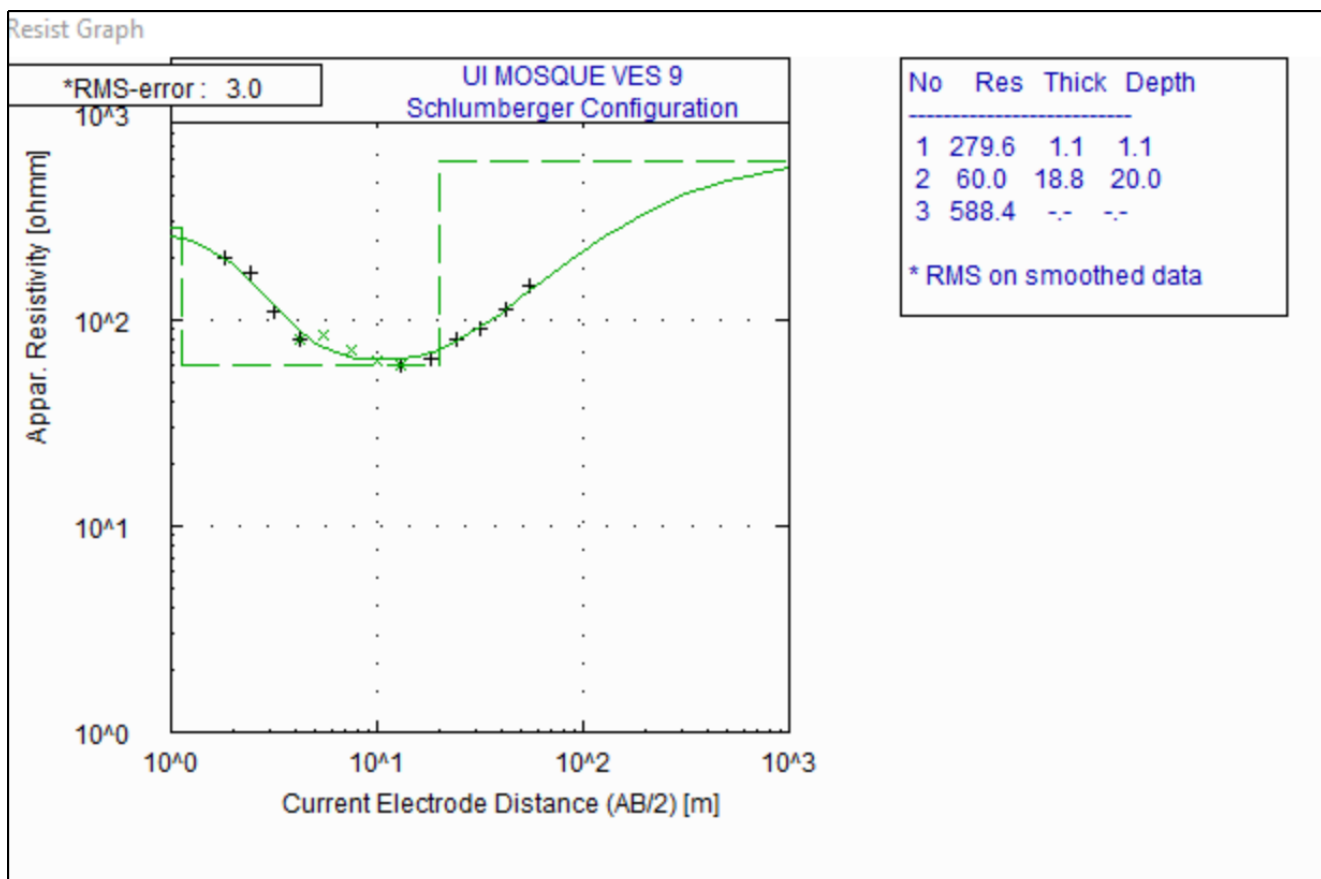


Figure 4.10: Graphical Representation of VES 9

The resistivity pattern shown in fig. 4.10 indicates a **K-Type Curve**. The resistivity and thickness data for the layers are as follows: Layer 1 has a resistivity of 279.6 $\Omega\cdot\text{m}$ and a thickness of 1.1 m, corresponding to a depth of 1.1 m. Layer 2 has a resistivity of 60.0 $\Omega\cdot\text{m}$ and a thickness of 18.8 m, extending to a depth of 19.9 m. Layer 3 has a resistivity of 588.4 $\Omega\cdot\text{m}$ and extends beyond the measured depth. This pattern is typical of geological settings where a resistive layer (e.g., dry sand/gravel) overlies a conductive layer (e.g., clay or water-saturated soil) and is underlain by a highly resistive layer (e.g., bedrock).

For foundation suitability, Layer 1 (0 - 1.1 m) is suitable for shallow foundations if compacted, but may require removal if loose or unstable. Layer 2 (1.1 - 19.9 m) presents poor foundation conditions due to low resistivity, indicating potential compressibility or water saturation, necessitating deep foundations (e.g., piles) to bypass this layer. Layer 3 (below 19.9 m) is ideal for foundation support if bedrock is confirmed, as it provides a stable and strong base.

4.3.10 VES 10 Station at UI Mosque

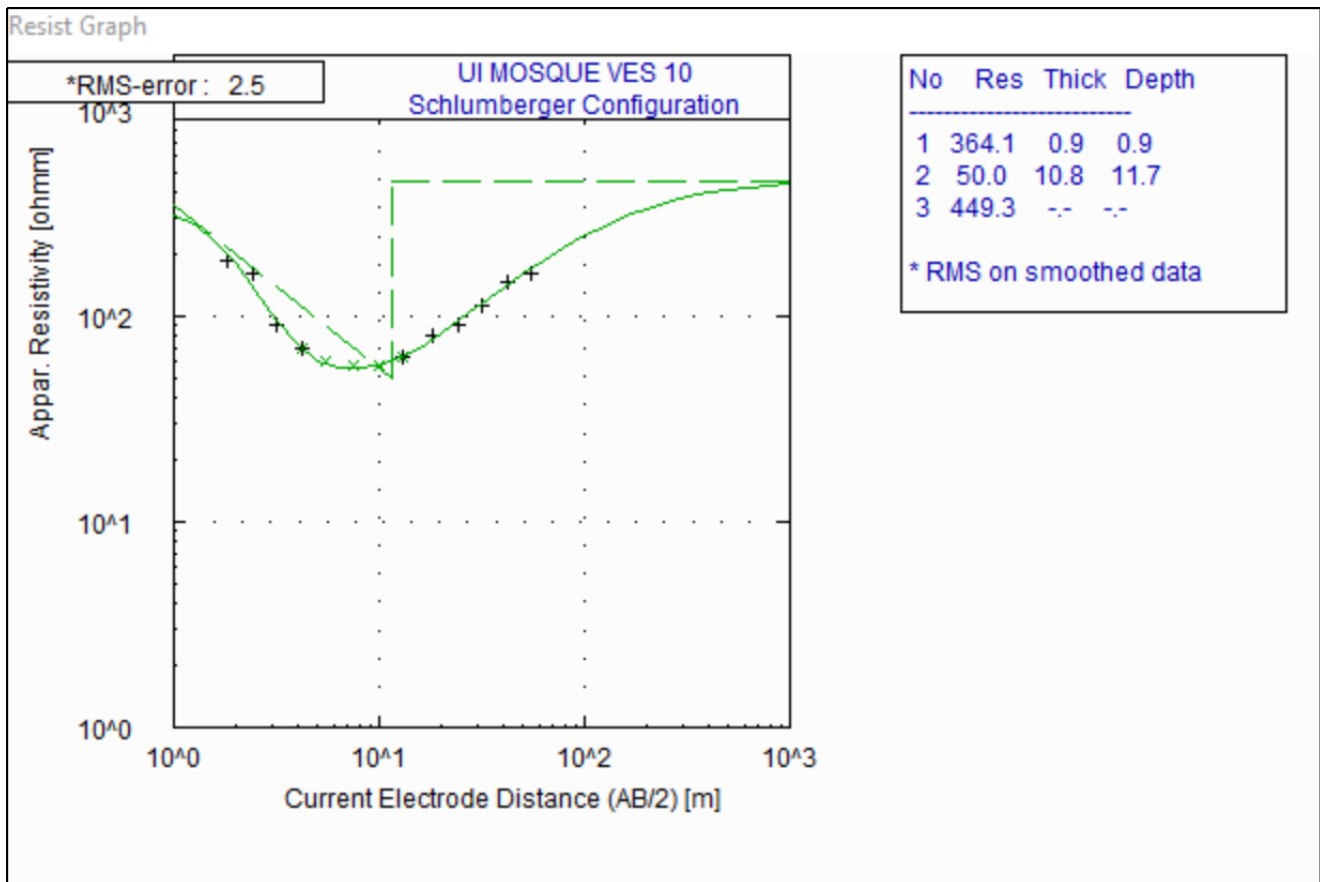


Figure 4.11: Graphical Representation of VES 10

The resistivity pattern in above fig. 4.11 indicates an **H-Type Curve**, characterized by a low-resistivity layer (Layer 2) sandwiched between two high-resistivity layers (Layer 1 and Layer 3). This is typical of geological settings where a conductive layer (e.g., clay or water-saturated soil) is overlain and underlain by more resistive materials (e.g., dry sand/gravel and bedrock). The resistivity and thickness data for the layers are as follows: Layer 1 has a resistivity of $364.1 \Omega\cdot m$ and a thickness of 0.9 m, corresponding to a depth of 0.9 m. Layer 2 has a resistivity of $50.0 \Omega\cdot m$ and a thickness of 10.8 m, extending to a depth of 11.7 m. Layer 3 has a resistivity of $449.3 \Omega\cdot m$ and extends beyond the measured depth. The lithology interpretation suggests that Layer 1, with high resistivity, likely represents dry or resistive material, such as gravel or dry sand. Layer 2, with significantly lower resistivity, indicates a conductive layer, which could be clay-rich soil or water-saturated sand. Layer 3, with very high resistivity, suggests bedrock or dense, compacted material.

For foundation suitability, Layer 1 (0–0.9 m) is suitable for shallow foundations if compacted, but may require removal if loose or unstable. Layer 2 (0.9–11.7 m) presents poor foundation conditions due to low resistivity, indicating potential compressibility or water saturation, necessitating deep foundations (e.g., piles) to bypass this layer. Layer 3 (below 11.7 m) is ideal for foundation support if bedrock is confirmed, as it provides a stable and strong base.

4.3.11 VES 1 Station at AAH

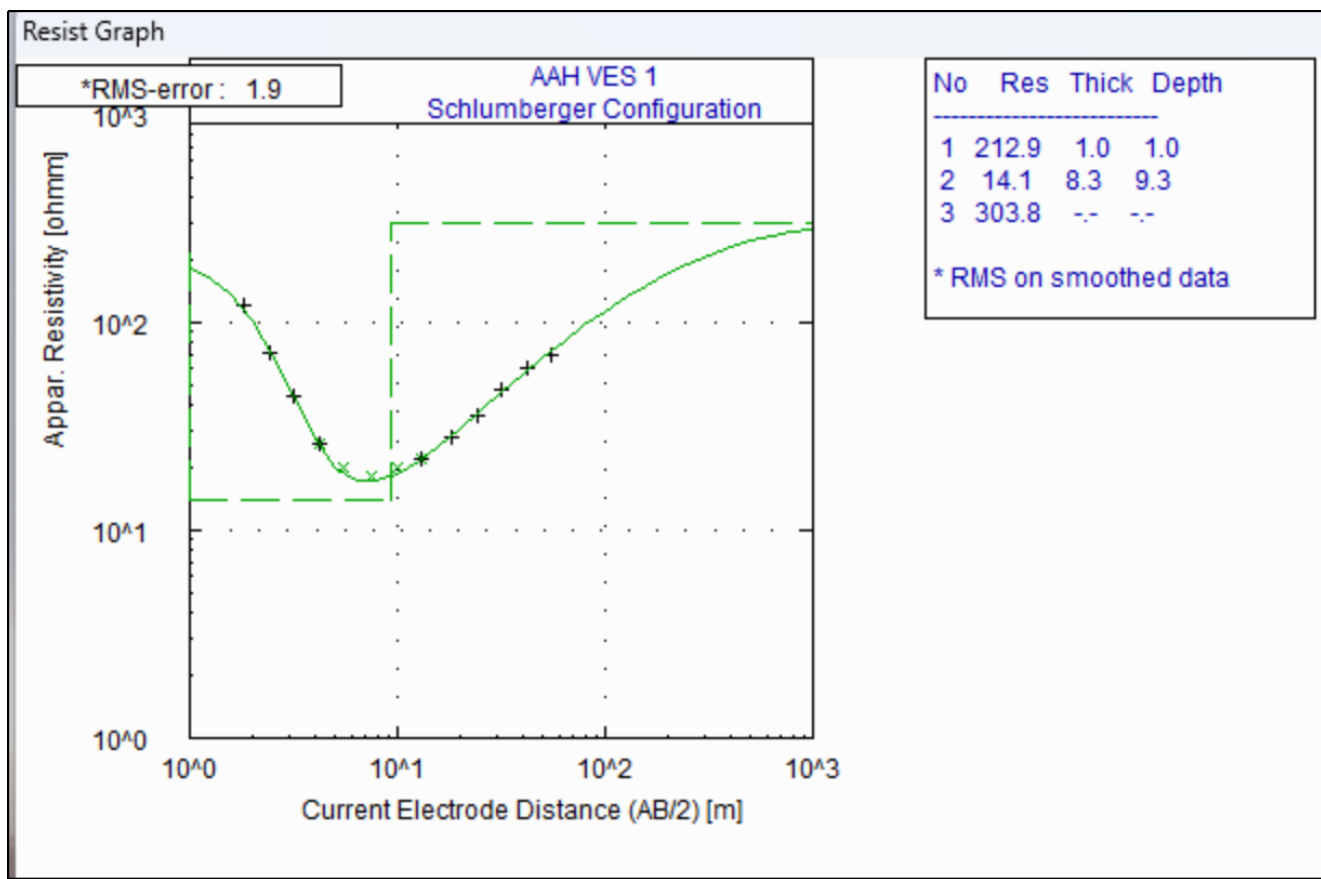


Figure 4.12: Graphical Representation of VES 1

In fig. 4.12, the resistivity significantly drops in Layer 2 and then increases in Layer 3 in fig. 4.122, which aligns with the **H-Type Curve**. This is characterized by a low-resistivity layer (Layer 2) sandwiched between two high-resistivity layers (Layer 1 and Layer 3). This configuration is typical for weathered basement or clay layers underlain by fresh bedrock. The resistivity and thickness data for the layers are as follows: Layer 1 has a resistivity of $212.9 \Omega m$ and a thickness of 1.0 m, corresponding to a depth of 1.0 m. Layer 2 has a resistivity of $14.1 \Omega m$ and a thickness of 8.3 m, extending to a depth of 9.3 m. Layer 3 has a resistivity of $303.8 \Omega m$.

The lithology interpretation for the layers is as follows: Layer 1, with moderate resistivity, likely represents dry, resistive material such as sand or laterite. Layer 2, with a very low resistivity, suggests a conductive layer, possibly clay-rich, water-saturated soil, or a highly weathered zone. Layer 3, with high resistivity, indicates a return to resistive material, likely fractured rock or fresh basement.

4.3.12 VES 2 Station at AAH

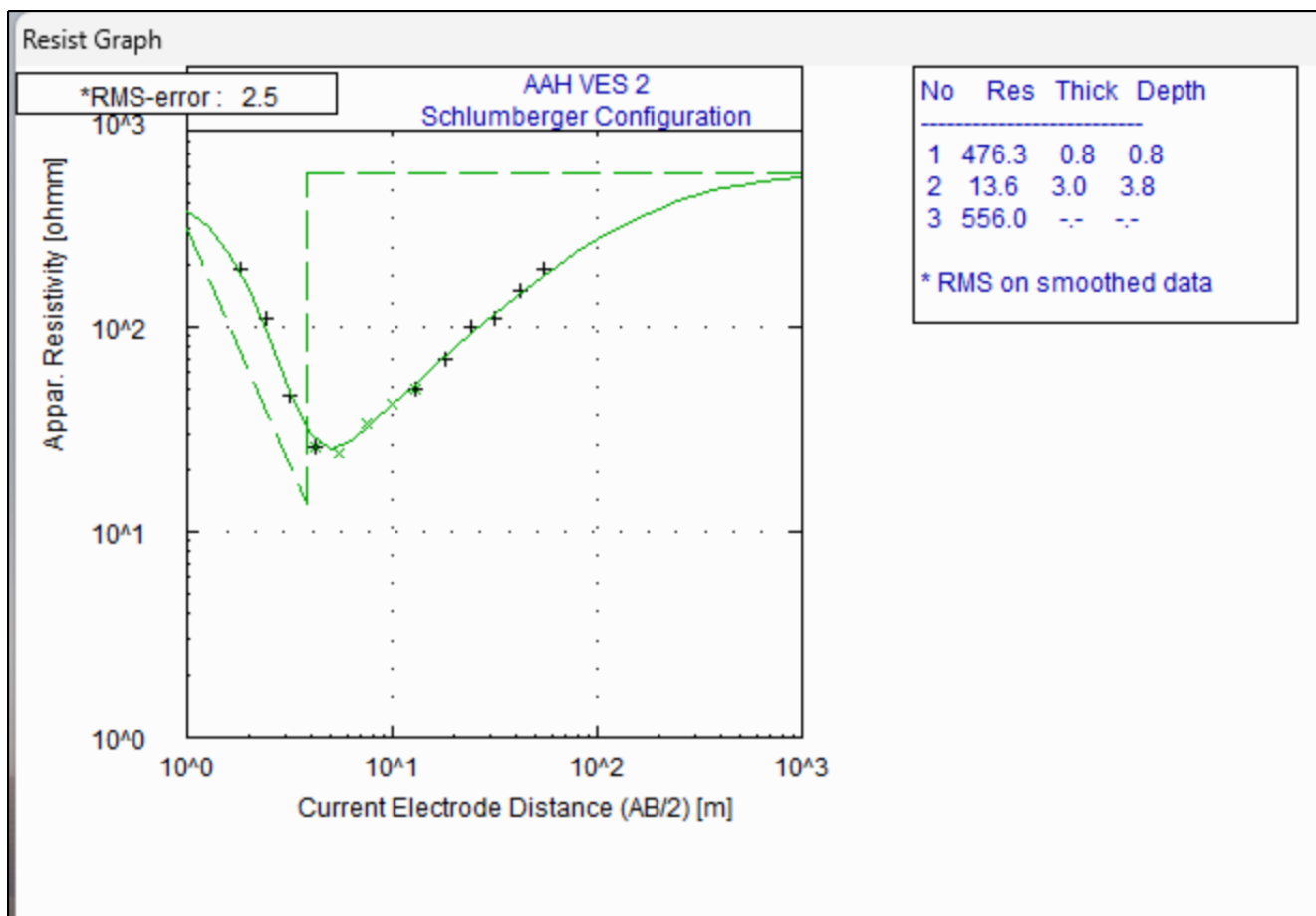


Figure 4.13: Graphical Representation of VES 2

In fig. 4.13, the resistivity and thickness data for the layers are as follows: Layer 1 has a resistivity of $476.3 \Omega \text{ m}$ and a thickness of 0.8 m . Layer 2 has a resistivity of $13.6 \Omega \text{ m}$ and a thickness of 3.0 m . Layer 3 has a resistivity of $556.0 \Omega \text{ m}$. The resistivity decreases significantly in Layer 2 and then increases again in Layer 3, suggesting an **H-Type Curve**. This is typical of a low-resistivity layer (Layer 2) sandwiched between two high-resistivity layers (Layer 1 and Layer 3), often indicative of a weathered basement or clay layer beneath resistive material.

The lithology interpretation for the layers is as follows: Layer 1, with high resistivity, likely represents dry, resistive material such as sand or laterite. Layer 2, with very low resistivity, indicates a conductive layer, likely clay-rich, water-saturated soil, or weathered material. Layer 3, with a very high resistivity, suggests solid or fractured basement rock.

4.3.13 VES 3 Station at AAH

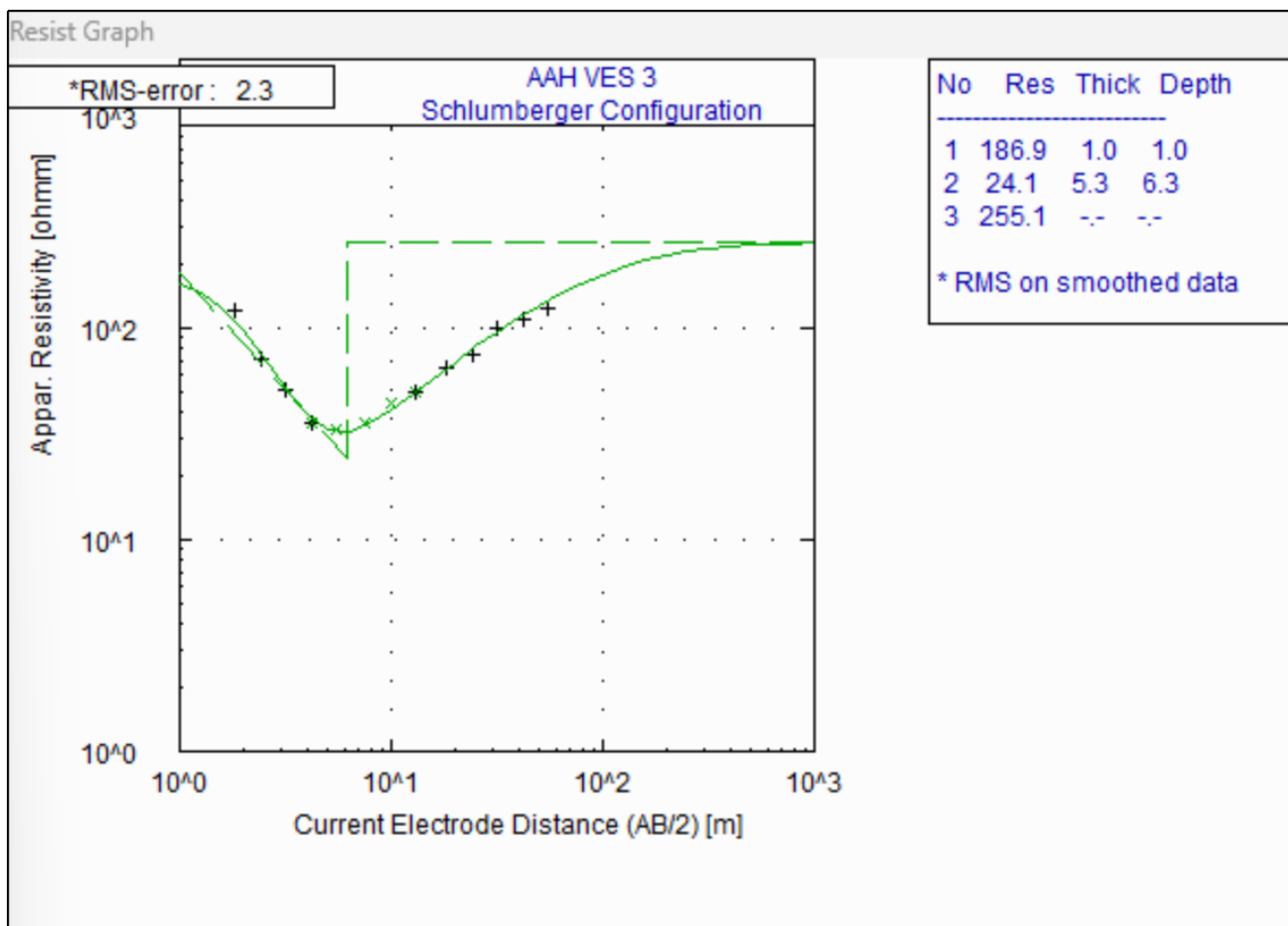


Figure 4.14: Graphical Representation of VES 3

The resistivity and thickness data for the layers in fig. 4.14 are as follows: Layer 1 has a resistivity of $186.9 \Omega \text{ m}$ and a thickness of 1.0 m , corresponding to a depth of 1.0 m . Layer 2 has a resistivity of $24.1 \Omega \text{ m}$ and a thickness of 5.3 m , extending to a depth of 6.3 m . Layer 3 has a resistivity of $255.1 \Omega \text{ m}$. The lithology interpretation suggests that Layer 1, with moderate resistivity, likely represents dry, resistive material such as sand or laterite. Layer 2, with very low resistivity, indicates a conductive layer, possibly clay-rich, water-saturated soil, or a weathered zone. Layer 3, with high resistivity, points to solid or fractured basement rock. The resistivity decreases in Layer 2 and then increases again in Layer 3, aligning with an **H-Type Curve**, which is characterized by a low-resistivity layer (Layer 2) sandwiched between two high-resistivity layers (Layer 1 and Layer 3), typically indicative of weathered basement or clay layers underlain by fresh bedrock.

4.3.14 VES 4 Station at AAH

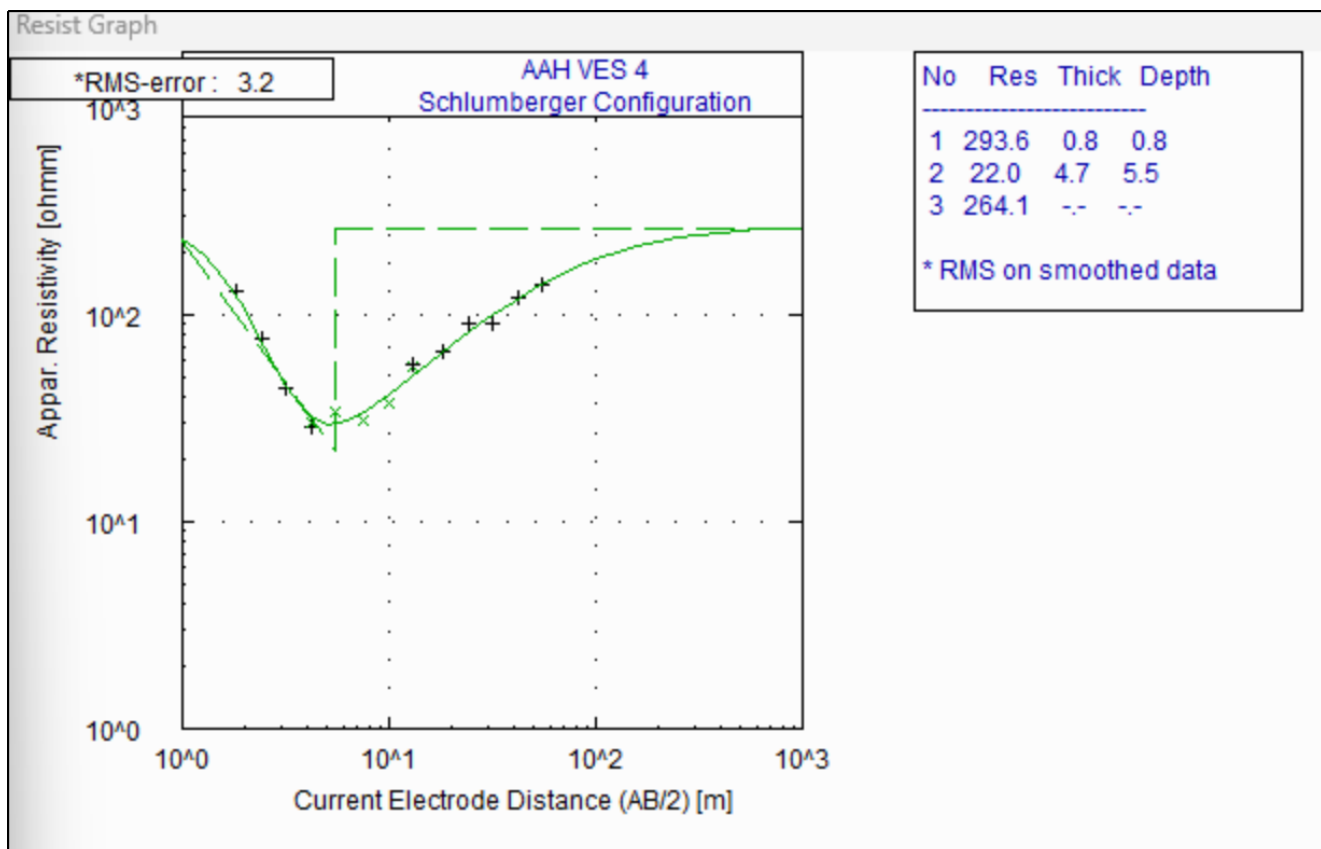


Figure 4.15: Graphical Representation of VES 4

The resistivity and thickness data for the layers in fig. 4.15 are as follows: Layer 1 has a resistivity of $293.6 \Omega \text{ m}$ and a thickness of 0.8 m , corresponding to a depth of 0.8 m . Layer 2 has a resistivity of $22.0 \Omega \text{ m}$ and a thickness of 4.7 m , extending to a depth of 5.5 m . Layer 3 has a resistivity of $264.1 \Omega \text{ m}$.

The lithology interpretation suggests that Layer 1, with high resistivity, likely represents dry, resistive material such as sand or laterite. Layer 2, with a much lower resistivity, indicates a conductive layer, possibly clay-rich, water-saturated soil, or a weathered zone. Layer 3, with moderate resistivity, likely represents a transition to solid or fractured basement rock. The resistivity decreases in Layer 2 and then increases in Layer 3, aligning with an **H-Type Curve**, characterized by a low-resistivity layer (Layer 2) sandwiched between two high-resistivity layers (Layer 1 and Layer 3), which is typically indicative of a weathered basement or clay layer beneath resistive material.

4.3.15 VES 5 Station at AAH

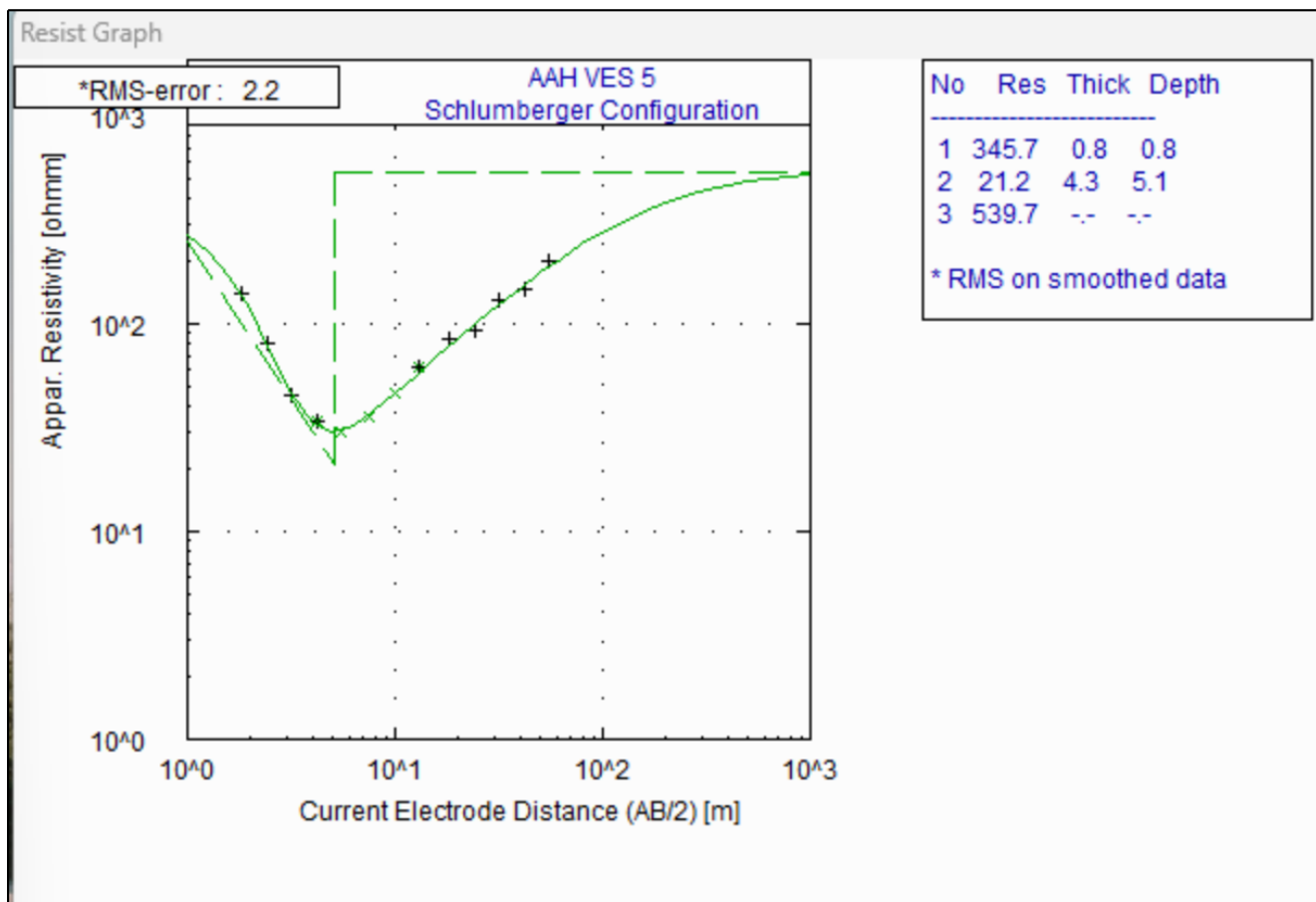


Figure 4.16: Graphical Representation of VES 5

The resistivity and thickness data for the layers in fig. 4.16 are as follows: Layer 1 has a resistivity of $345.7 \Omega \text{ m}$ and a thickness of 0.8 m , corresponding to a depth of 0.8 m . Layer 2 has a resistivity of $21.2 \Omega \text{ m}$ and a thickness of 4.3 m , extending to a depth of 5.1 m . Layer 3 has a resistivity of $539.7 \Omega \text{ m}$. The lithology interpretation suggests that Layer 1, with high resistivity, likely represents dry, resistive material such as sand or laterite. Layer 2, with much lower resistivity, indicates a conductive layer, possibly clay-rich, water-saturated soil, or a weathered zone. Layer 3, with a very high resistivity, suggests solid or fractured basement rock.

The resistivity decreases in Layer 2 and then increases in Layer 3, indicating an **H-Type Curve**, characterized by a low-resistivity layer (Layer 2) sandwiched between two high-resistivity layers (Layer 1 and Layer 3), typical of weathered basement or clay layers underlain by fresh bedrock.

4.3.16 VES 6 Station at AAH

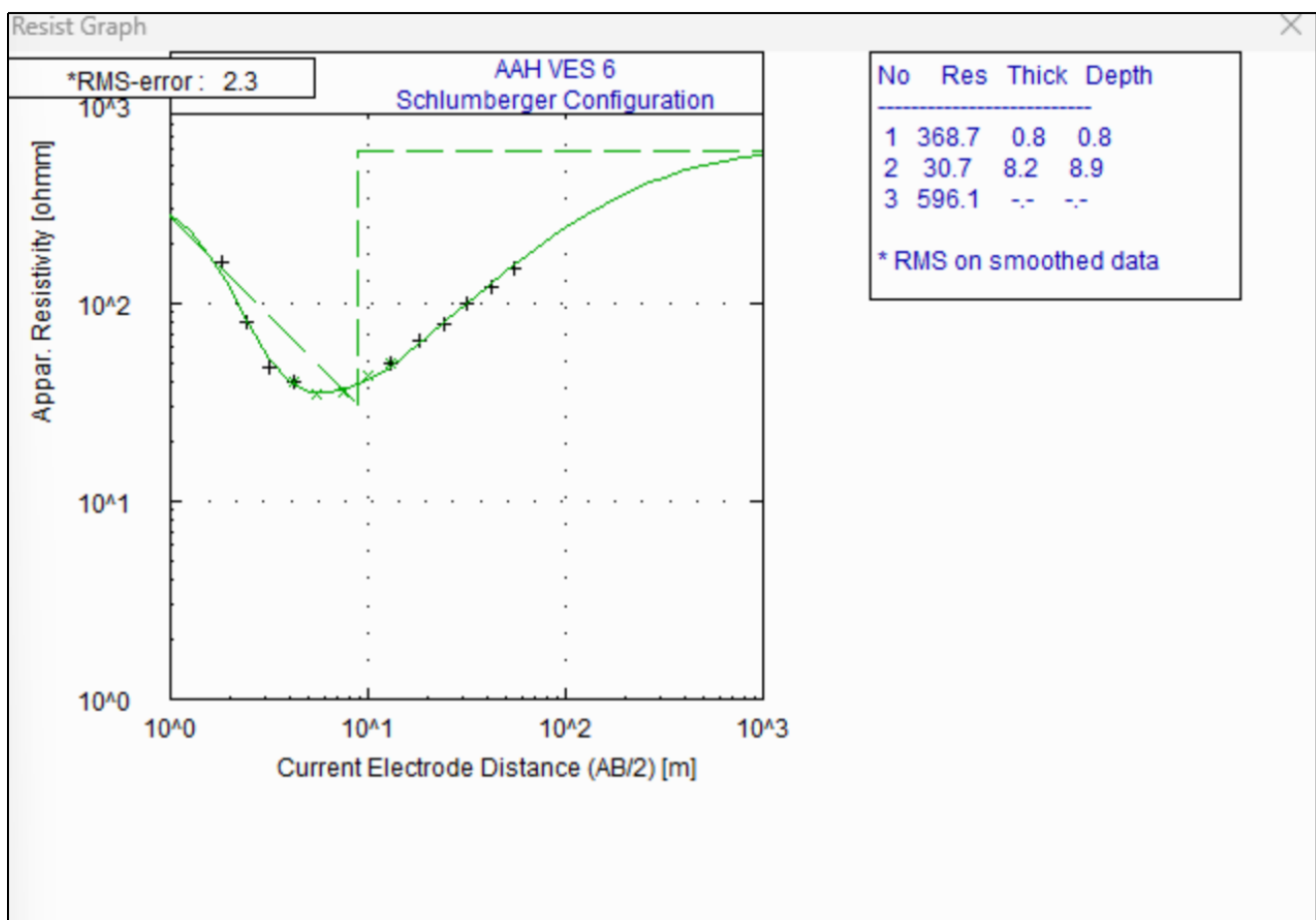


Figure 4.17: Graphical Representation of VES 6

The resistivity and thickness data for the layers in fig. 4.17 are as follows: Layer 1 has a resistivity of $368.7 \Omega m$ and a thickness of 0.8 m, corresponding to a depth of 0.8 m. Layer 2 has a resistivity of $30.7 \Omega m$ and a thickness of 8.2 m, extending to a depth of 8.9 m. Layer 3 has a resistivity of $596.1 \Omega m$. The lithology interpretation suggests that Layer 1, with high resistivity, likely represents dry, resistive material such as sand or laterite. Layer 2, with a lower resistivity, indicates a conductive layer, possibly clay-rich, water-saturated soil, or a weathered zone. Layer 3, with very high resistivity, suggests solid or fractured basement rock.

The resistivity decreases in Layer 2 and then increases in Layer 3, aligning with an **H-Type Curve**, characterized by a low-resistivity layer (Layer 2) sandwiched between two high-resistivity layers (Layer 1 and Layer 3), indicative of a weathered basement or clay layer beneath resistive material.

4.3.17 VES 7 Station at AAH

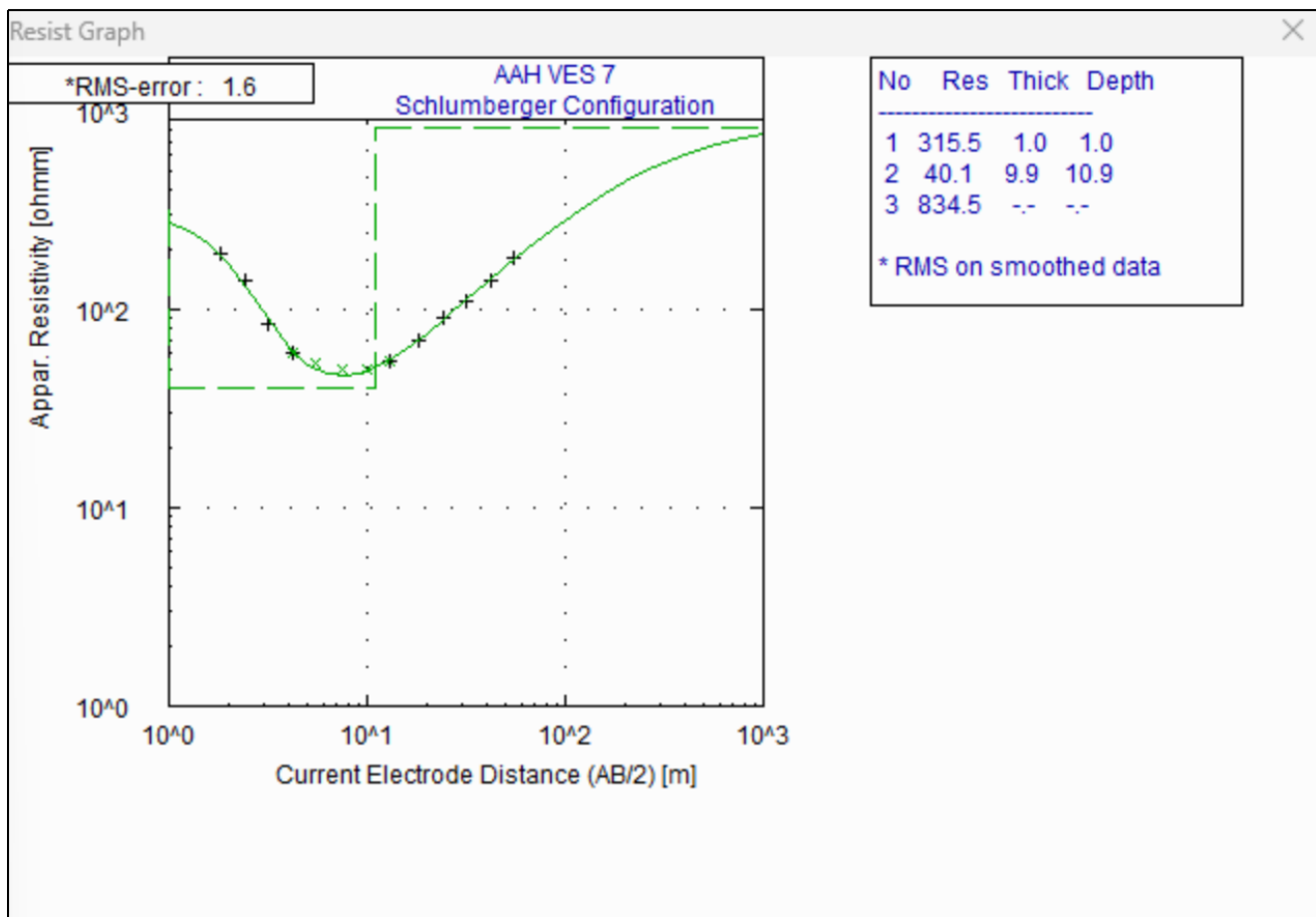


Figure 4.18: Graphical Representation of VES 7

The resistivity and thickness data for the layers in fig. 4.18 are as follows: Layer 1 has a resistivity of $315.5 \Omega m$ and a thickness of $1.0 m$, corresponding to a depth of $1.0 m$. Layer 2 has a resistivity of $40.1 \Omega m$ and a thickness of $9.9 m$, extending to a depth of $10.9 m$. Layer 3 has a resistivity of $834.5 \Omega m$. The lithology interpretation suggests that Layer 1, with high resistivity, likely represents dry, resistive material such as sand or laterite. Layer 2, with much lower resistivity, indicates a conductive layer, possibly clay-rich, water-saturated soil, or a weathered zone. Layer 3, with very high resistivity, points to solid or fractured basement rock.

The resistivity decreases in Layer 2 and then increases again in Layer 3, fitting an **H-Type Curve**, characterized by a low-resistivity layer (Layer 2) sandwiched between two high-resistivity layers (Layer 1 and Layer 3), typically indicative of weathered basement or clay layers underlain by fresh bedrock.

4.3.18 VES 8 Station at AAH

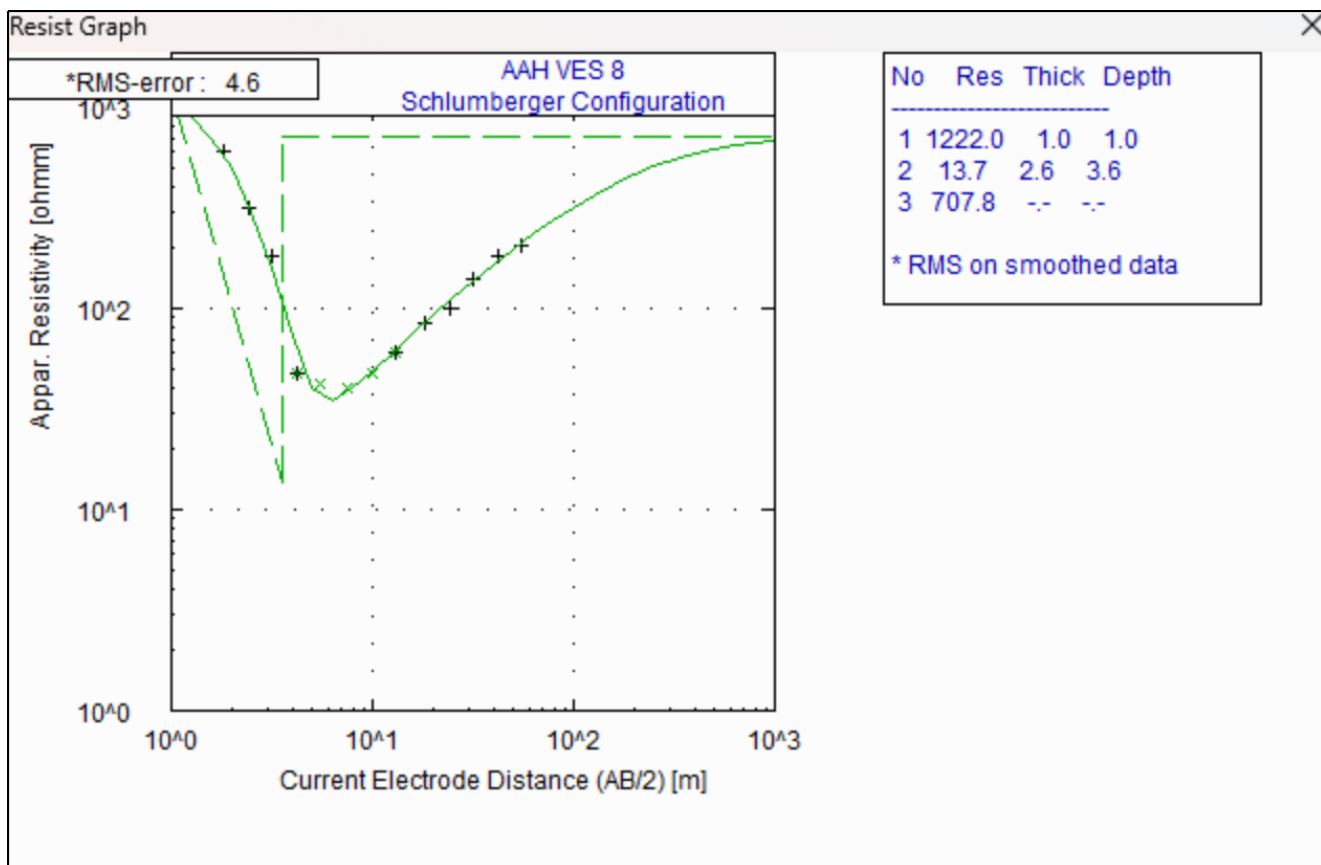


Figure 4.19: Graphical Representation of VES 8

The resistivity and thickness data for the layers in fig. 4.19 are as follows: Layer 1 has a resistivity of $1222.0 \Omega m$ and a thickness of $1.0 m$, corresponding to a depth of $1.0 m$. Layer 2 has a resistivity of $13.7 \Omega m$ and a thickness of $2.6 m$, extending to a depth of $3.6 m$. Layer 3 has a resistivity of $707.8 \Omega m$. The lithology interpretation suggests that Layer 1, with very high resistivity, represents fresh bedrock or basement rock. Layer 2, with very low resistivity, indicates a conductive layer, likely clay-rich or water-saturated soil. Layer 3, with high resistivity, points to solid or fractured basement rock. The resistivity decreases in Layer 2 and then increases again in Layer 3, fitting an **H-Type Curve**, characterized by a low-resistivity layer (Layer 2) sandwiched between two high-resistivity layers (Layer 1 and Layer 3), indicative of a weathered basement or clay layer beneath resistive material.

4.3.19 VES 9 Station at AAH

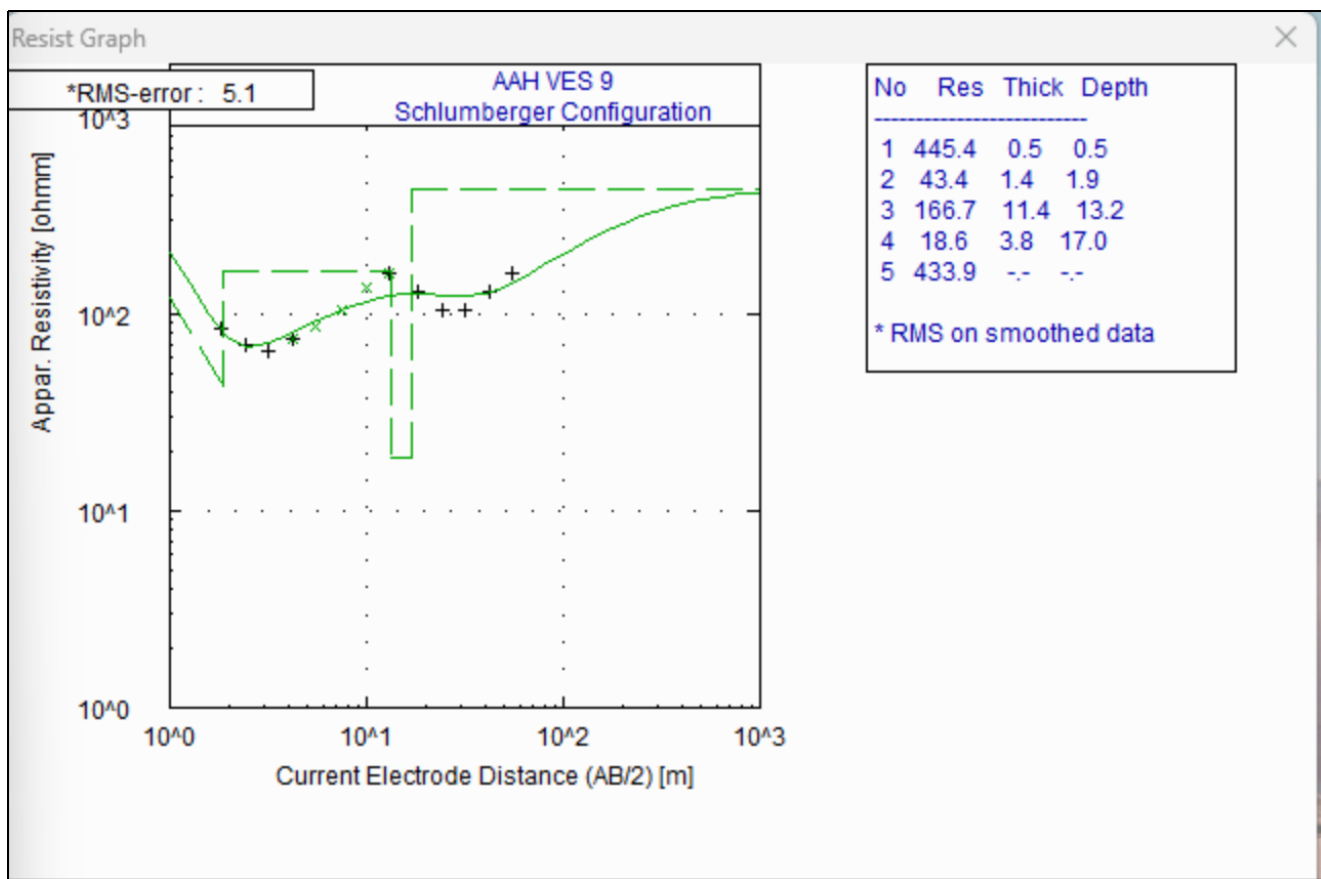


Figure 4.20: Graphical Representation of VES 9

The resistivity pattern shown in fig. 4.20 indicates a **KHK-Type Curve**. The resistivity and thickness data for the layers are as follows: Layer 1 has a resistivity of $445.4 \Omega\cdot m$ and a thickness of 0.5m, corresponding to a depth of 0.5m. Layer 2 has a resistivity of $43.4 \Omega\cdot m$ and a thickness of 1.4 m, extending to a depth of 1.9 m. Layer 3 has a resistivity of $166.7 \Omega\cdot m$ and a thickness of 11.4 m, reaching a depth of 13.2 m. Layer 4 has a resistivity of $18.6 \Omega\cdot m$ and a thickness of 3.8 m, extending to a depth of 17.0 m. Layer 5 has a resistivity of $433.9 \Omega\cdot m$ and extends beyond the measured depth.

The lithology interpretation suggests that: Layer 1, with high resistivity, represents dry or compacted material, such as laterite or dry sand. Layer 2, with significantly lower resistivity, could indicate clay or water-saturated soil. Layer 3, with increased resistivity, suggests compacted rock or unsaturated sandstone. Layer 4, with very low resistivity, points to a highly conductive, water-bearing formation or clayey material. Layer 5, with high resistivity, may represent a consolidated bedrock or a dry formation beneath the surveyed depth.

For foundation suitability: Layer 1 (0–0.5 m) may be suitable for shallow foundations if compact. Layer 2 (0.5–1.9 m) requires evaluation due to possible instability. Layer 3 (1.9–13.2 m) is more stable and can support deep foundations. Layer 4 (13.2–17.0 m) should be assessed for load-bearing capacity before construction. Layer 5 (below 17.0 m) might be suitable for deep

foundation anchorage, depending on its geological characteristics.

4.3.20 VES 10 Station at AAH

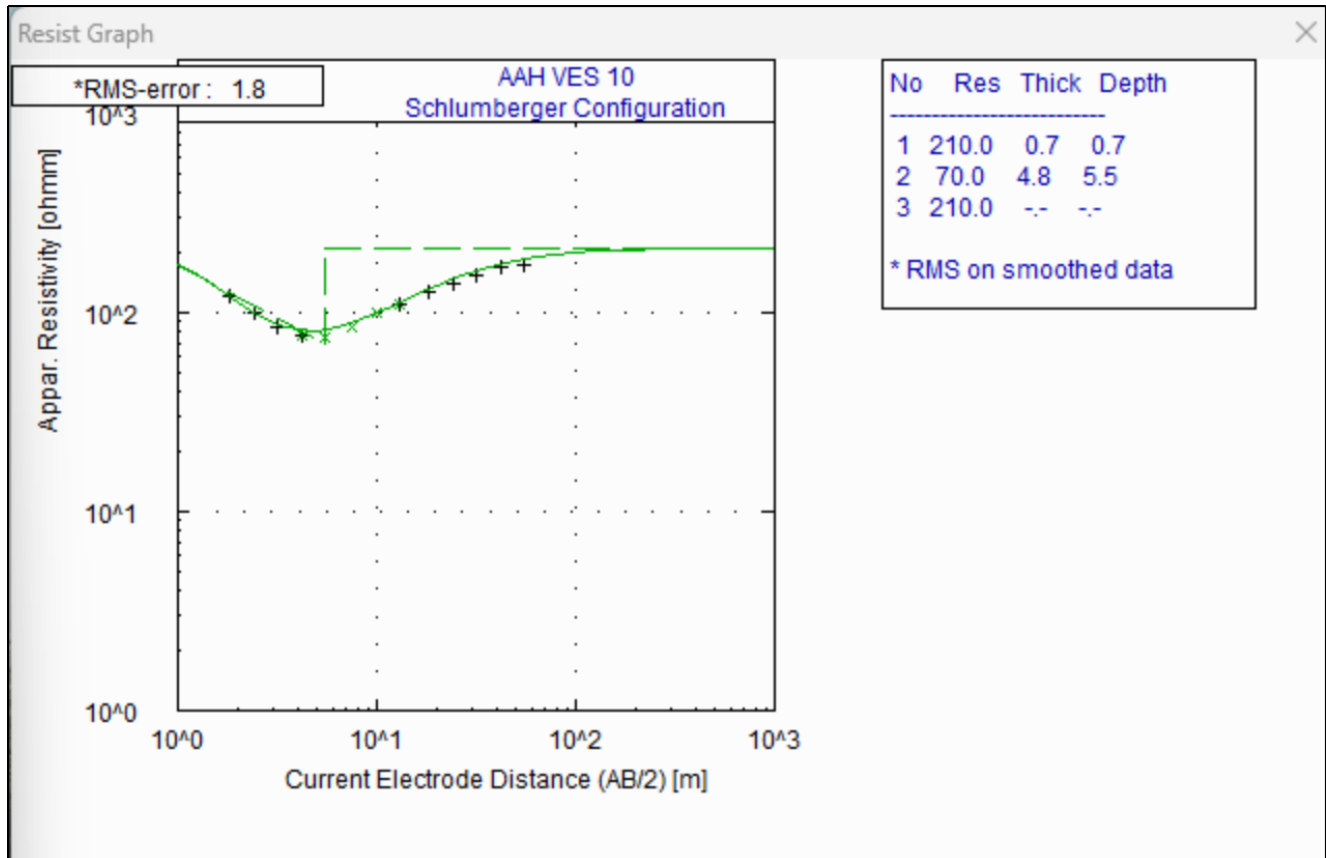
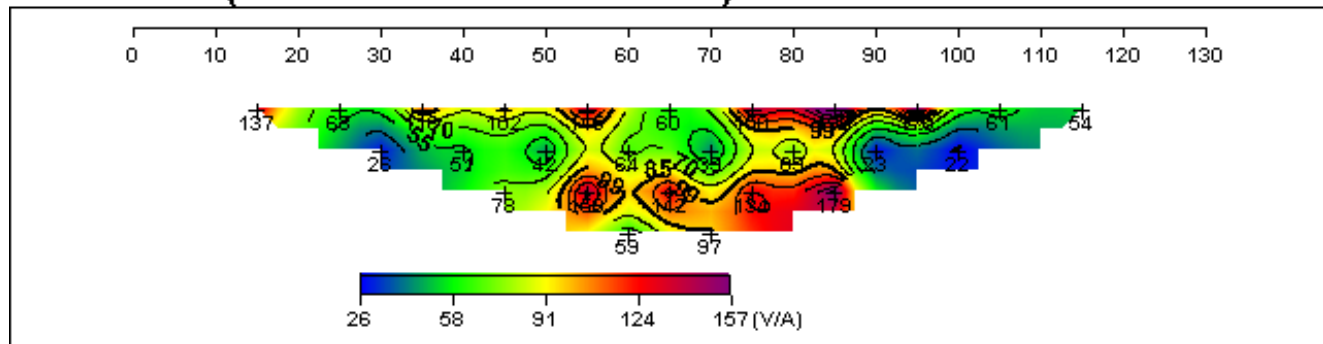


Figure 4.21: Graphical Representation of VES 10

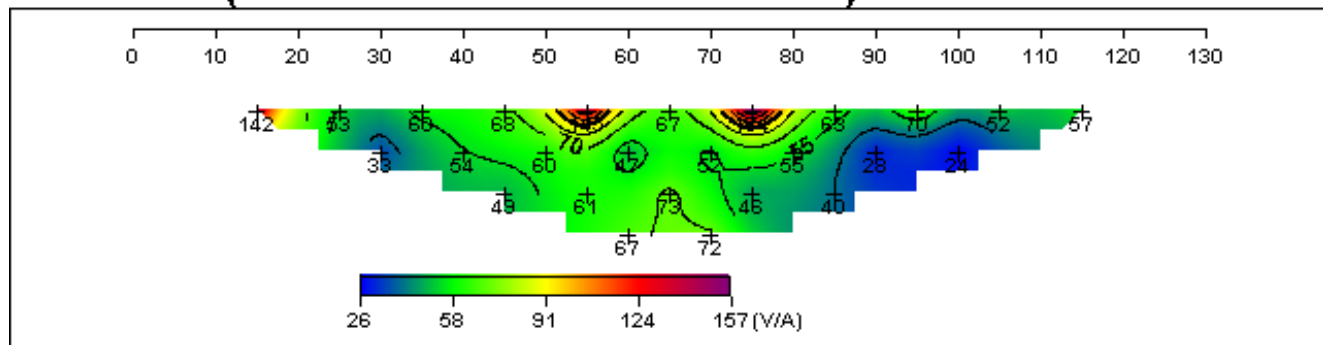
In fig. 4.21, the resistivity and thickness data for the layers are as follows: Layer 1 has a resistivity of $210.0 \Omega \text{ m}$ and a thickness of 0.7 m , corresponding to a depth of 0.7 m . Layer 2 has a resistivity of $70.0 \Omega \text{ m}$ and a thickness of 4.8 m , extending to a depth of 5.5 m . Layer 3 has a resistivity of $210.0 \Omega \text{ m}$. The lithology interpretation suggests that Layer 1, with moderate resistivity, likely represents dry or resistive material. Layer 2, with lower resistivity, indicates a conductive layer, possibly clay-rich or water-saturated soil. Layer 3, with high resistivity, suggests solid or fractured basement rock. The resistivity pattern indicates an **H-Type Curve**, with a low-resistivity layer (Layer 2) sandwiched between two high-resistivity layers (Layer 1 and Layer 3), typical of weathered basement or clay-rich layers beneath resistive material.

4.4 Constant Separation Traversing Data Interpretation

PROFILE 1 (Field Data Pseudosection)



PROFILE 1 (Theoretical Data Pseudosection)



PROFILE 1 (2-D Resistivity Structure)

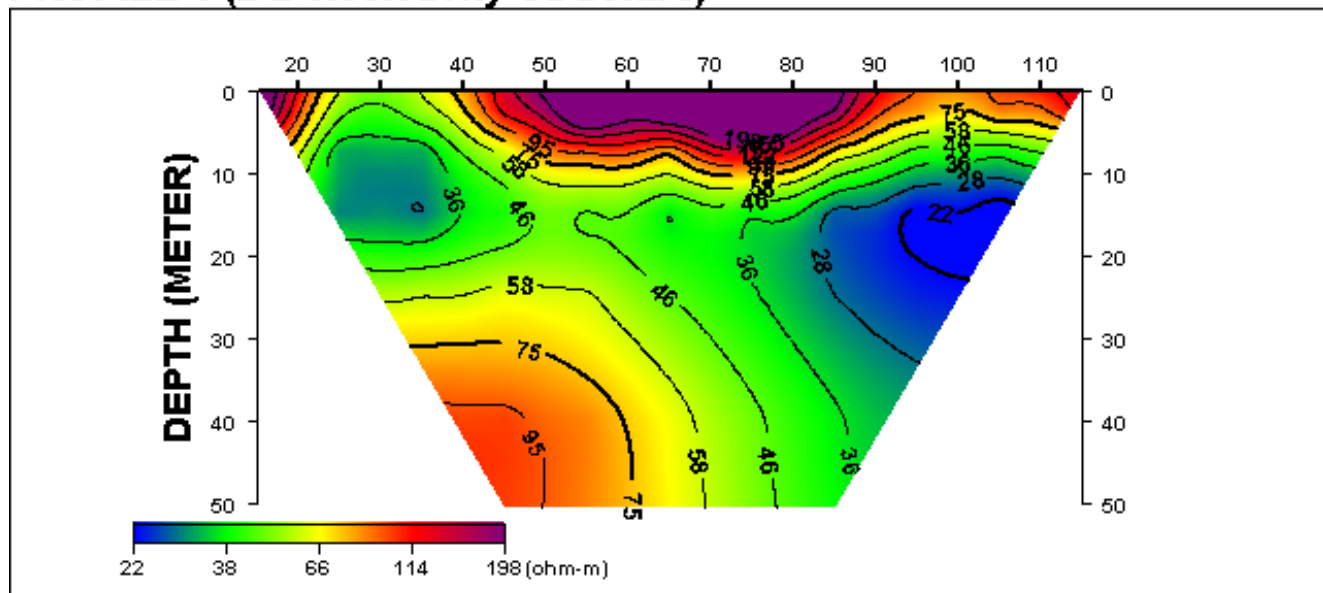
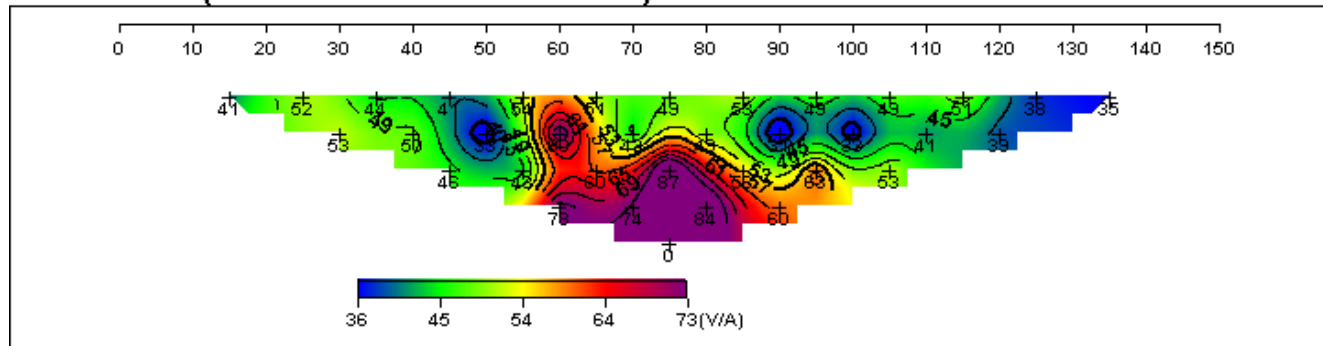
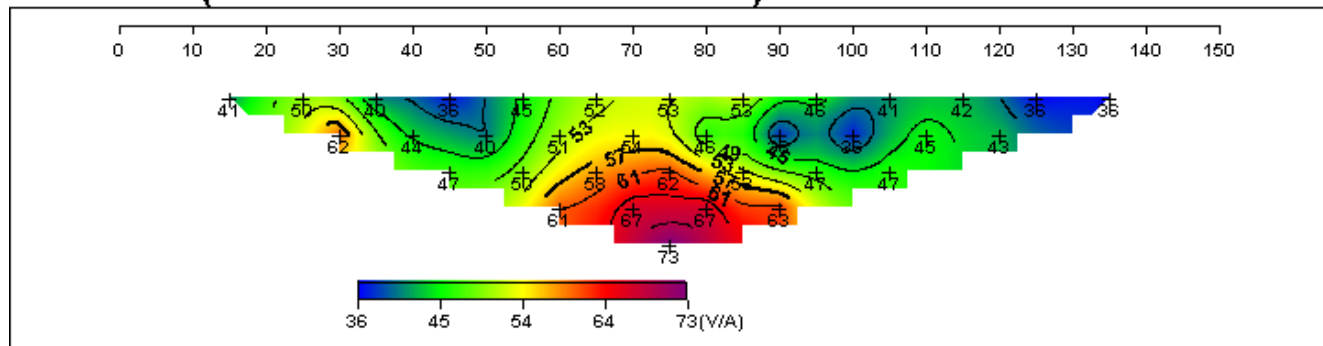


Figure 4.22: 2D View of CST Profile 1

PROFILE 2 (Field Data Pseudosection)



PROFILE 2 (Theoretical Data Pseudosection)



PROFILE 2 (2-D Resistivity Structure)

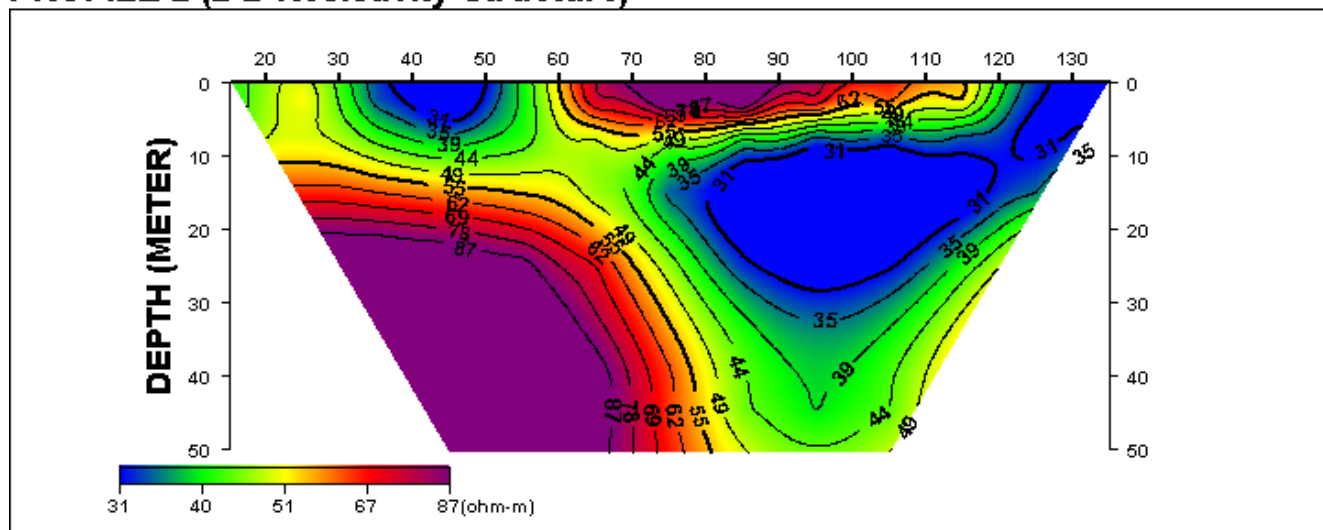
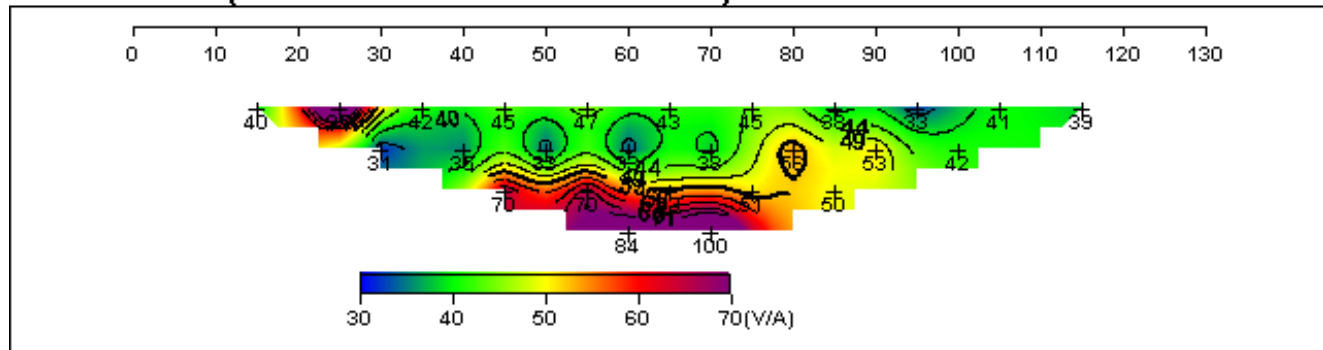
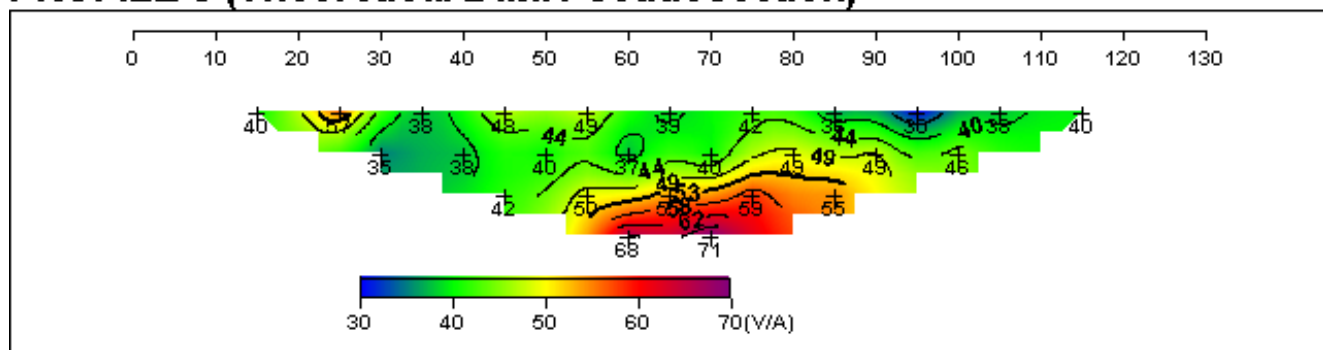


Figure 4.23: 2D View of CST Profile 2

PROFILE 3 (Field Data Pseudosection)



PROFILE 3 (Theoretical Data Pseudosection)



PROFILE 3 (2-D Resistivity Structure)

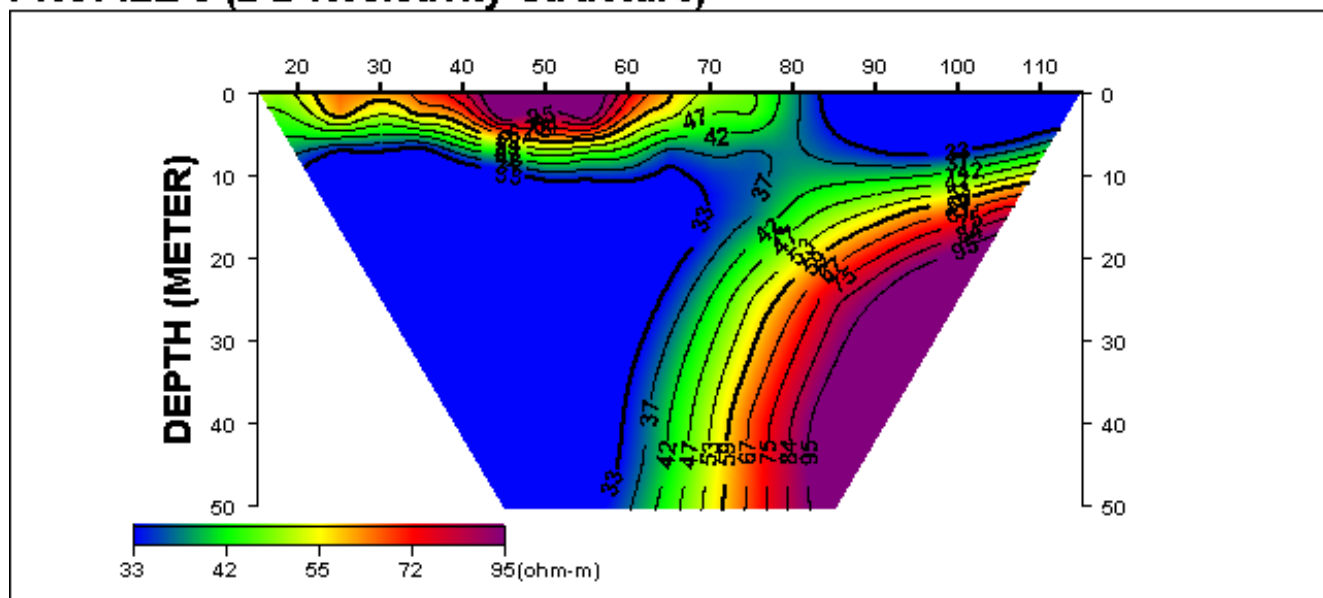
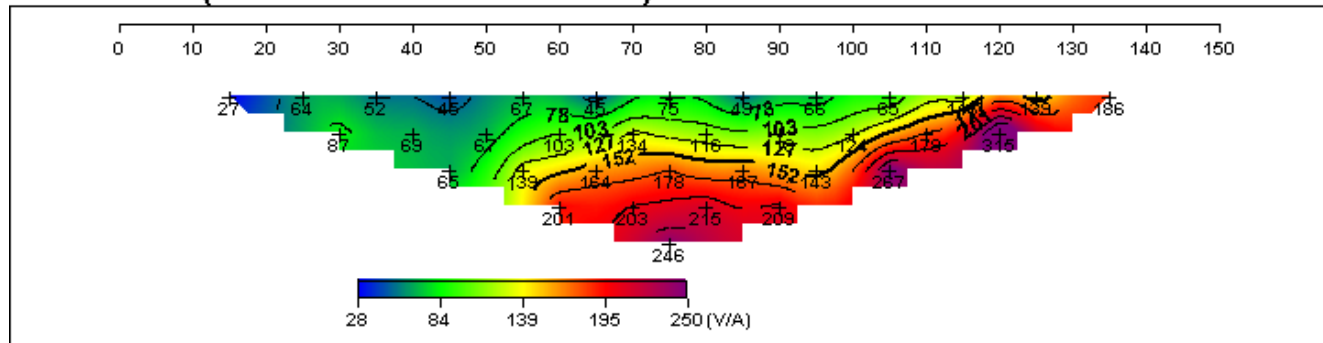
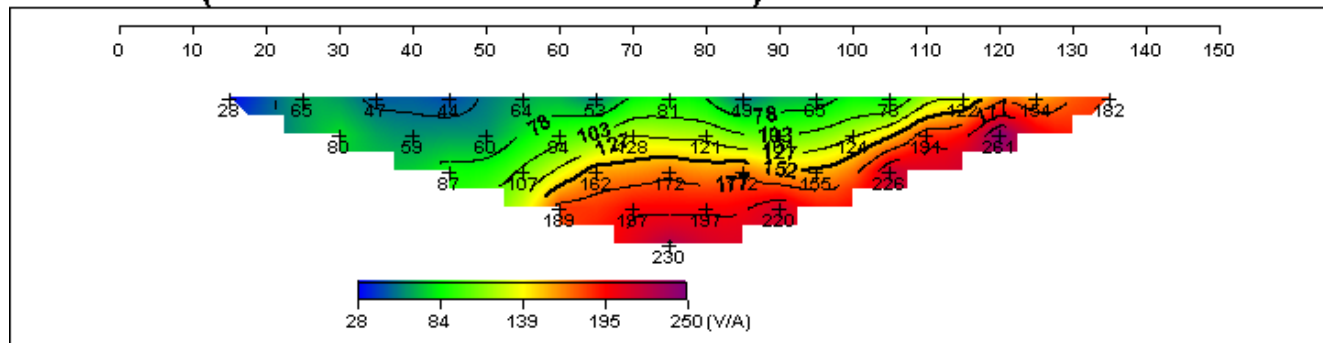


Figure 4.24: 2D View of CST Profile 3

PROFILE 1 (Field Data Pseudosection)



PROFILE 1 (Theoretical Data Pseudosection)



PROFILE 1 (2-D Resistivity Structure)

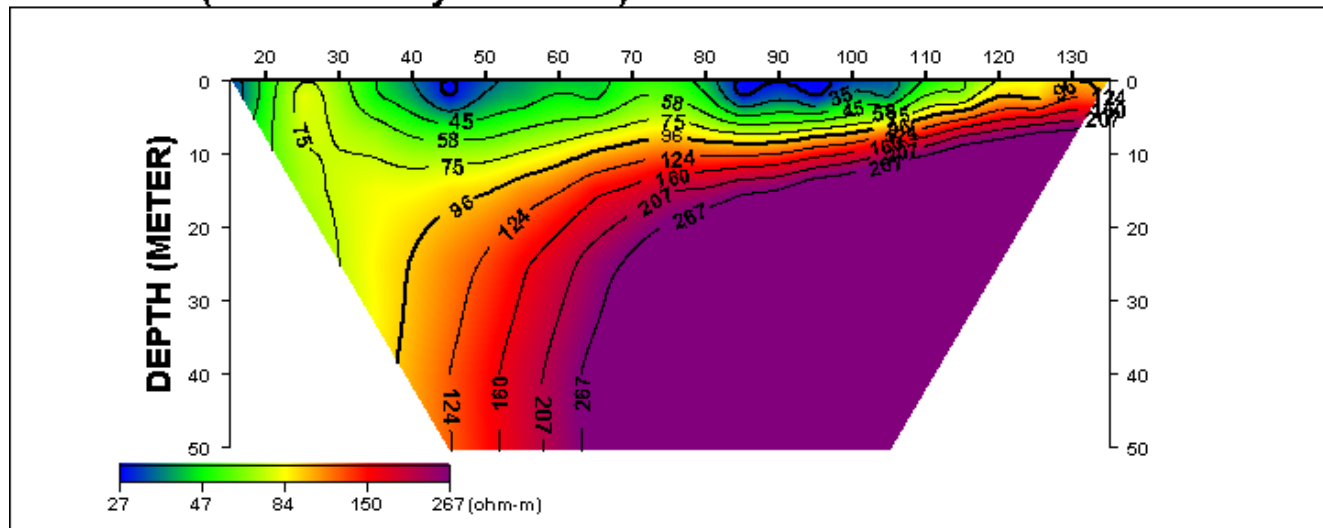
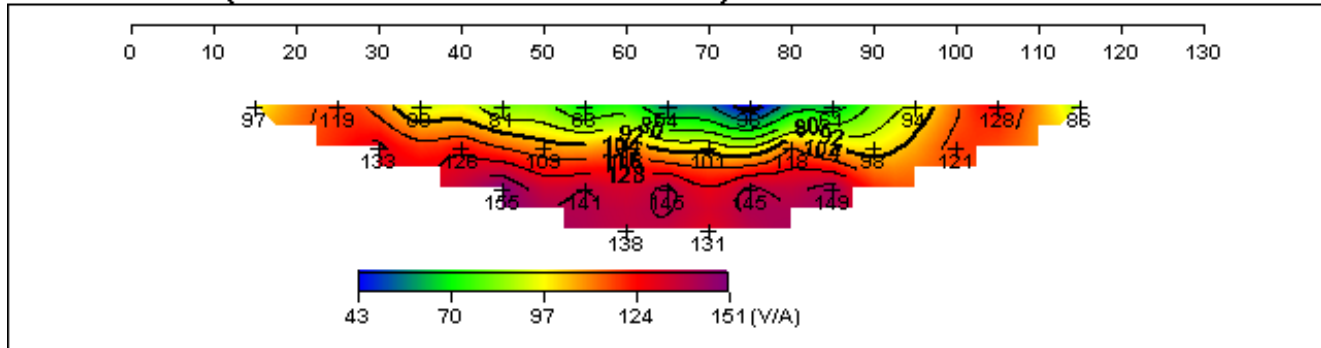
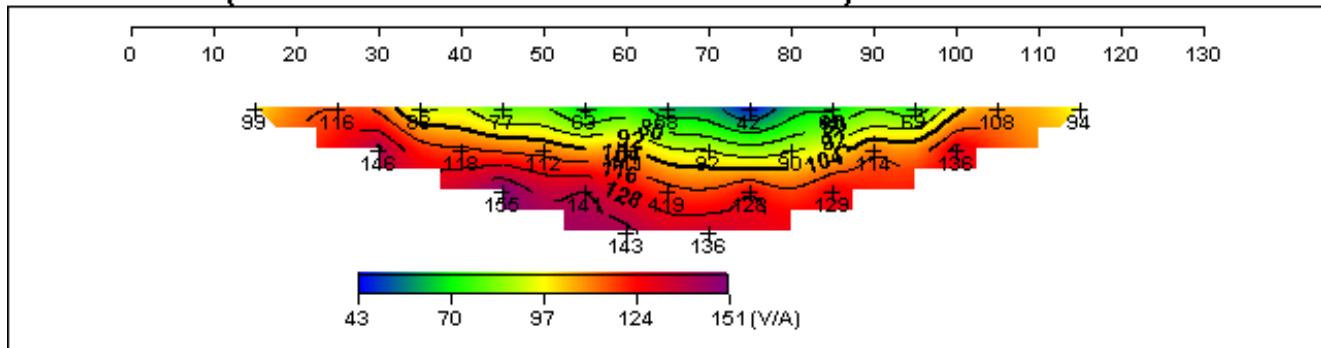


Figure 4.25: 2D View of CST Profile 1 at AAH

PROFILE 2 (Field Data Pseudosection)



PROFILE 2 (Theoretical Data Pseudosection)



PROFILE 2 (2-D Resistivity Structure)

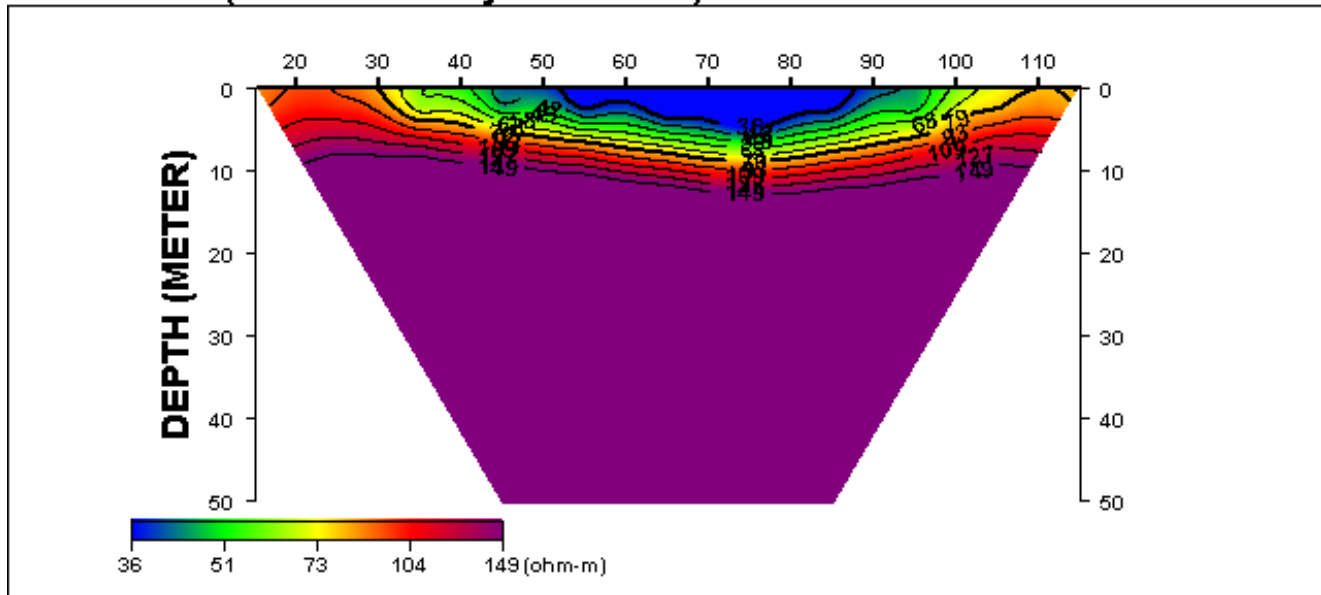


Figure 4.26: 2D View of CST Profile 2 at AAH

4.5 Interpretation of the Profiles

4.5.1 Resistivity Variations

1. **Field Data Pseudosection:** Red colors (e.g., 250 V/A) indicate high resistivity, suggesting coarse-grained materials like sand and gravel. Blue colors (e.g., 26 V/A) suggest low

- resistivity, indicating saturated, fine-grained materials like clay or silt.
2. **Theoretical Data Pseudosection:** Similar resistivity trends as the field data, with smoother variations.
 3. **2-D Resistivity Structure:** Red colors (e.g., 267 Ωm) shown in Figure 4.27 represent high resistivity, while blue colors (e.g., 22 Ωm) shown in Figure 4.24 represent low resistivity.

4.5.2 Profile 1 at UI Mosque

Fig. 4.22: Geological features inferred from the resistivity data include an estimated depth to bedrock around 50 meters, evidenced by increasing resistivity with depth. Abrupt changes in resistivity, such as transitions from low to high resistivity zones, may indicate potential faults or fractures. Low resistivity zones near the surface suggest areas with potential groundwater presence. For foundation design, high resistivity zones likely indicate coarse-grained soils suitable for bearing loads, while low resistivity zones suggest fine-grained soils that may require careful consideration due to potential settlement issues. Abrupt resistivity changes warrant careful evaluation for foundation stability. Furthermore, the depth to bedrock and the presence of saturated zones will influence the potential for foundation settlement. Construction considerations include potentially easier excavation in high resistivity zones and the possible need for dewatering measures in low resistivity zones.

4.5.3 Profile 2 at UI Mosque

Fig. 4.23: The 2-D resistivity structure suggests potential variations in subsurface materials, with higher resistivity zones (red colors, e.g., 87 ohm-m) likely representing less conductive materials such as coarse-grained soils or bedrock, and lower resistivity zones (blue colors, e.g., 31 ohm-m) potentially indicating more conductive materials such as fine-grained soils or saturated zones. Abrupt changes in resistivity within the profile may indicate potential faults or fractures. Regarding foundation design, the resistivity data can help assess the suitability of the ground for different foundation types. Higher resistivity zones may be more suitable for shallow foundations, while lower resistivity zones may require careful consideration due to potential settlement issues and may necessitate deeper foundations or ground improvement measures.

4.5.4 Profile 3 at UI Mosque

Fig. 4.24: The 2-D resistivity structure of Profile 3 provides insights into the subsurface conditions. A likely depth to bedrock of around 50 meters is suggested by an overall increase in resistivity with depth. Abrupt changes in resistivity, such as the shift from low to high resistivity around the 70-meter mark, may indicate potential faults or fractures. The presence of low resistivity zones, particularly evident in the central portion of the profile, suggests areas with potentially higher moisture content or groundwater presence.

These geological features have significant implications for foundation design. High resistivity zones (red) likely indicate coarse-grained soils, which generally offer good bearing capacity. Conversely, low resistivity zones (blue) suggest fine-grained soils, which may have lower bearing capacity and higher potential for settlement. Abrupt resistivity changes, potentially indicating faults or fractures, require careful consideration for foundation stability. Moreover, the depth to bedrock and the presence of low resistivity zones influence the potential for foundation settlement. Areas with lower resistivity may be more prone to settlement and may require deeper foundations or ground improvement measures.

4.5.5 Profile 1 at AAH

Fig. 4.25: Profile 1 reveals significant resistivity variations. The 2-D resistivity structure suggests a likely depth to bedrock beyond 50 meters, indicated by the continued increase in resistivity with depth. Abrupt changes in resistivity, such as the shift from low to high resistivity zones, may indicate potential faults or fractures. Low resistivity zones, particularly evident near the surface, suggest areas with potentially higher moisture content or groundwater presence. High resistivity zones likely indicate coarse-grained soils, while low resistivity zones suggest fine-grained soils. These variations have important implications for foundation design. High resistivity zones may be suitable for shallow foundations, while low resistivity zones may require careful consideration due to potential settlement issues and may necessitate deeper foundations or ground improvement measures. Abrupt resistivity changes require careful evaluation for foundation stability.

4.5.6 Profile 2 at AAH

Fig. 4.26: Profile 2 reveals significant resistivity variations. The 2-D resistivity structure suggests a likely depth to bedrock beyond 50 meters, indicated by the continued increase in resistivity with depth. Abrupt changes in resistivity within the profile, such as the shift from low resistivity (blue) to high resistivity (red) in different sections, may indicate potential faults or fractures. Low resistivity zones (blue colors), especially near the surface, suggest areas with potentially higher moisture content or groundwater presence.

These geological features have important implications for foundation design. High resistivity zones (red) likely indicate coarse-grained soils like sand and gravel, which generally have good bearing capacity. Conversely, low resistivity zones (blue) suggest fine-grained soils like clay and silt, which may have lower bearing capacity and higher potential for settlement. Abrupt resistivity changes, potentially indicating faults or fractures, require careful consideration for foundation stability. Moreover, the depth to bedrock and the presence of low resistivity zones (indicating potentially saturated soils) will influence the potential for foundation settlement. Areas with lower resistivity may be more prone to settlement and may require deeper foundations or ground improvement measures.

4.6 Geoelectric Section along the Profiles using Surfer

4.6.1 UI Mosque Profile 1 Geoelectric Section

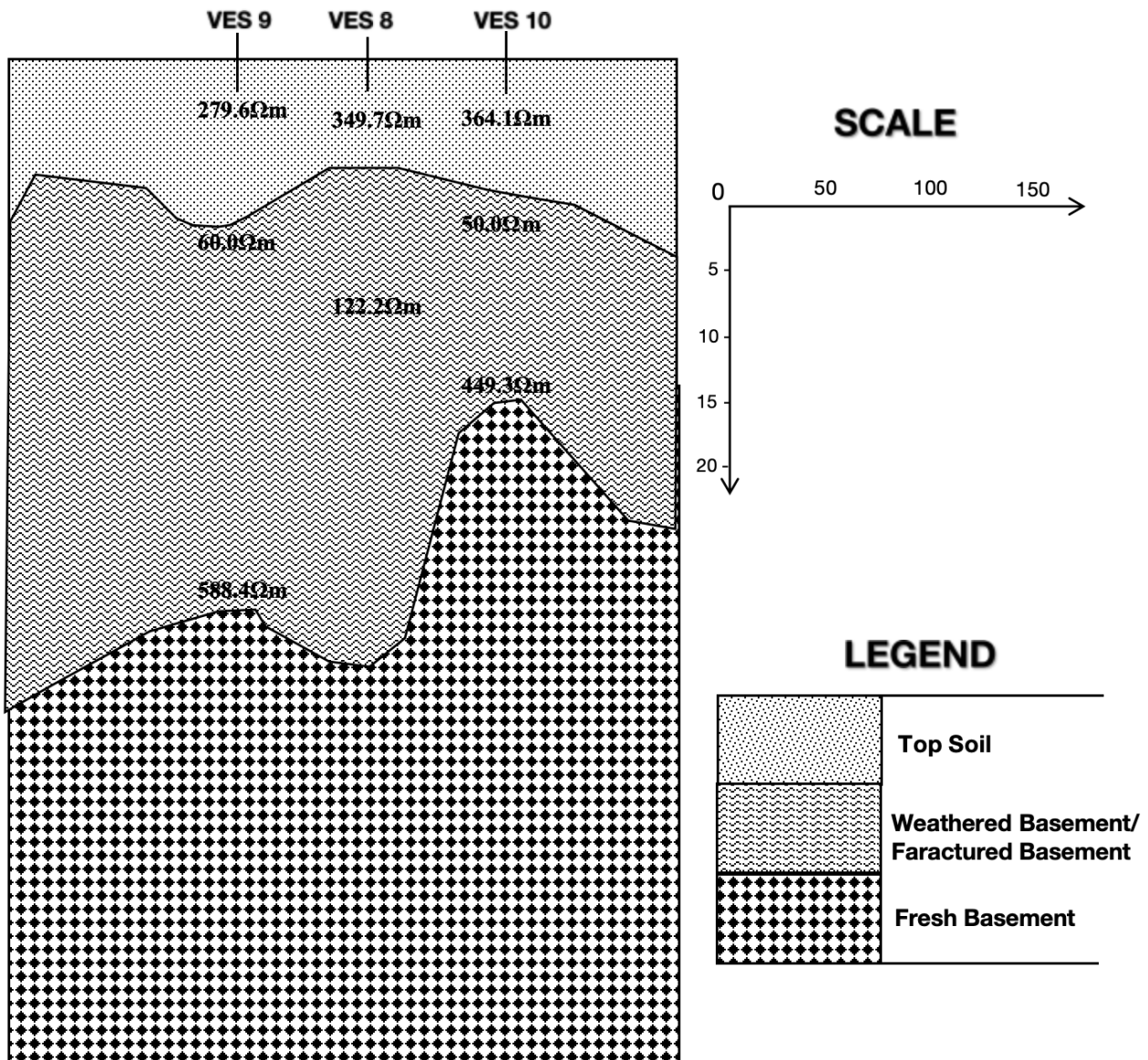


Figure 4.27: Geoelectric Section along Profile 1 at UI Mosque using Surfer

4.6.2 UI Mosque Profile 2 Geoelectric Section

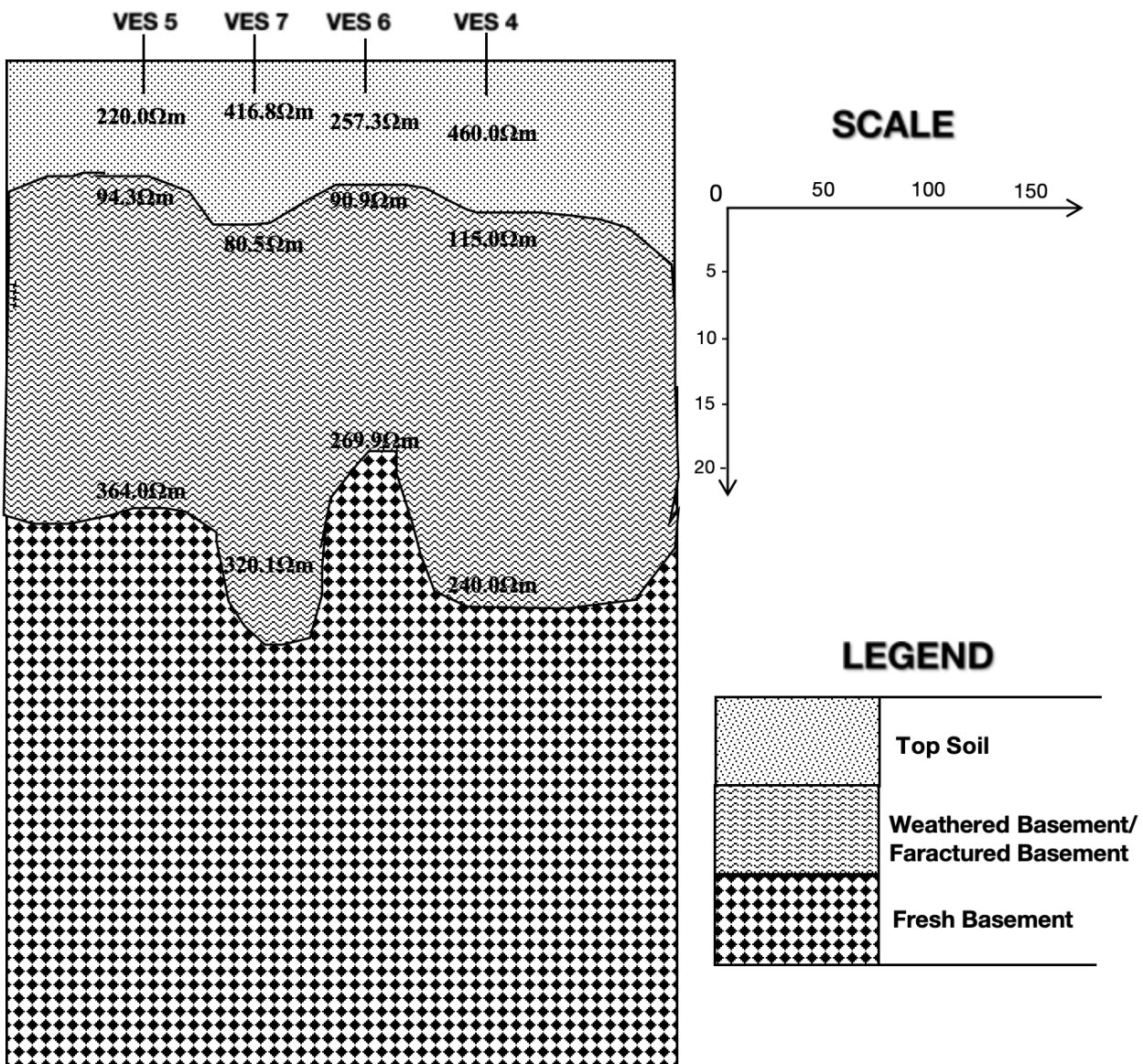


Figure 4.28: Geoelectric Section along Profile 2 at UI Mosque using Surfer

4.6.3 UI Mosque Profile 3 Geoelectric Section

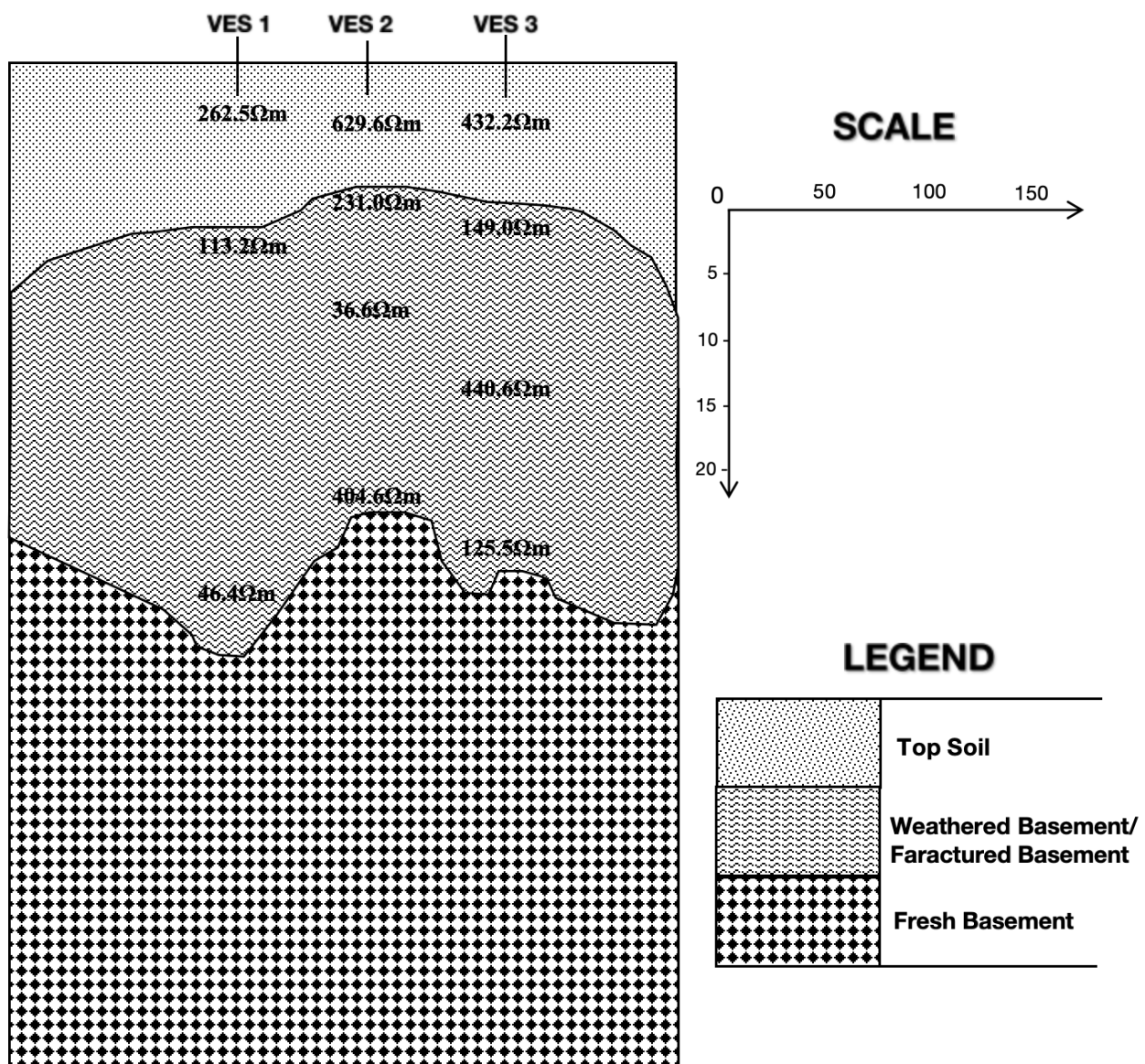


Figure 4.29: Geoelectric Section along Profile 3 at UI Mosque using Surfer

4.6.4 Abubakar Abdulsalam Hall Profile 1 Geoelectric Section

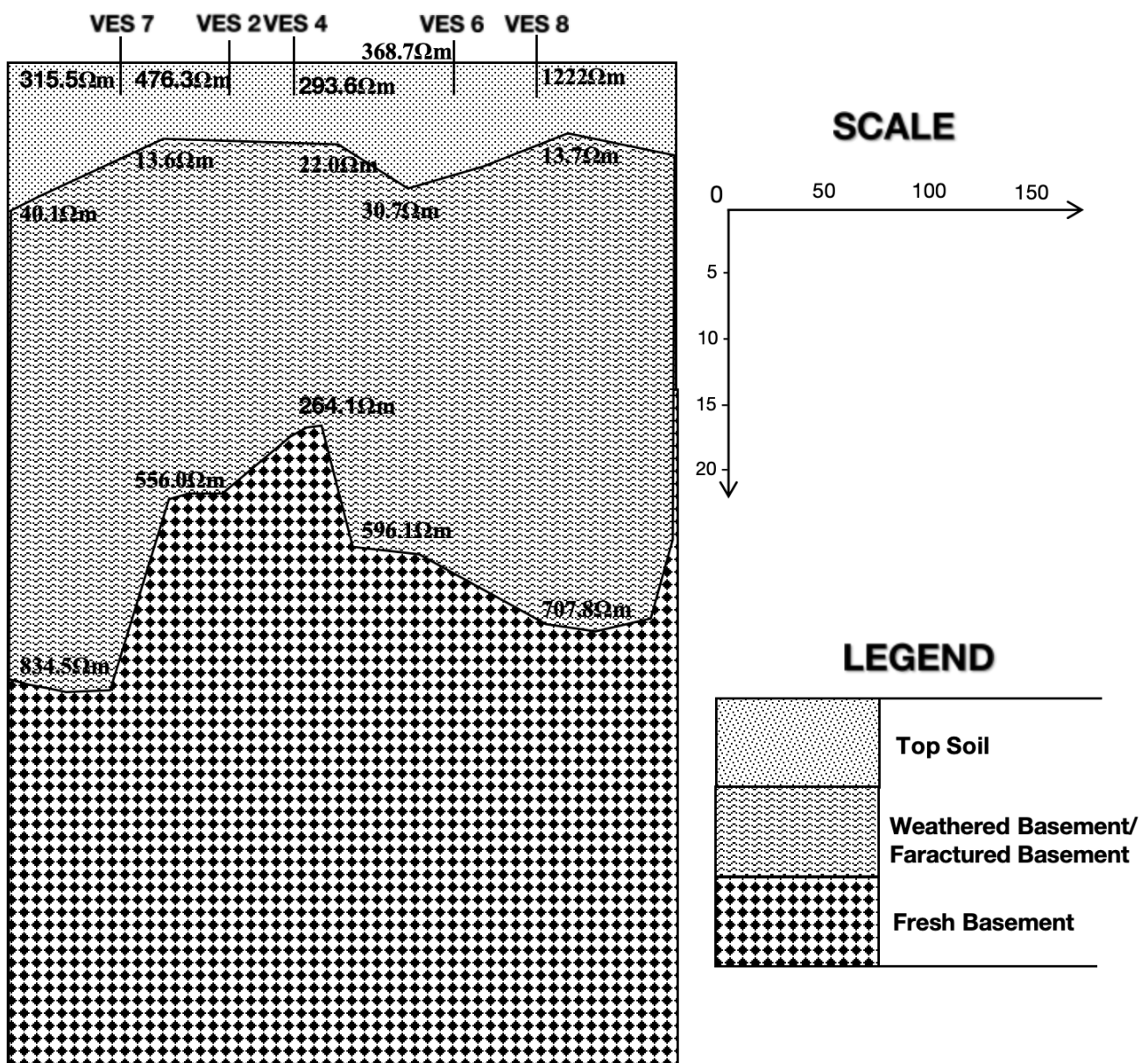


Figure 4.30: Geoelectric Section along Profile 1 at AAH using Surfer

4.6.5 Abubakar Abdulsalam Hall Profile 2 Geoelectric Section

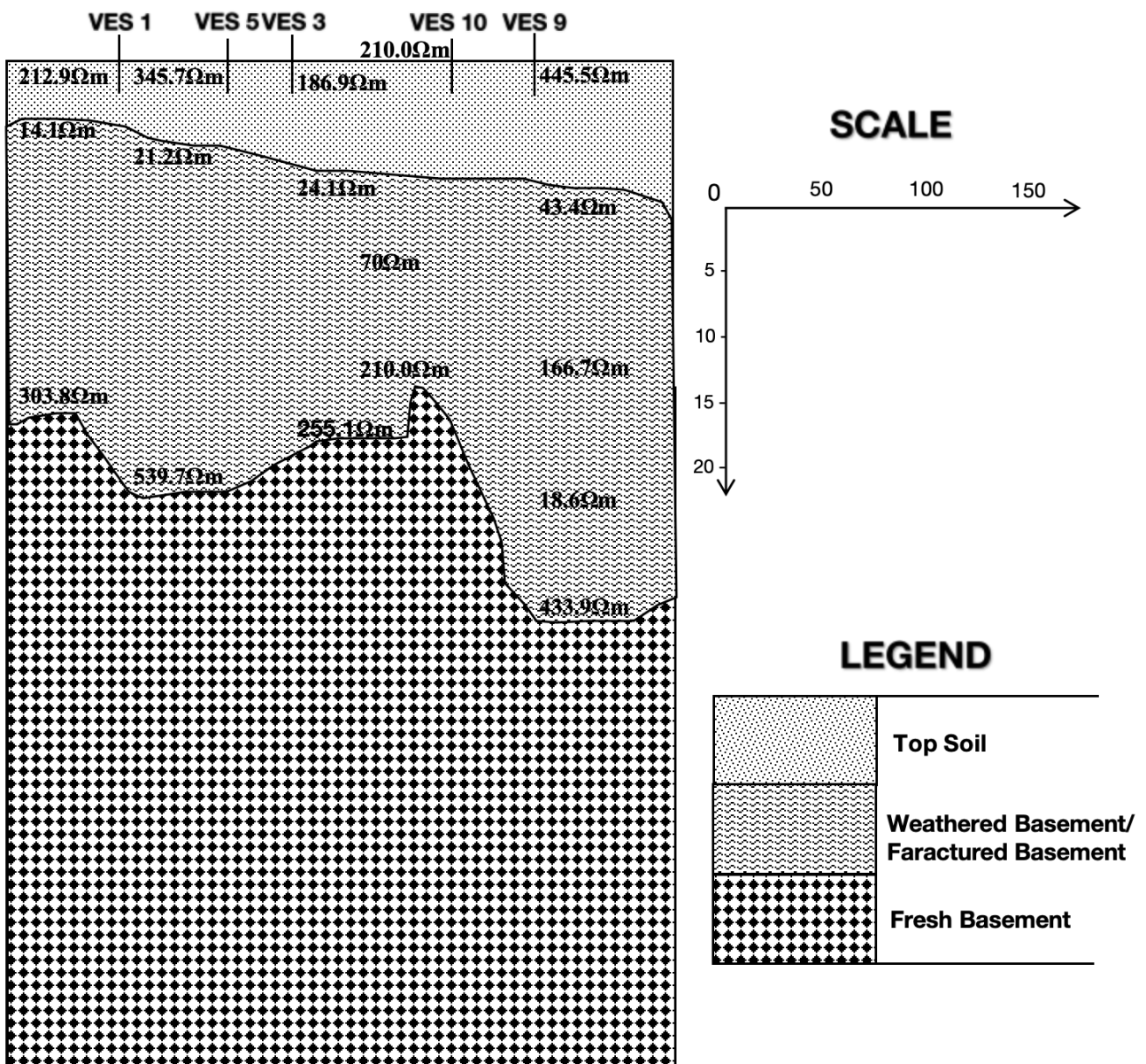


Figure 4.31: Geoelectric Section along Profile 2 at AAH using Surfer

4.7 Geoelectric Parameters and the Inferred Lithology of the Study Area

The Electrical Sounding curves from the interpreted results obtained in the previous section in both study areas shown that the two area underlain by three distinct layers in most parts. The Tables below gives the summary of the geoelectric parameters and the model interpretation of the layers.

4.7.1 Model Interpretation of Layers for UI Mosque Study Area

VES	Geoelectric Parameters				Curve Type
	Possible Lithology	Resistivity (Ωm)	Thickness (m)	Depth (m)	
VES 1	Topsoil	262.5	1.0	1.0	Q
	Weathered Basement	113.2	3.0	4.0	
	Fresh bedrock	46.4	Undetermined	Undetermined	
VES 2	Topsoil	629.6	0.8	0.8	QH
	Weathered Basement	231.0	3.5	4.3	
	Clay-rich soil	36.6	11.6	15.9	
	Basement Rock	404.6	Undetermined	Undetermined	
VES 3	Topsoil	432.2	1.1	1.1	HQ
	Weathered Basement	149.0	4.4	5.4	
	Basement Rock	440.6	10.0	15.4	
	Fresh bedrock	364.1	Undetermined	Undetermined	
VES 4	Topsoil	460.0	1.0	1.0	H
	Weathered Basement	115.0	10.5	11.5	
	Fresh bedrock	240.0	Undetermined	Undetermined	
VES 5	Topsoil	220.0	1.0	1.0	H
	Weathered Basement	94.3	21	22	
	Fresh bedrock	364.0	Undetermined	Undetermined	
VES 6	Topsoil	257.3	1.0	1.0	H
	Weathered Basement	90.9	9.0	10.0	
	Fresh bedrock	269.9	Undetermined	Undetermined	
VES 7	Topsoil	416.8	1.1	1.1	H

VES	Geoelectric Parameters				Curve Type
	Possible Lithology	Resistivity (Ωm)	Thickness (m)	Depth (m)	
	Weathered Basement	80.5	10.1	11.6	
	Fresh bedrock	320.1	Undetermined	Undetermined	
VES 8	Topsoil	349.7	1.0	1.0	Q
	Weathered Basement	122.2	6.6	7.6	
	Fresh bedrock	27.7	Undetermined	Undetermined	
VES 9	Topsoil	279.6	1.1	1.1	H
	Weathered Basement	60.0	18.8	20.0	
	Fresh bedrock	588.4	Undetermined	Undetermined	
VES 10	Topsoil	364.1	0.9	0.9	H
	Weathered Basement	50.0	10.8	11.7	
	Fresh bedrock	449.3	Undetermined	Undetermined	

Table 4.1: Interpretation of Layers at UI Mosque Study Area

4.7.2 Model Interpretation of Layers for AAH Study Area

VES	Geoelectric Parameters				Curve Type
	Possible Lithology	Resistivity (Ωm)	Thickness (m)	Depth (m)	
VES 1	Topsoil	212.9	1.0	1.0	H
	Weathered Basement	141.1	8.3	9.3	
	Fresh bedrock	303.8	Undetermined	Undetermined	
VES 2	Topsoil	476.3	0.8	0.8	H
	Weathered Basement	13.6	3.0	3.8	

VES	Geoelectric Parameters				Curve Type
	Possible Lithology	Resistivity (Ωm)	Thickness (m)	Depth (m)	
	Fresh bedrock	556.0	Undetermined	Undetermined	
VES 3	Topsoil	186.9	1.0	1.0	H
	Weathered Basement	24.1	5.3	6.3	
	Fresh bedrock	255.1	Undetermined	Undetermined	
VES 4	Topsoil	293.6	0.8	0.8	H
	Weathered Basement	22.0	4.7	5.5	
	Fresh bedrock	264.1	Undetermined	Undetermined	
VES 5	Topsoil	345.7	0.8	0.8	H
	Weathered Basement	21.2	4.3	5.1	
	Fresh bedrock	539.7	Undetermined	Undetermined	
VES 6	Topsoil	368.7	0.8	0.8	H
	Weathered Basement	30.7	8.2	8.9	
	Fresh bedrock	596.1	Undetermined	Undetermined	
VES 7	Topsoil	315.5	1.0	1.0	H
	Weathered Basement	40.1	9.9	10.9	
	Fresh bedrock	834.5	Undetermined	Undetermined	
VES 8	Topsoil	1222.0	1.0	1.0	H
	Weathered Basement	13.7	2.6	3.6	
	Fresh bedrock	707.8	Undetermined	Undetermined	
VES 9	Topsoil	445.4	0.5	0.5	KHK
	Clay or water-saturated	43.4	1.4	1.9	

VES	Geoelectric Parameters				Curve Type
	Possible Lithology	Resistivity (Ωm)	Thickness (m)	Depth (m)	
	Compacted Rock / unsaturated sandstone	166.7	11.4	13.2	
	High Conductive (water-saturated)	18.6	3.8	17.0	
	Fresh bedrock	433.9	Undetermined	Undetermined	
VES 10	Topsoil	210.0	0.7	0.7	H
	Weathered Basement	70.0	4.8	5.5	
	Fresh bedrock	210.0	Undetermined	Undetermined	

Table 4.2: Interpretation of Layers at AAH Study Area

CHAPTER 5: SUMMARY, CONCLUSION, AND RECOMMENDATIONS

5.1 SUMMARY

This project explored the application of electrical resistivity methods, including Vertical Electrical Sounding (VES) and Constant Separation Traversing (CST), to investigate subsurface characteristics for geophysical purposes. The project emphasized the integration of field data acquisition, processing, and interpretation techniques to develop resistivity models that provide insights into subsurface lithology and structural anomalies.

The methodology employed standard configurations such as Schlumberger for depth-specific studies and Wenner for horizontal resistivity variations, leveraging their strengths in capturing diverse geophysical features. The data acquisition process involved systematic profiling of the study area, with rigorous calibration and correction techniques applied to ensure accuracy. Advanced software tools, such as WINRESIST and DIPROWIN, were utilized to process and invert apparent resistivity values into true resistivity models, revealing detailed curves for VES and 2D subsurface images for CST.

This project underscores the importance of geoelectrical techniques as cost-effective, non-invasive tools for subsurface investigations, contributing to resource exploration, environmental studies, and civil engineering projects.

5.2 RECOMMENDATIONS

Based on the findings and observations from this project, the following recommendations are proposed:

1. **Enhanced Data Acquisition Strategies:** Future surveys should prioritize denser electrode spacing and extended profiles to capture more detailed resistivity variations. This is particularly important in areas with complex geology or high groundwater potential.

2. **Use of Advanced Inversion Techniques:** Leveraging emerging algorithms and 3D inversion software can enhance the accuracy and interpretability of resistivity data. Researchers should also consider the use of machine learning and artificial intelligence tools for automated data analysis and pattern recognition.
3. **Environmental Monitoring and Adaptation:** Environmental factors such as soil moisture, temperature, and anthropogenic interference significantly influence resistivity measurements. Efforts should be made to monitor and compensate for these variables during data acquisition and processing.
4. **Capacity Building and Training:** Continuous training of geophysicists and engineers in the latest resistivity technologies and software tools is essential to ensure the effective implementation of geophysical surveys. Workshops, certifications, and collaborations with research institutions can enhance expertise in the field.
5. **Further Research:** Future studies should focus on improving resistivity interpretation by conducting controlled field experiments in well-characterized areas. These studies can help refine resistivity models and develop standardized protocols for subsurface investigations.

By addressing these recommendations, the reliability and applicability of electrical resistivity methods can be significantly enhanced, paving the way for more impactful contributions to geology, hydrology, and engineering.

5.3 CONCLUSION

The project demonstrated the use of electrical resistivity methods in delineating subsurface structures within the study areas. The Schlumberger and Wenner configurations proved to be complementary techniques, effectively capturing vertical and lateral resistivity variations, respectively.

By applying practical curve matching techniques and employing advance software tools, the study produced high-resolution resistivity profiles that provided critical insights into subsurface conditions. The results confirmed the presence of lithological boundaries, aquiferous zones, and potential weak structural areas, validating the reliability of the adopted geophysical methods.

While this project achieved its objectives, it also revealed the limitations of geoelectrical methods, particularly their sensitivity to environmental factors and the inherent ambiguities in resistivity interpretation. Addressing these limitations through the recommendations like multi-method integration and advanced processing techniques will further enhance the reliability of subsurface investigations.

REFERENCES

- Adagunodo, T. A., Sunmonu, L. A., Salako, K. A. (2013). Geophysical investigation into the cause of structural failure in a building at Ogbomoso, Southwestern Nigeria. IOSR Journal of Applied Physics, 3(4), 08-16.
- Adetoyinbo, A. A., Bello, A. K., Magi, F. F. (2023). Subsurface Characteristics and Evaluation of Groundwater Potential Zone of Idi-Ayunre, Southwest, Nigeria. International Journal of Science Academic Research, 4(6), 5714-5721.
- Adeyemi, G. O., Bello, A. A. (2020). Geophysical and hydrogeological investigation of groundwater potential in part of Lagos State, Southwestern Nigeria. Journal of Applied Sciences and Environmental Management, 24(1), 57-63.
- Afuwai Gwazah, Cyril. (2019). Investigation of the inhomogeneity of subsurface structures at various VES points at Samaru-Zaria, Northern-Nigeria ARTICLE INFORMATION ABSTRACT. 1. 55-62.
- Agada, P. O., Ibuot, J. C., Oseghale, A. D. (2013). Geoelectrical investigation of groundwater potential in Emohua LGA, Rivers State, Nigeria. International Journal of Scientific Engineering Research, 4(9), 1745-1751.
- Akintoye, A. E., Olorunfemi, M. O., Ojo, J. S. (2018). Geoelectrical investigation of groundwater potential and aquifer vulnerability in a typical basement complex environment: A case study of Ado-Ekiti, Southwestern Nigeria. Nigerian Journal of Technological Development, 15(1), 1-10.
- Amadi, A., et al. (2012). Architect's and Geologist's View on the Causes of Building Failures in Nigeria. Modern Applied Science, 6(6), 31.
- Annan, A. P. (2005). Ground Penetrating Radar: Principles, Procedures, and Applications. Sensors & Software Inc.
- Anomohanran, O. (2013). Seismic refraction method: A technique for determining the thickness

of stratified substratum. American Journal of Applied Sciences, 10(8), 857-863.

Bermúdez, M. A., González-Serna, J. M., Martín-Crespo, T. (2020). Application of electrical resistivity tomography to the detection of subsurface cavities.

Binley, A. (2015). Tools and Techniques: Electrical Methods. In G. Schubert (Ed.), Treatise on Geophysics (Vol. 11, pp. 233-259). Cambridge, MA: Elsevier Science. doi:10.1016/B978-0-444-53802-4.00192-5.

Caldwell, T. G., Bibby, H. M., & Brown, C. (2004). The magnetotelluric phase tensor. Geophysical Journal International, 158(2), 457-469.

Coker, J. O. (2012). Geoelectrical investigation of groundwater potential in Mubi, Adamawa State, Nigeria. Journal of Geology and Mining Research, 4(2), 35-40.

Emilio, M., Riccardi, U. (2010). Geophysical methods applied to engineering and environmental problems. Springer, 1-10.

Eze, C. L., Ugwu, S. A., Okoye, C. O. (2017). Geoelectrical investigation of groundwater potential in Enugu State, Southeastern Nigeria. Journal of Earth System Science, 126(5), 68.

Falae, P. O. (2014). Geophysical survey using Vertical Electrical Sounding (VES) at Ibese, Southwestern Nigeria. Asia Pacific Journal of Energy and Environment, 1(2), pages.

Farinde, O. A., Enikanselu, P. A. (2015). Geophysical investigation of road pavement instability along Ibadan–Ife Expressway, Southwestern Nigeria. Journal of Applied Geology and Geophysics, 3(1), 01-09.

Griffiths, D. H., Barker, R. D. (1993). Two-dimensional resistivity imaging and modeling in areas of complex geology. Journal of Applied Geophysics, 29(3-4), 211-226.

Ismaila, A. A., Akanbi, E. S. (2019). Geophysical investigation of groundwater potential in part of Ilorin, Southwestern Nigeria. Nigerian Journal of Technological Development, 16(1), 1-8.

Jamaluddin, & Umar, Emi. (2018). Identification of subsurface layer with Wenner-Schlumberger arrays configuration geoelectrical method. IOP Conference Series: Earth and Environmental Science. 118. 012006. 10.1088/1755-1315/118/1/012006.

James, D. A., Olatunji, S. O. (2019). Geophysical investigation of groundwater potential in part

of Ibadan metropolis, Southwestern Nigeria. Journal of Applied Sciences and Environmental Management, 23(2), 311-316.

Kunetz, G. (1966). Principles of Direct Current Resistivity Prospecting. Gebrüder Borntraeger.

Kværno, S. H., Øygarden, L. (2006). The Influence of Freeze-Thaw Cycles and Soil Moisture on Aggregate Stability of Three Soils in Norway. *Catena*, 67(3), 175-182.

Lapenna, V., Lorenzo, P., Perrone, A., Piscitelli, S., Rizzo, E., Sdao, F. (2005). 2D electrical resistivity imaging of some complex landslides in the Lucanian Apennine chain, southern Italy. *Geophysics*, 70(3), B11-B18.

Loke, M.H. (2011). Electrical Resistivity Surveys and Data Interpretation. In: Gupta, H.K. (eds) Encyclopedia of Solid Earth Geophysics. Encyclopedia of Earth Sciences Series. Springer, Dordrecht.

Loke, M. H. (2016). Tutorial: 2-D and 3-D electrical imaging surveys. Geotomo Software, Malaysia.

Ogunseye, T. T., Bello, A. K., Ozegin, K. O., Akpotor, J. N. (2022). Geochemical Soil Analysis for Groundwater Quality at Mokola Area, Ibadan, Southwestern Nigeria. *IOSR Journal of Applied Geology and Geophysics*.

Olayemi, O. M., Ojo, J. S., Olorunfemi, M. O. (2021). Geoelectrical assessment of groundwater potential in a typical basement complex terrain: A case study of Iwaraja, Southwestern Nigeria. *Nigerian Journal of Technological Development*, 18(1), 1-9.

Ozevin, D., Dindarloo, S. R. (2017). Acoustic emission monitoring of corrosion in prestressed concrete structures. *Journal of Materials in Civil Engineering*, 29(10), 04017193.

Pearson, Autumn & Carroll, Kenneth & Rucker, Dale & Tsai, Peter & Fuchs, Erek. (2023). Electrical Resistivity Mapping of Lower Rio Grande River-Groundwater Interactions.

Sanuade, Oluseun Amosun, Joel & Oyeyemi, Kehinde & Olaojo, Abayomi & Fagbemigun, Tokunbo & Faloyo, Jane. (2019). Analysis of principles of equivalence and suppression in resistivity sounding technique. *Journal of Physics: Conference Series*. 1299. 012065. 10.1088/1742-6596/1299/1/012065.

Reynolds, J. M. (2011). An Introduction to Applied and Environmental Geophysics (2nd ed.). Wiley-Blackwell.

Sharma, P. V. (1986). Geophysical Methods in Geology (2nd ed.). Elsevier.

Soupios, P., Papazachos, C., Sarris, A., Vallianatos, F., Makris, J., Vafidis, A. (2006). Estimation of aquifer parameters from surficial geophysical methods: A case study of Keritis Basin in Crete. Journal of Hydrology, 338(1-2), 122-131.

Steeple, D. W., Chilton, J. (2001). Groundwater exploration using seismic refraction and electrical resistivity methods in a karst area of southeastern Minnesota. Geophysics, 66(2), 482-489.

Telford, W. M., Geldart, L. P., Sheriff, R. E. (1990). Applied Geophysics (2nd ed.). Cambridge University Press.

Warner, M. (2004). Seismic reflection inversion: Methods, pitfalls, and applications. European Association of Geoscientists Engineers, 22(5), 123-136.

Wiwattanachang N., & Giao, P.. (2011). Monitoring crack development in fiber concrete beam by using electrical resistivity imaging. Journal of Applied Geophysics - J APPL GEOPHYS. 75. 294-304. 10.1016/j.jappgeo.2011.06.009.

<https://egsciences.com/service/vertical-electrical-sounding>

<https://geologyscience.com/geology-branches/geophysics/electrical-resistivity-surveys>

https://archive.epa.gov/esd/archive-geophysics/web/html/resistivity_methods.html

<https://www.epa.gov/environmental-geophysics/electrical-resistivity>

Appendix

- Vertical Electrical Sounding Resistivity Field Records

Location: Emotan Lane, University of Ibadan Central Mosque, Ibadan.

Instrument: Campus Omega Resistivity Meter

Array Type: Schlumberger Array

Coordinates	VES 1	VES 2	VES 3	VES 4	VES 5	VES 6	VES 7	VES 8	VES 9	VES 10
Latitudes:	7.446810	7.446895	7.446926	7.446710	7.446727	7.446721	7.446720	7.446580	7.446531	7.446532
Longitudes:	3.899718	3.899828	3.899930	3.899940	3.899400	3.899898	3.899641	3.899755	3.899717	3.899836

Current Electrode (AB/2) M	Potential Electrode (MN/2) M	Geometric Factor (K)	R1 (Ω)	KR1 (ΩM)	R2 (Ω)	KR2 (ΩM)	R3 (Ω)	KR3 (ΩM)	R4 (Ω)	KR4 (ΩM)	R5 (Ω)	KR5 (ΩM)
1.0	0.25	5.89	44.25	261	101	594	62.46	368	80.24	473	38	224
1.3	0.25	10.23	21.65	221	55.21	565	32.25	402	36.23	371	20	205
1.8	0.25	19.97	10.18	203	20.01	400	16.47	329	13.54	270	8.19	164
2.4	0.25	35.80	5.24	188	10.26	367	8.17	292	7.10	254	6.14	220
3.2	0.25	63.96	2.34	150	4.45	284	7.55	482	3.22	206	2.74	175
4.2	0.25	110.46	1.156	128	2.36	261	1.76	194	1.68	186	1.38	152
4.2	1	26.14	5.115	134	7.48	196	7.49	196	7.11	186	5.88	154
5.5	1	45.95	2.338	107	4.02	185	3.71	170	2.55	117	2.96	136
7.5	1	86.79	0.974	85	1.613	140	1.294	112	1.811	157	1.46	127
10	1	155.53	0.437	68	0.683	107	0.779	121	2.67	415	0.630	98
13	1	263.93	0.296	78	0.229	60	1.225	323	1.44	380	0.360	95
13	2.5	102.27	0.365	37	0.591	60	3.109	318	2.89	296	0.929	95
18	2.5	199.67	0.194	39	0.215	43	1.380	276	0.516	103	0.541	108
24	2.5	358.03	0.105	38	0.372	133	0.780	253	0.243	87	0.307	110
32	2.5	639.55	0.080	51	0.134	86	0.383	245	0.148	96	0.192	123
42	2.5	1104.57	0.043	50	0.078	86	0.207	229	0.174	192	0.134	148
55	2.5	1896.98	0.023	43	0.067	127	0.093	176	0.091	173	0.114	216

Table 5.1: VES 1-5 Data obtained from Filed Work at UI Mosque

Current Electrode (AB/2) M	Potential Electrode (MN/2) M	Geometric Factor (K)	R6 (Ω)	KR6 (ΩM)	R7 (Ω)	KR7 (ΩM)	R8 (Ω)	KR8 (ΩM)	R9 (Ω)	KR9 (ΩM)	R10 (Ω)	KR10 (ΩM)
1.0	0.25	5.89	45.00	265	70.13	413	56.50	333	60.13	354	71.94	424
1.3	0.25	10.23	22.86	234	30.18	309	27.43	280	30.24	309	33.12	339
1.8	0.25	19.97	11.13	222	10.97	210	10.69	213	9.27	185	10.35	207
2.4	0.25	35.80	7.00	251	6.24	223	5.76	206	3.97	142	4.098	146
3.2	0.25	63.96	3.74	239	2.89	184	2.90	186	1.387	89	1.716	110
4.2	0.25	110.46	2.32	256	1.84	148	1.34	148	0.828	91	0.832	92
4.2	1.0	26.14	10.25	268	5.66	148	5.70	149	0.290	90	0.287	92
5.5	1.0	45.95	3.67	168	2.32	106	2.415	111	1.852	85	1.958	90
7.5	1.0	86.79	1.59	138	1.35	117	0.676	59	0.808	70	0.712	62
10.0	1.0	155.53	0.64	101	0.61	95	0.271	42	0.406	63	0.352	55
13	1	263.93	0.43	114	0.36	96	0.287	76	0.228	60	0.221	58
13	2.5	102.27	1.09	112	1.05	97	0.743	76	0.596	61	0.587	60
18	2.5	199.67	0.60	120	0.52	110	0.255	51	0.441	88	0.425	85
24	2.5	358.03	0.34	123	0.31	114	0.134	48	0.232	83	0.220	79
32	2.5	639.55	0.22	146	0.19	124	0.055	35	0.122	78	0.117	75
42	2.5	1104.57	0.17	193	0.13	150	0.027	30	0.095	105	0.288	318
55	2.5	1896.98	0.12	241	0.11	208	0.039	74	0.078	148	0.227	431

Table 5.2: VES 6-10 Data obtained from Filed Work at UI Mosque

Location: Appleton Road, Abubakar Abdulsalam Hall, UI, Ibadan.

Instrument: Campus Omega Resistivity Meter

Array Type: Schlumberger Array

Coordinates	VES 1	VES 2	VES 3	VES 4	VES 5	VES 6	VES 7	VES 8	VES 9	VES 10
Latitudes:	7.43943° N	7.43941° N	7.43926° N	7.43939° N	7.43938° N	7.43938° N	7.43938° N	7.43940° N	7.43915° N	7.43923° N
Longitudes:	3.89507° E	3.89495° E	3.89521° E	3.89499° E	3.89512° E	3.89507° E	3.894515° E	3.89523° E	3.89519° E	3.89529° E

Current Electrode (AB/2) M	Potential Electrode (MN/2) M	Geometric Factor (K)	R1 (Ω)	KR1 (ΩM)	R2 (Ω)	KR2 (ΩM)	R3 (Ω)	KR3 (ΩM)	R4 (Ω)	KR4 (ΩM)	R5 (Ω)	KR5 (ΩM)
1.0	0.25	5.89	40.89	241	52.29	308	30.76	181	40.89	241	53.75	317
1.3	0.25	10.23	17.34	177	23.03	236	18.37	188	19.06	195	20.36	208
1.8	0.25	19.97	5.84	117	9.49	190	6.13	122	6.52	130	4.288	86
2.4	0.25	35.80	1.898	68	4.24	152	2.01	72	2.11	76	1.639	59
3.2	0.25	63.96	0.591	38	1.561	100	0.803	51	0.691	44	0.699	45
4.2	0.25	110.46	0.232	26	0.591	65	0.328	36	0.266	29	0.268	30
4.2	1.0	26.14	1.031	27	2.48	65	1.38	36	1.15	30	1.186	31
5.5	1.0	45.95	0.813	37	0.646	30	0.718	33	0.747	34	0.696	32
7.5	1.0	86.79	0.207	18	0.22	19	0.412	36	0.355	31	0.338	29
10.0	1.0	155.53	0.128	20	0.103	16	0.256	40	0.239	37	0.152	24
13	1	263.93	0.083	22	0.0875	23	0.216	57	0.211	56	0.209	55
13	2.5	102.27	0.225	23	0.3925	40	0.049	5	0.56	57	0.55	56
18	2.5	199.67	0.14	28	0.871	174	0.36	72	0.33	66	0.417	83
24	2.5	358.03	0.091	33	0.312	112	0.232	83	0.252	90	0.256	92
32	2.5	639.55	0.14	90	0.227	145	0.123	79	0.142	91	0.194	124
42	2.5	1104.57	0.01	11	0.138	152	0.097	107	0.109	120	0.134	148
55	2.5	1896.98	0.092	175	0.093	176	0.066	125	0.074	140	0.115	218

Table 5.3: VES 1-5 Data obtained from Filed Work at AAH

Current Electrode (AB/2) M	Potential Electrode (MN/2) M	Geometric Factor (K)	R6 (Ω)	KR6 (ΩM)	R7 (Ω)	KR7 (ΩM)	R8 (Ω)	KR8 (ΩM)	R9 (Ω)	KR9 (ΩM)	R10 (Ω)	KR10 (ΩM)
1.0	0.25	5.89	72.56	427	60.35	355	188	1107	61.51	362	48.36	285
1.3	0.25	10.23	31.14	319	23.45	240	84.54	865	15.27	156	14.85	152
1.8	0.25	19.97	7.49	150	10.12	202	33.21	663	4.37	87	5.46	109
2.4	0.25	35.80	1.68	60	5.25	188	9.14	327	2.079	74	2.46	88
3.2	0.25	63.96	0.58	37	2.63	168	1.794	115	1.276	82	1.33	85
4.2	0.25	110.46	0.356	39	0.679	75	0.433	48	0.631	70	0.72	80
4.2	1.0	26.14	1.49	39	2.91	76	1.87	49	2.72	71	3.09	81
5.5	1.0	45.95	0.753	35	1.175	54	0.613	28	1.509	69	1.63	75
7.5	1.0	86.79	0.449	39	0.55	48	0.152	13	1.855	161	0.98	85
10.0	1.0	155.53	0.276	43	0.257	40	0.306	48	1.742	271	0.69	107
13	1	263.93	0.2	53	0.22	58	0.276	73	0.695	183	0.44	116
13	2.5	102.27	0.528	54	0.567	58	0.694	71	1.78	182	1.12	115
18	2.5	199.67	0.485	97	0.416	83	0.494	99	0.696	139	0.66	132
24	2.5	358.03	0.221	79	0.257	92	0.376	135	0.297	106	0.385	138
32	2.5	639.55	0.343	219	0.172	110	0.187	120	0.159	102	0.231	148
42	2.5	1104.57	0.212	234	0.121	134	0.163	180	0.139	154	0.141	156
55	2.5	1896.98	0.05	95	0.095	180	0.08	152	0.088	167	0.126	239

Table 5.4: VES 6 - 10 Data obtained from Field Work at AAH

- Constant Separation Traversing Resistivity Field Records

Location: Appleton Road, Abubakar Abdulsalam Hall, UI, Ibadan.

Instrument: Omega Resistivity Meter

Array Type: Wenner Array

Profiles	Starting Latitudes:	Starting Longitudes:	Ending Latitudes:	Ending Longitudes:
Profile 1 (150m)	7.43927° N	3.89424° E	7.43945° N	3.89558° E
Profile 2 (130m)	7.44024° N	3.89497° E	7.43908° N	3.89508° E

10m Electrode Spacing

Electrodes Position (m)	Geometric Factor (K)	R1 (Ω)	KR1 (Ωm)	R2 (Ω)	KR2 (Ωm)
0, 10, 20, 30	62.84	0.429	26.95836	1.57	98.6588
10, 20, 30, 40	62.84	1.018	63.97112	1.897	119.20748
20, 30, 40, 50	62.84	0.826	51.90584	1.423	89.42132
30, 40, 50, 60	62.84	0.714	44.86776	1.294	81.31496
40, 50, 60, 70	62.84	1.069	67.17596	1.043	65.54212
50, 60, 70, 80	62.84	0.713	44.80492	0.862	54.16808
60, 70, 80, 90	62.84	1.19	74.7796	0.575	36.133
70, 80, 90, 100	62.84	0.782	49.14088	0.974	61.20616
80, 90, 100, 110	62.84	1.043	65.54212	1.501	94.32284
90, 100, 110, 120	62.84	1.345	84.5198	2.044	128.44496
100, 110, 120, 130	62.84	1.846	116.00264	1.363	85.65092
110, 120, 130, 140	62.84	2.217	139.31628	-	-
120, 130, 140, 150	62.84	2.959	185.94356	-	-

20m Electrode Spacing					
Electrodes Position (m)	Geometric Factor (K)	R1 (Ω)	KR1 (Ωm)	R2 (Ω)	KR2 (Ωm)
0, 20, 40, 60	125.68	0.689	86.59352	1.061	133.34648
10, 30, 50, 70	125.68	0.547	68.74696	1.000	125.68
20, 40, 60, 80	125.68	0.533	66.98744	0.871	109.46728
30, 50, 70, 90	125.68	0.823	103.43464	0.923	116.00264
40, 60, 80, 100	125.68	1.069	134.35192	0.802	100.79536
50, 70, 90, 110	125.68	0.923	116.00264	0.94	118.1392
60, 80, 100, 120	125.68	0.94	118.1392	0.777	97.65336
70, 90, 110, 130	125.68	0.983	123.54344	0.966	121.40688
80, 100, 120, 140	125.68	1.423	178.84264	-	-
90, 110, 130, 150	125.68	2.51	315.4568	-	-

30m Electrode Spacing					
Electrodes Position (m)	Geometric Factor (K)	R1 (Ω)	KR1 (Ωm)	R2 (Ω)	KR2 (Ωm)
0, 30, 60, 90	188.52	0.344	64.85088	0.820	154.5864
10, 40, 70, 100	188.52	0.739	139.31628	0.749	141.20148
20, 50, 80, 110	188.52	0.871	164.20092	0.771	145.34892
30, 60, 90, 120	188.52	0.942	177.58584	0.768	144.78336
40, 70, 100, 130	188.52	0.888	167.40576	0.788	148.55376
50, 80, 110, 140	188.52	0.760	143.2752	-	-
60, 90, 120, 150	188.52	1.414	266.56728	-	-

40m Electrode Spacing					
Electrodes Position (m)	Geometric Factor (K)	R1 (Ω)	KR1 (Ωm)	R2 (Ω)	KR2 (Ωm)
0, 40, 80, 120	251.36	0.799	200.83664	0.550	138.248
10, 50, 90, 110	251.36	0.806	202.59616	0.522	131.20992
20, 60, 100, 140	251.36	0.854	214.66144	-	-
30, 70, 110, 150	251.36	0.832	209.13152	-	-

50m Electrode Spacing					
Electrodes Position (m)	Geometric Factor (K)	R1 (Ω)	KR1 (Ωm)	R2 (Ω)	KR2 (Ωm)
120,130,140,150	314.2	0.783	246.0186	-	-

Location: Emotan Lane, University of Ibadan Central Mosque, Ibadan.

Instrument: Omega Resistivity Meter

Array Type: Wenner Array

Profiles	Starting Latitudes:	Starting Longitudes:	Ending Latitudes:	Ending Longitudes:
Profile 1 (130m)	7.446567° N	3.899063° E	7.446538° N	3.900243° E
Profile 2 (150m)	7.446634° N	3.899220° E	7.446908° N	3.900401° E
Profile 3 (130m)	7.446661° N	3.899393° E	7.447051° N	3.900334° E

10m Electrode Spacing							
Electrodes Position (m)	Geometric Factor (K)	R1 (Ω)	KR1 (Ωm)	R2 (Ω)	KR2 (Ωm)	R (Ω)	KR3 (Ωm)
0,10,20,30	62.84	2.182	137.1169	0.656	41.22304	0.643	40.40612
10,20,30,40	62.84	1.000	62.84	0.823	51.71732	1.518	95.39112
20,30,40,50	62.84	1.843	115.8141	0.707	44.42788	0.667	41.91428
30,40,50,60	62.84	1.621	101.8636	0.646	40.59464	0.717	45.05628
40,50,60,70	62.84	2.306	144.909	0.854	53.66536	0.748	47.00432
50,60,70,80	62.84	0.957	60.13788	0.817	51.34028	0.688	43.23392
60,70,80,90	62.84	2.381	149.622	0.778	48.88952	0.710	44.6164
70,80,90,100	62.84	3.157	198.3859	0.848	53.28832	0.599	37.64116
80,90,100,110	62.84	2.700	169.668	0.783	49.20372	0.521	32.73964
90,100,110,120	62.84	0.976	61.33184	0.778	48.88952	0.646	40.59464
100,110,120,130	62.84	0.862	54.16808	0.818	51.40312	0.620	38.9608
110,120,130,140	62.84	-	-	0.604	37.95536	-	-
120,130,140,150	62.84	-	-	0.559	35.12756	-	-

20m Electrode Spacing

Electrodes Position (m)	Geometric Factor (K)	R1 (Ω)	KR1 (Ωm)	R2 (Ω)	KR2 (Ωm)	R (Ω)	KR3 (Ωm)
0,20,40,60	125.68	0.209	26.26712	0.425	53.414	0.243	30.54024
10,30,50,70	125.68	0.402	50.52336	0.396	49.76928	0.278	34.93904
20,40,60,80	125.68	0.334	41.97712	0.265	33.3052	0.264	33.17952
30,50,70,90	125.68	0.507	63.71976	0.640	80.4352	0.261	32.80248
40,60,80,100	125.68	0.311	39.08648	0.342	42.98256	0.305	38.3324
50,70,90,110	125.68	0.550	69.124	0.392	49.26656	0.443	55.67624
60,80,100,120	125.68	0.186	23.37648	0.249	31.29432	0.424	53.28832
70,90,110,130	125.68	0.172	21.61696	0.260	32.6768	0.331	41.60008
80,100,120,140	125.68	-	-	0.330	41.4744	-	-
90,110,130,150	125.68	-	-	0.310	38.9608	-	-

30m Electrode Spacing

Electrodes Position (m)	Geometric Factor (K)	R1 (Ω)	KR1 (Ωm)	R2 (Ω)	KR2 (Ωm)	R (Ω)	KR3 (Ωm)
0,30,60,90	188.52	0.415	78.2358	0.245	46.1874	0.373	70.31796
10,40,70,100	188.52	0.839	158.1683	0.227	42.79404	0.373	70.31796
20,50,80,110	188.52	0.754	142.1441	0.317	59.76084	0.280	52.7856
30,60,90,120	188.52	0.709	133.6607	0.470	88.6044	0.273	51.46596
40,70,100,130	188.52	0.948	178.717	0.297	55.99044	0.264	49.76928
50,80,110,140	188.52	-	-	0.335	63.1542	-	-
60,90,120,150	188.52	-	-	0.279	52.59708	-	-

40m Electrode Spacing

Electrodes Position (m)	Geometric Factor (K)	R1 (Ω)	KR1 (Ωm)	R2 (Ω)	KR2 (Ωm)	R (Ω)	KR3 (Ωm)
0,40,80,120	251.36	0.236	59.32096	0.311	78.17296	0.333	83.70288
10,50,90,130	251.36	0.384	96.52224	0.295	74.1512	0.396	99.53856
20,60,100,140	251.36	-	-	0.336	84.45696	-	-
30,70,110,150	251.36	-	-	0.239	60.07504	-	-

50m Electrode Spacing

Electrodes Position (m)	Geometric Factor (K)	R1 (Ω)	KR1 (Ωm)	R2 (Ω)	KR2 (Ωm)	R (Ω)	KR3 (Ωm)
120,130,140,150	62.84	-	-	0.559	35.12756	-	-